Chapter 3
Generic channel models

3.1 Physical propagation mechanisms

- Reflection, diffraction and scattering are three basic propagation mechanism.
- They occur depending on the size L of the object compared with the wavelength λ.
  - When a plane electromagnetic wave encounters an obstacle much larger than the wavelength, i.e. $L \gg \lambda$, reflection occurs.
  - Diffraction happens when the obstacle's size is in the same order of the wavelength, i.e. $L \approx \lambda$.
  - Scattering happens when a plane wave encounters an obstacle much smaller than the wavelength, i.e. $L << \lambda$. This obstacle becomes a new source emitting waves towards multiple directions.

Diffraction

- Described by the Huygens-Fresnel principle and the principle of superposition of waves.
  - The wave propagation visualized by considering every point on a wave front as a point source for a secondary spherical wave.
  - The wave displacement at any subsequent point is the sum of these secondary waves.
- Sum of waves is determined by the relative phases as well as the amplitudes of the individual waves so that the summed amplitude of the waves can have any value between zero and the sum of the individual amplitudes.
- Diffraction patterns usually have a series of maxima and minima.

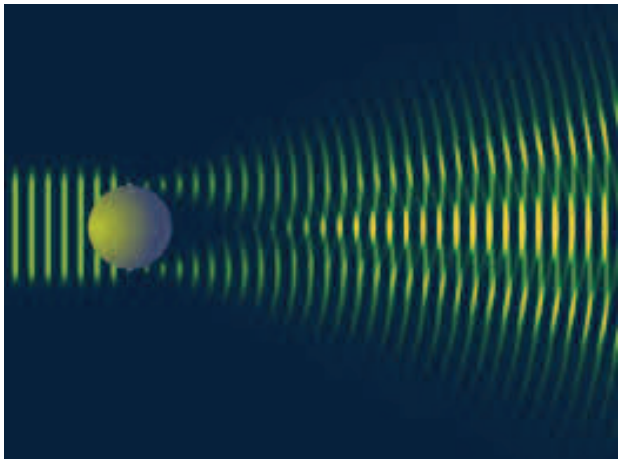

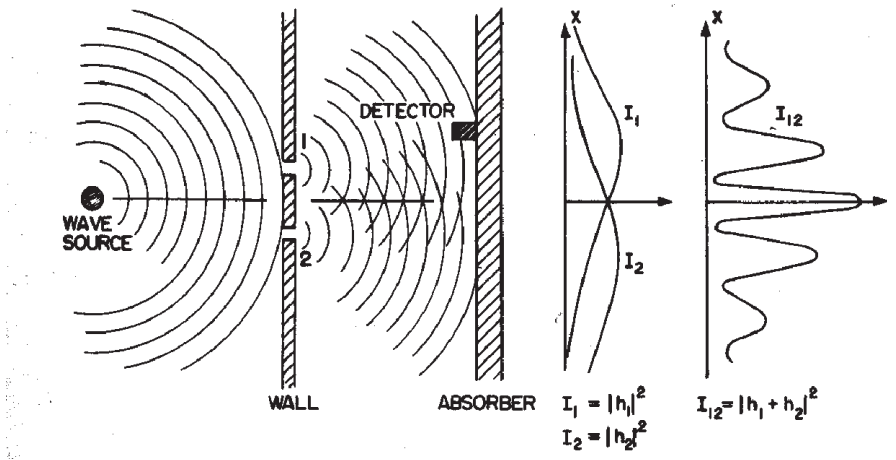

Experimental propagation constellation

- Parameter estimation algorithms estimated direction of arrival, direction of departure, delay, Doppler frequency and complex attenuation of plane waves
- With knowledge of the locations of the Tx and Rx, propagation paths especially for those with one-bounce can be constructed.

Estimated paths overlapping with the photographs of the background.

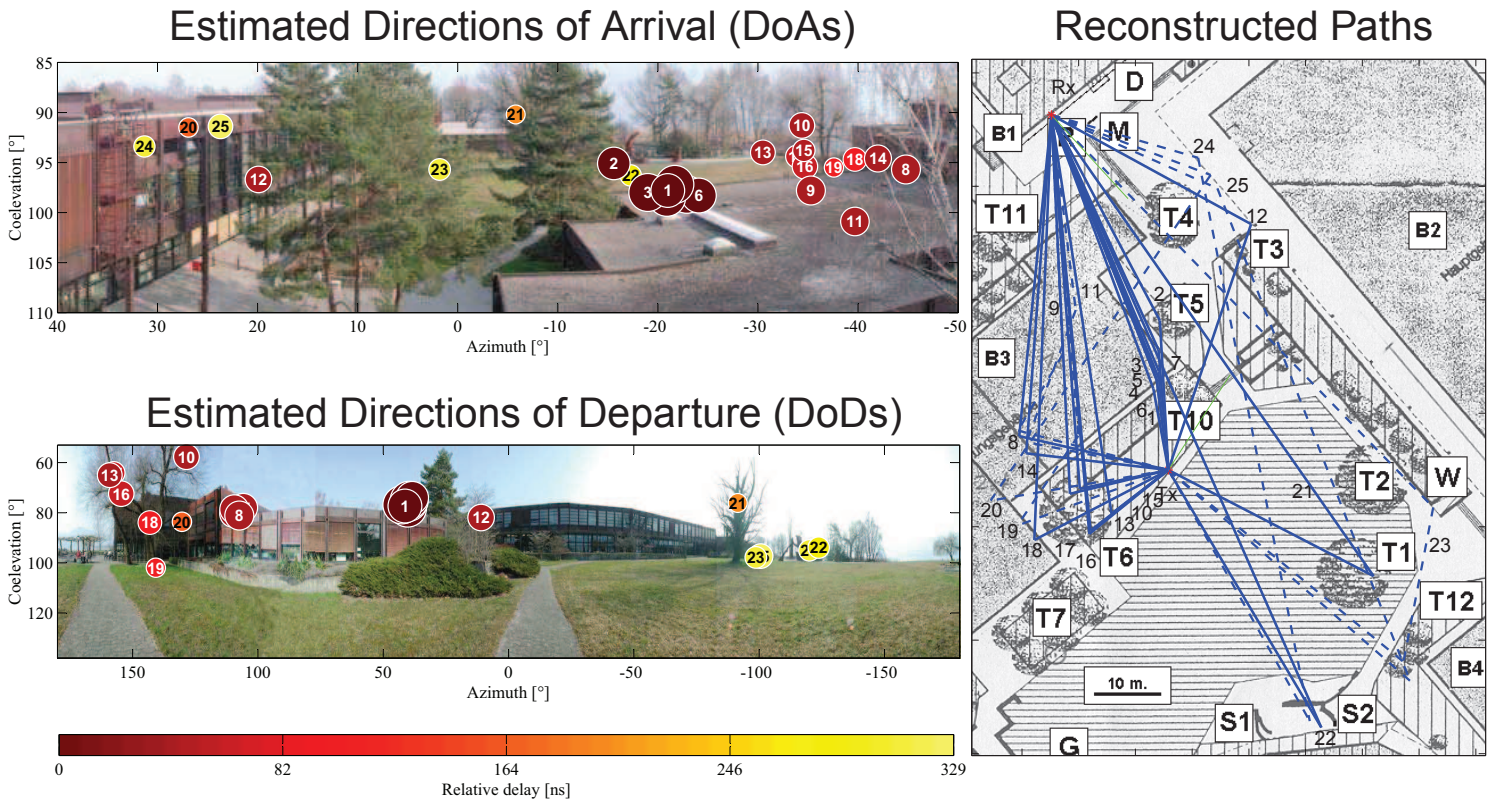

Identified propagation mechanism

- No. 1, to 6 paths are due to the diffraction at the edge of building "B3".

Estimated Directions of Arrival (DoAs)

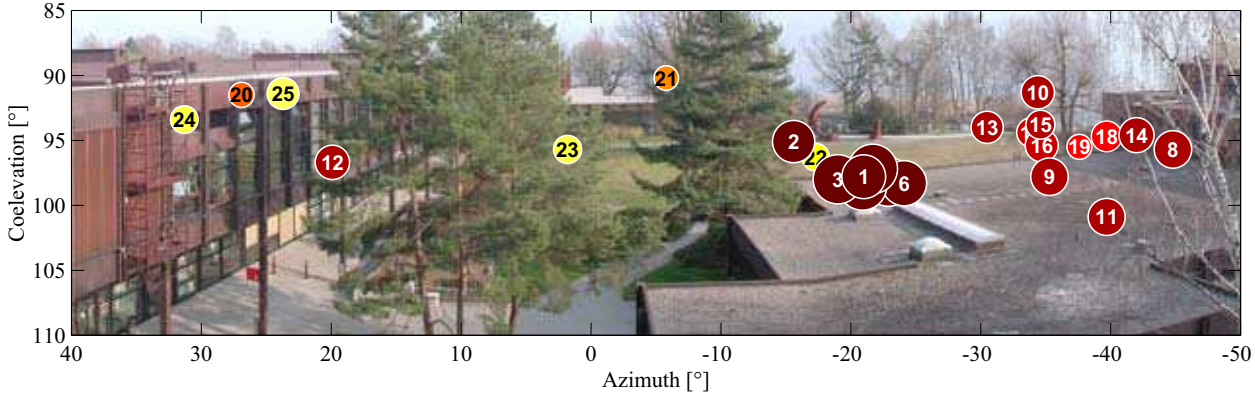

Estimated Directions of Departure (DoDs

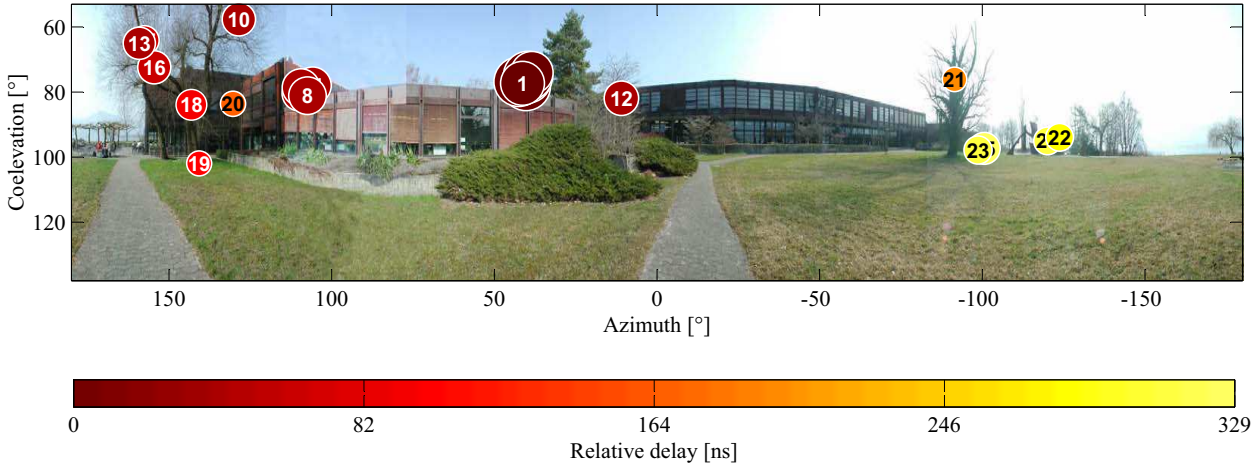

Reconstructed Paths

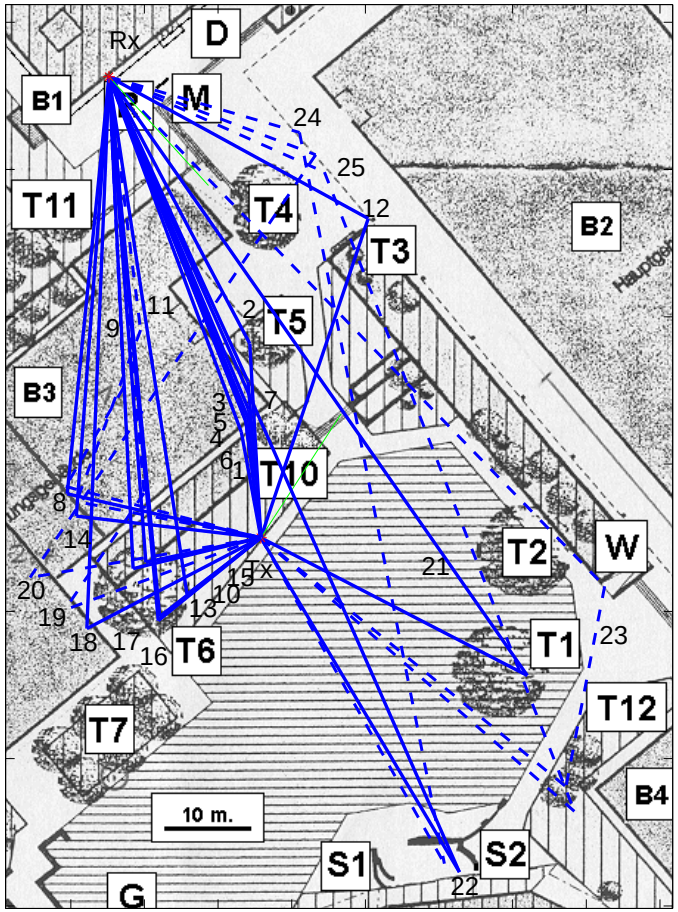

Identified propagation mechanism

- The paths no. 9 to 19 are more caused by the scattering due to the mixture of thin tree stems combined with the edges of the buildings.

Estimated Directions of Arrival (DoAs)

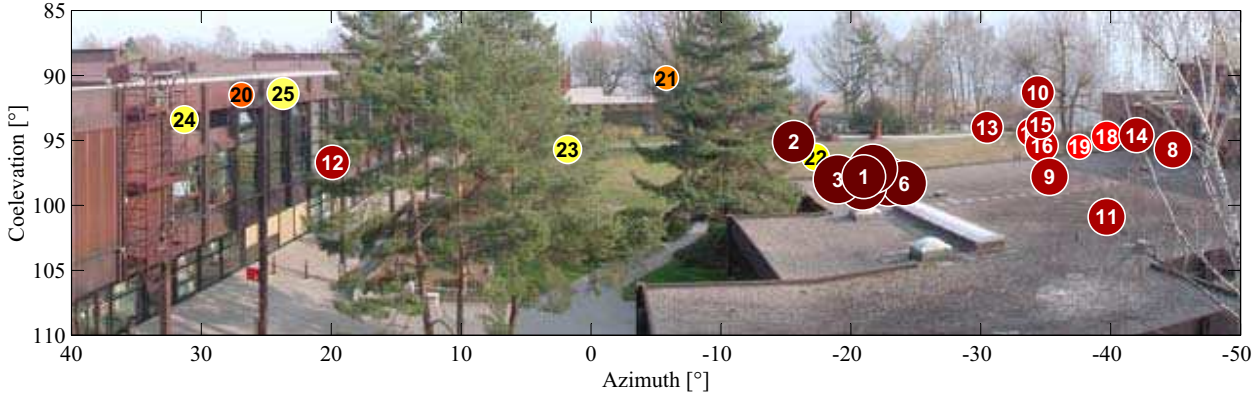

Estimated Directions of Departure (DoDs

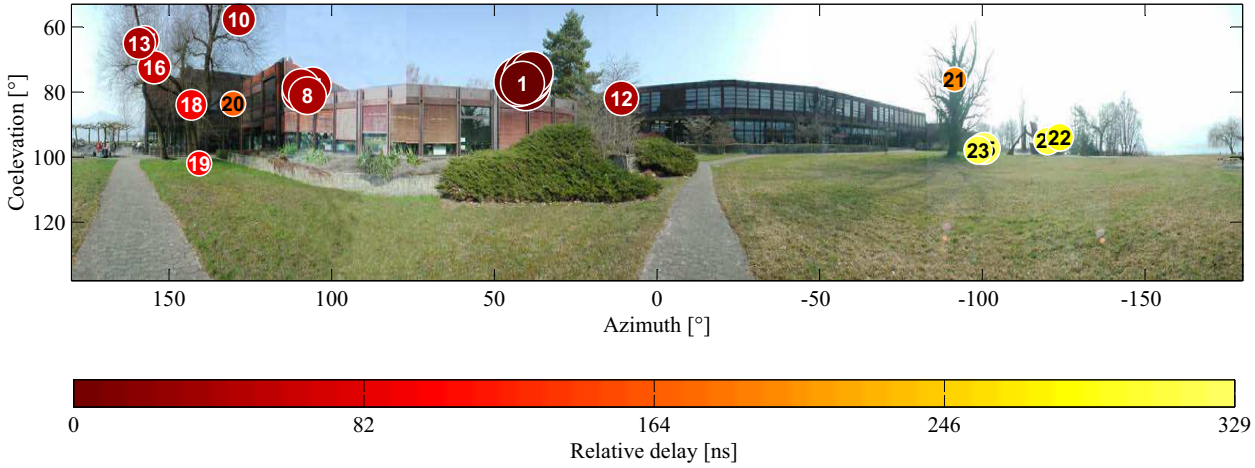

Reconstructed Paths

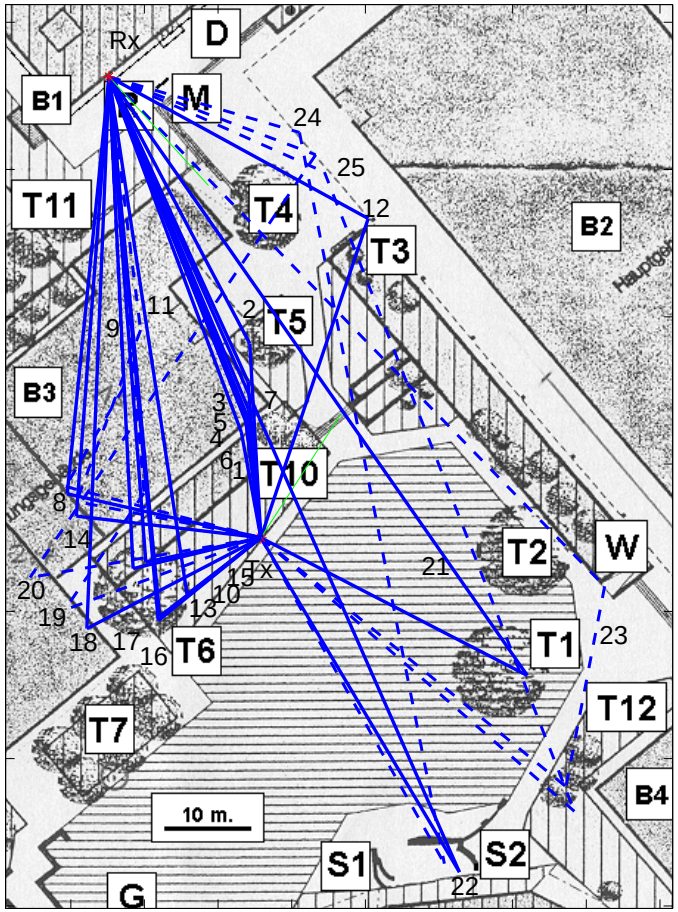

Identified propagation mechanism

- The paths no. 21, 22, 23, may be caused by the reflections of the sculptures, tree and the facade of the buildings in the environment.

Estimated Directions of Arrival (DoAs)

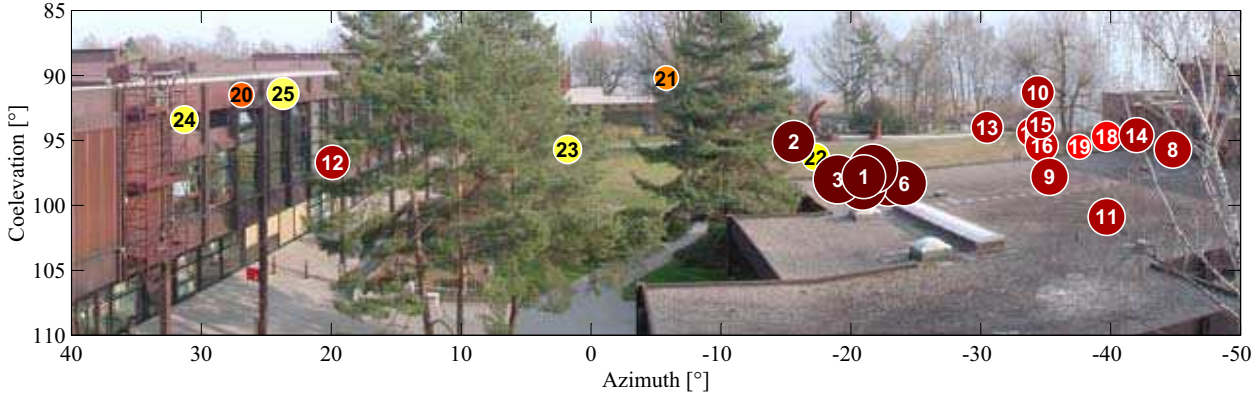

Estimated Directions of Departure (DoDs

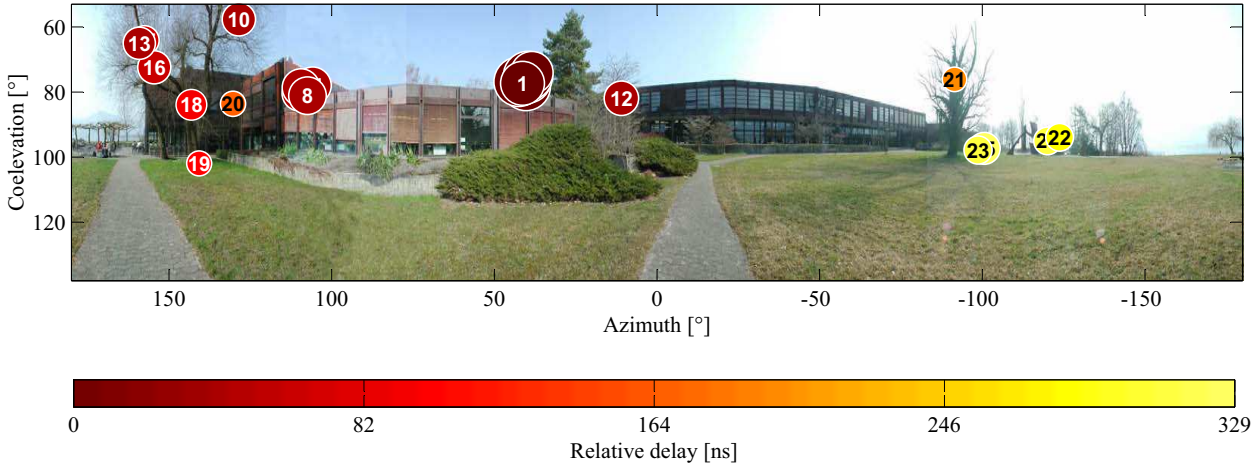

Reconstructed Path 21

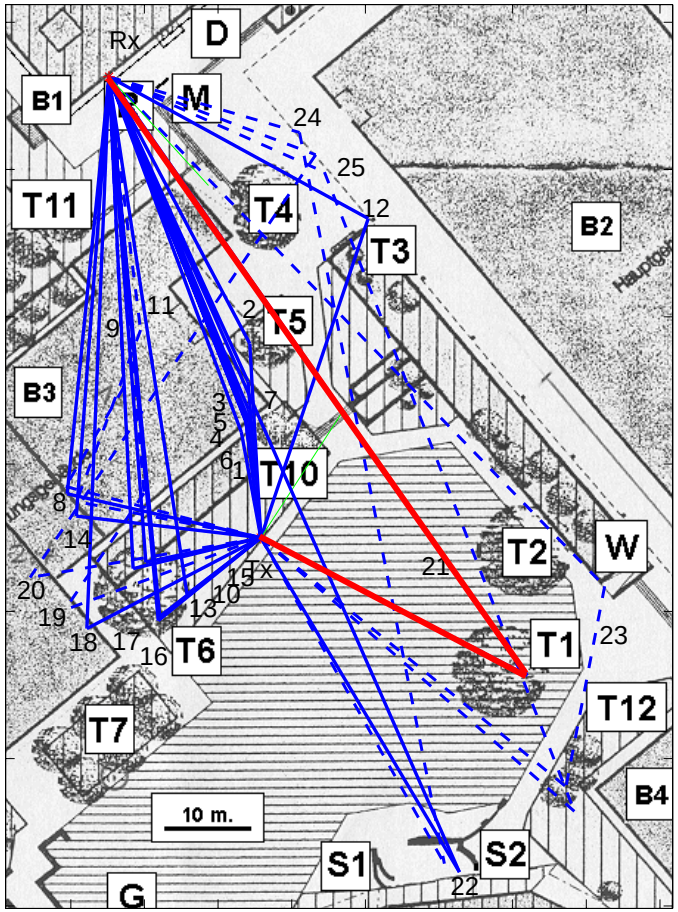

Identified propagation mechanism

- The paths no. 24, may be caused by the reflections of the sculptures and the facade of the buildings in the environment.

Estimated Directions of Arrival (DoAs)

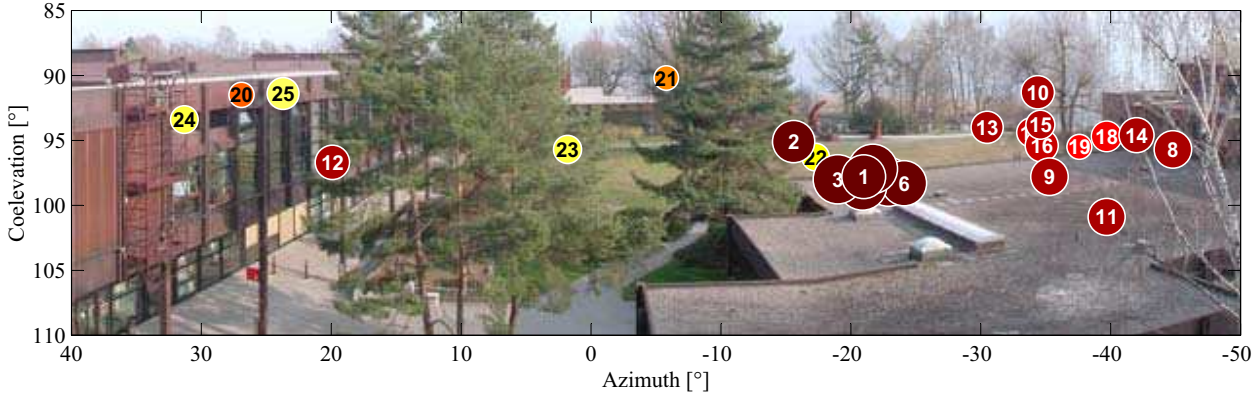

Estimated Directions of Departure (DoDs

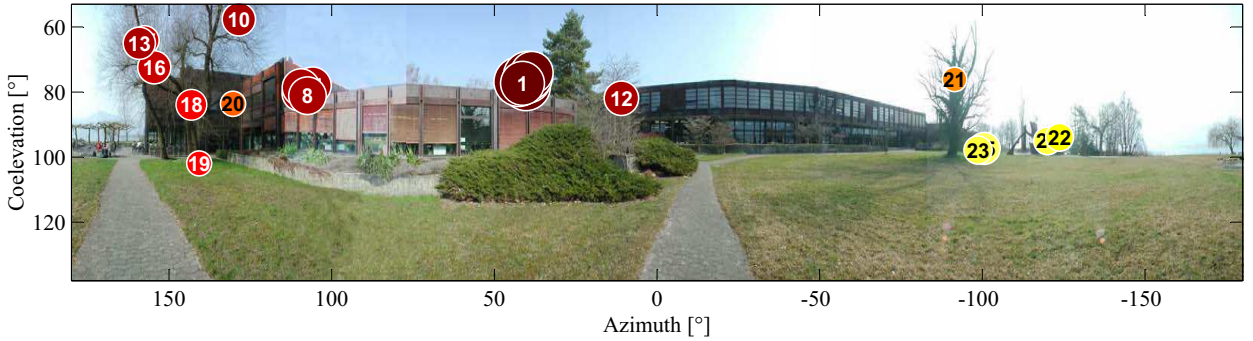

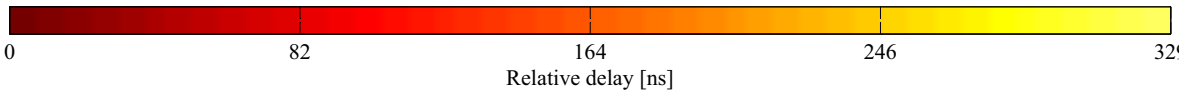

Reconstructed Path 24

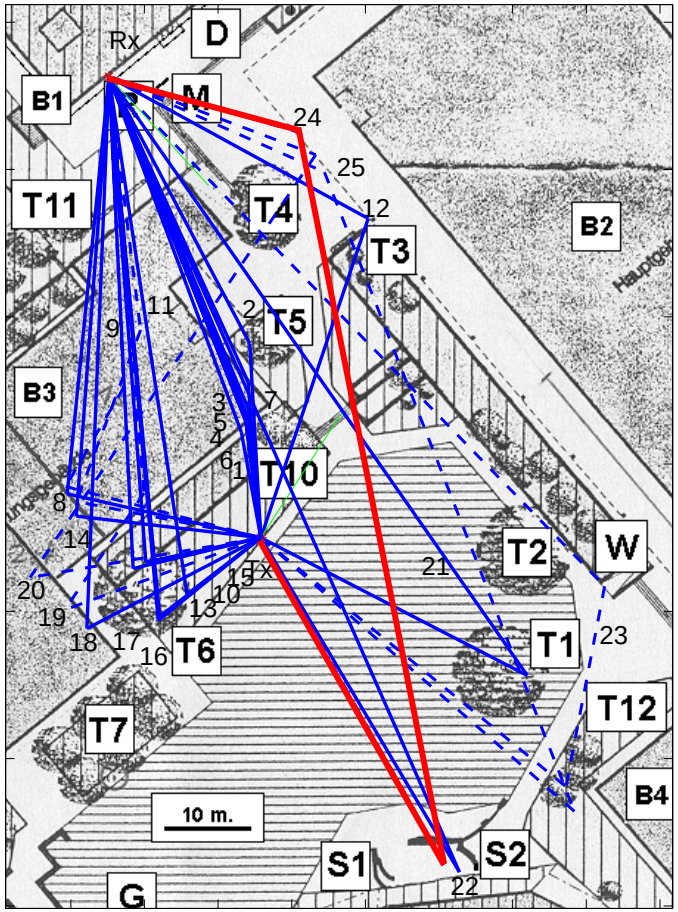

Mechanism identified by polarization properties

Estimated polarization:

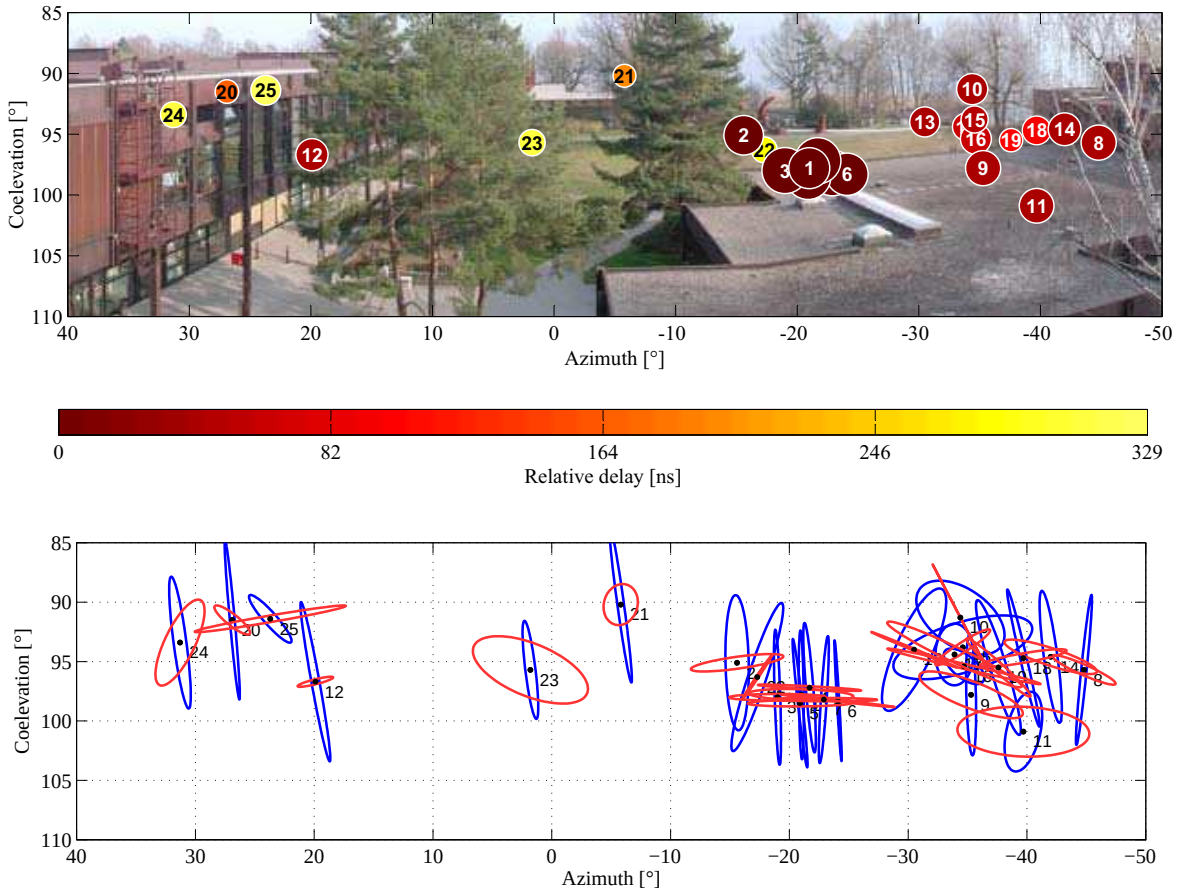

- Blue ellipses : polarization ellipses calculated using $\left[\hat{a}_{d,1,1} \quad \hat{a}_{d,2,1}\right]^{\mathrm{T}}$,
- Red ellipses : polarization ellipses calculated using $\left[\hat{a}_{d,1,2} \quad \hat{a}_{d,2,2}\right]^{\mathrm{T}}$.

Mechanism identified by polarization properties

Scatter plot of the estimated cross-polarization discrimination (XPD) of the individual paths:

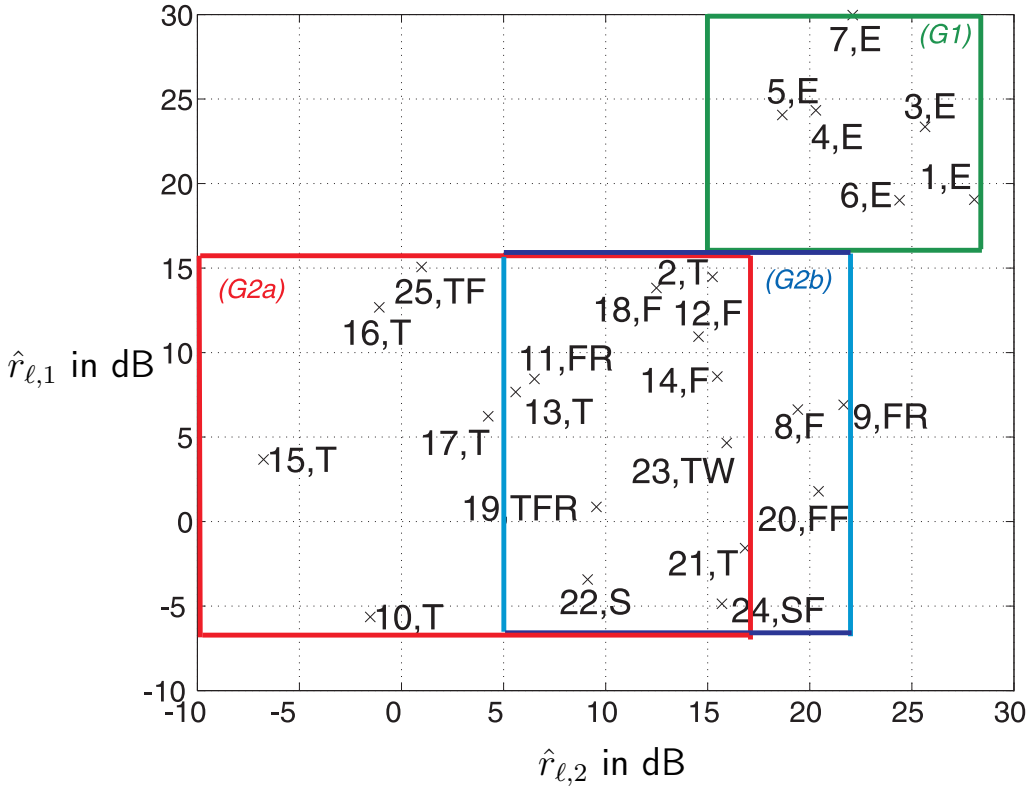

- $\hat{r}_{\ell,1} = \left|\hat{\alpha}_{\ell,1,1}/\hat{\alpha}_{\ell,2,1}\right|^2$ and $\hat{r}_{\ell,2} = \left|\hat{\alpha}_{\ell,2,2}/\hat{\alpha}_{\ell,1,2}\right|^2$
- The symbols denote the types of scatterers identified along the paths: facade (F), roof (R), edge (E) of buildings as well as tree (T), sculpture (S), and wall (W).

Mechanism identified by polarization properties

XPDs versus the interaction type:

Group	Interaction type/scatterers along the propagation path	XPDs in dB	
		$\hat{r}_{\ell,1}$	$\hat{r}_{\ell,2}$
1	Diffraction around the roof edge of B3	$[15, 28]$	$[16, 30]$
2a	Reflection/scattering by at least one tree	$[-10, 17]$	$[-6, 16]$
2b	Reflection/scattering only by man-made structures	$[5, 22]$	$[-6, 16]$

Modeling channels based on mechanism

- Modeling channel composition based on propagation mechanisms.
- Specular/reflected paths and the diffracted paths are identified.
- The former paths exhibit less path loss than the latter paths.

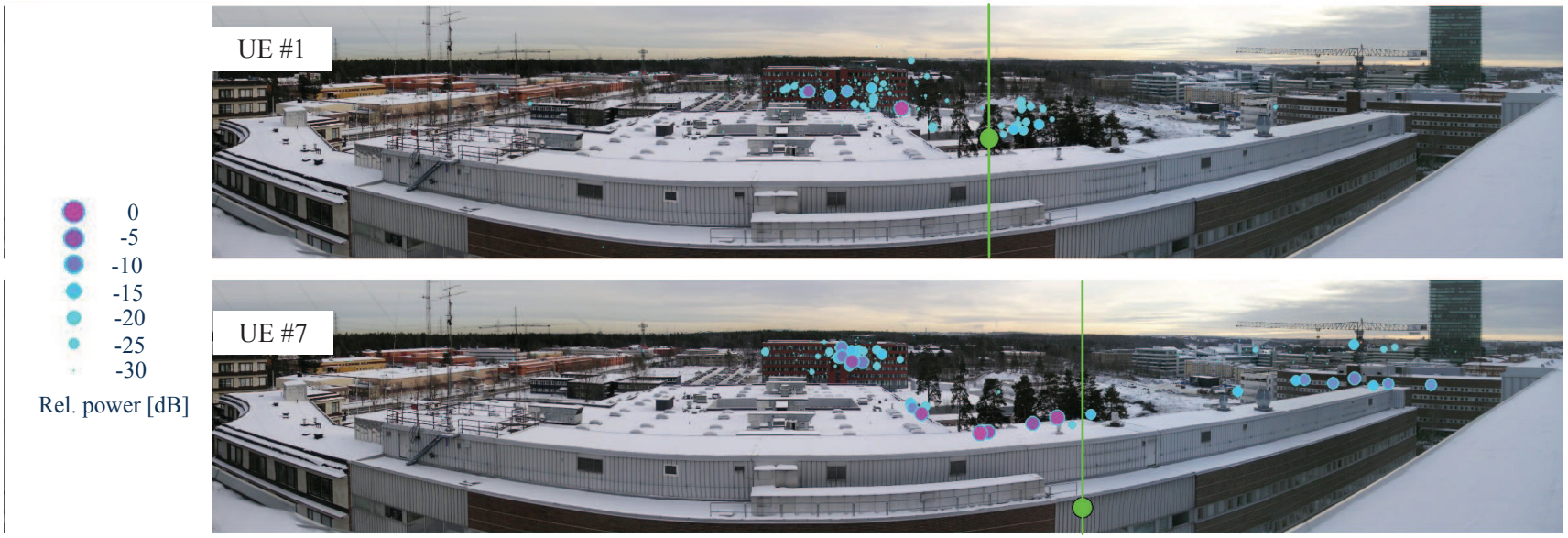

Figure 4. Estimated paths superimposed on a panoraic photograph taken from the BS location at the roof. The directions of the UE locations are indicated with green circles. It should be noted that the UEs are in NLOS conditions so that they are not visible from the BS.

Medbo, J.; Asplund, H.; Berg, J. E. & Jalden, N. Directional channel characteristics in elevation and azimuth at an urban macrocell base station Antennas and Propagation (EUCAP), 2012 6th European Conference on, 2012, 428-432

Modeling channels by mechanism [Medbo et al. 2012]

- Classification of paths as diffracted or specularly reflected done by means of the projected UE location h, which is obtained by extrapolating the estimated wave direction at the base station to the distance corresponding to the estimated delay.
- If h is on or near ground level, the wave is classified as specular
- If h is significantly above ground, e.g. more than half of the height of the closest obstructing building, then the path is classified as diffracted
- For this measurement the radio link at UE locations for which the excess loss is larger than 25 dB has a significant contribution from diffracted paths.

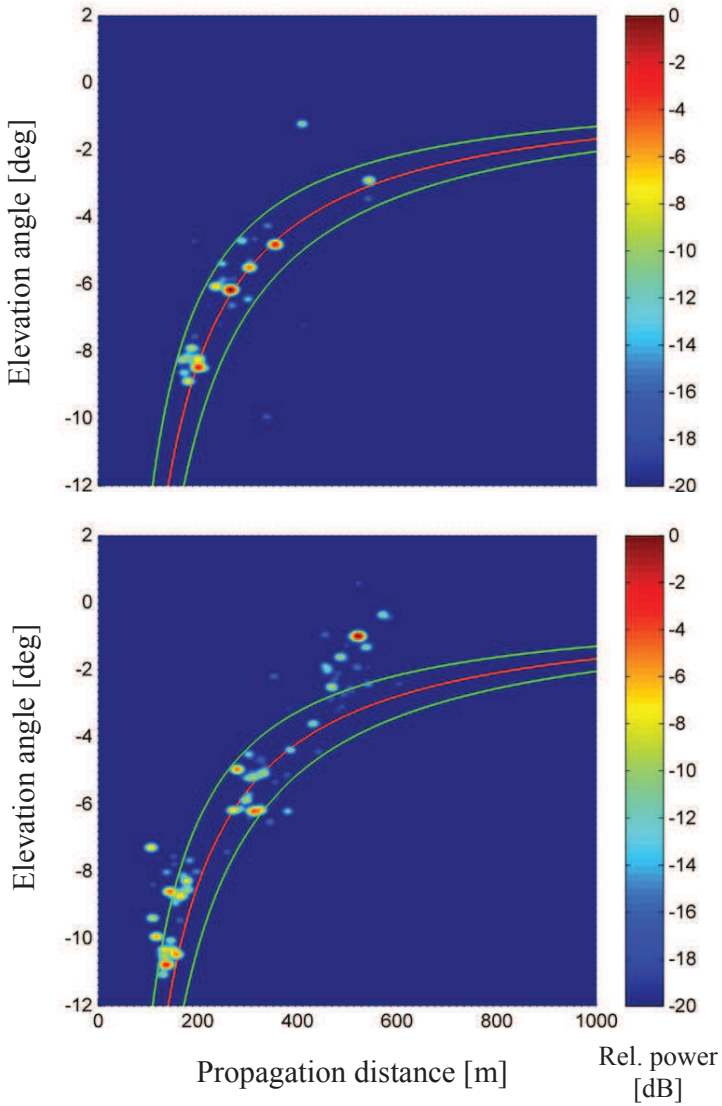

Figure 3. Power distributions in elevation angle and propagation distance for UE locations having excess loss less than 25 dB (upper) and higher than 25 dB (lower). Projected UE heights of -6.5, 0 and 6.5 m above ground are indicated with solid lines.

Chapter 3.2
Channel spread function

Diagram showing the dispersion of channel in multiple dimensions

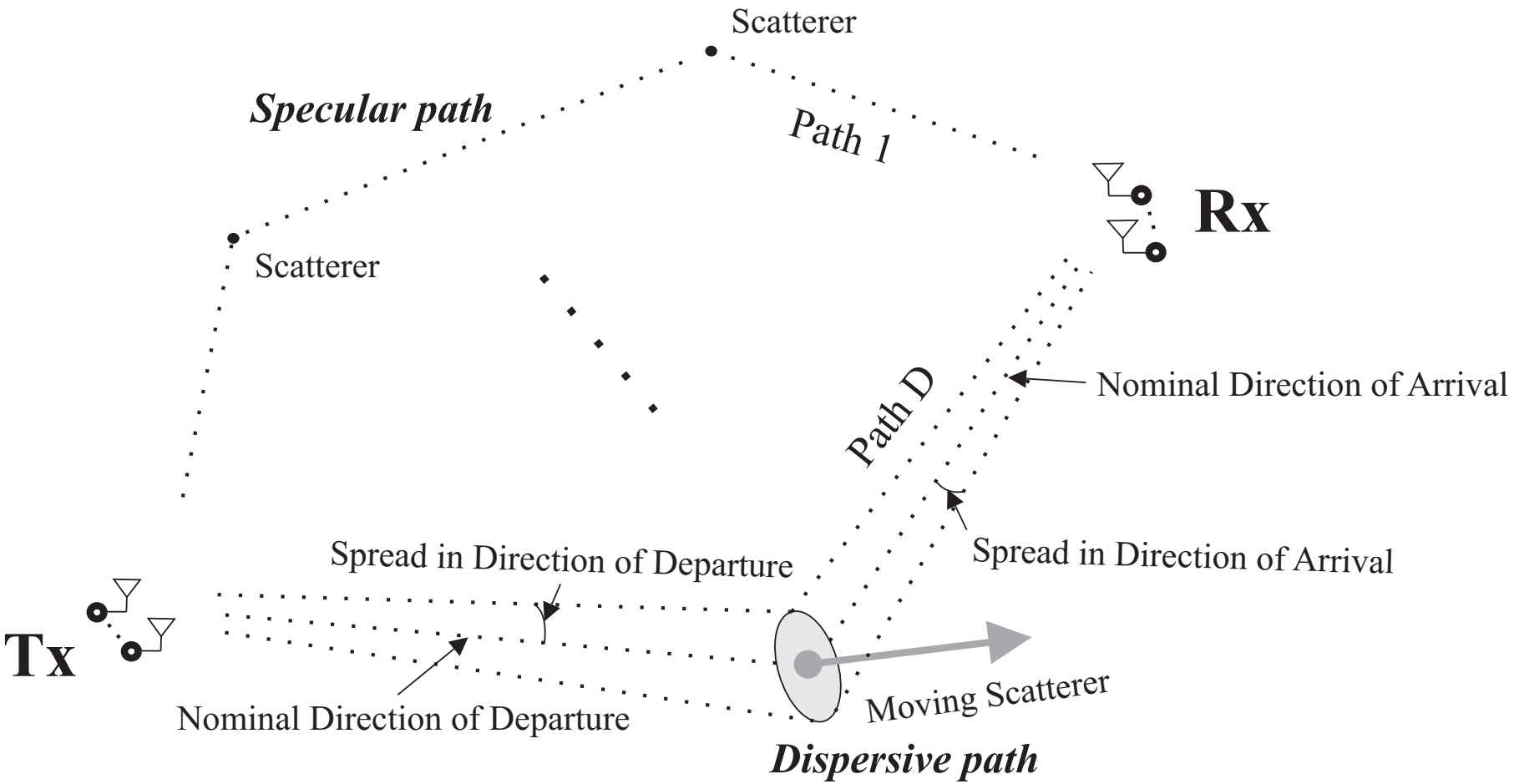

Signal model for received signal

In the case where L components are all specular path components, the output signal of the Rx antenna located at x_{Rx} while the Tx antenna located at x_{Tx} transmits signals can be written as

$$r(x_{\mathrm{Tx}}, x_{\mathrm{Rx}}; t) = \sum_{\ell=1}^{L} \alpha_\ell \exp\{j2\pi\lambda_0^{-1}(\mathbf{\Omega}_{\ell,\mathrm{Tx}} \cdot x_{\mathrm{Tx}})\} \exp\{j2\pi\lambda_0^{-1}(\mathbf{\Omega}_{\ell,\mathrm{Rx}} \cdot x_{\mathrm{Rx}})\} \exp\{j2\pi\nu_\ell t\} s(t-\tau_\ell). \quad (3)$$

where

- $s(t)$: the modulating signal at the input of the transmitter (Tx) antenna
- λ_0 : the wavelength.
- α_ℓ : complex amplitude
- τ_ℓ : delay
- $\mathbf{\Omega}_{\ell,\mathrm{Rx}}$: the incident direction
- $\mathbf{\Omega}_{\ell,\mathrm{Tx}}$: the departure direction
- ν_ℓ : the Doppler frequency

Direction of incidence characterized by Ω

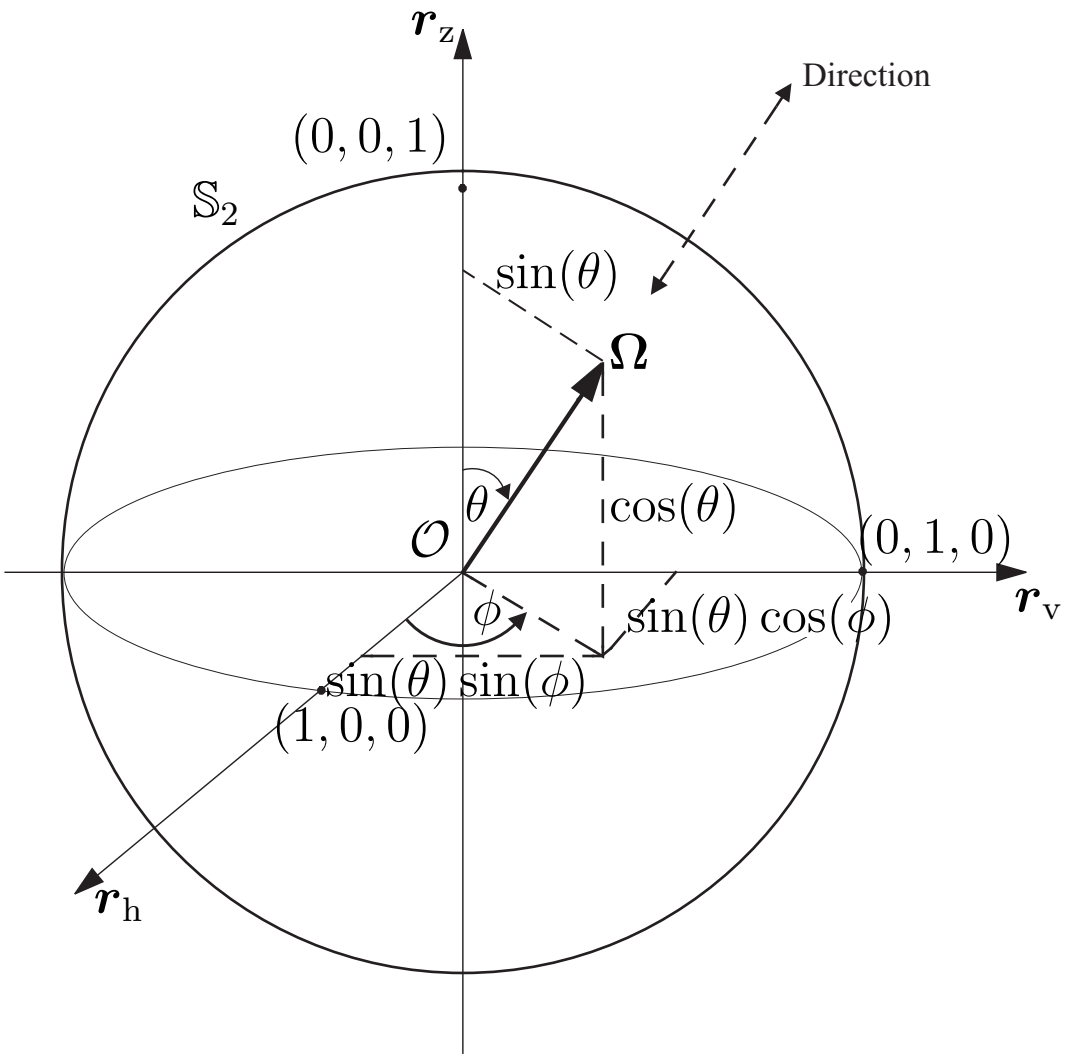

$$\boldsymbol{\Omega}_{\mathrm{Tx}} = \boldsymbol{e}(\phi_{\mathrm{Tx}}, \theta_{\mathrm{Tx}}) \doteq [\cos(\phi_{\mathrm{Tx}})\sin(\theta_{\mathrm{Tx}}), \sin(\phi_{\mathrm{Tx}})\sin(\theta_{\mathrm{Tx}}), \cos(\theta_{\mathrm{Tx}})]^{\mathrm{T}} \in \mathbb{S}_2$$

Bidirection-delay-Doppler spread function

$$r(x_{\mathrm{Tx}}, x_{\mathrm{Rx}}; t) = \int\int\int\int \exp\{j2\pi\lambda_0^{-1}(\mathbf{\Omega}_{\mathrm{Tx}} \cdot x_{\mathrm{Tx}})\} \exp\{j2\pi\lambda_0^{-1}(\mathbf{\Omega}_{\mathrm{Rx}} \cdot x_{\mathrm{Rx}})\} \exp\{j2\pi\nu t\} s(t-\tau) h(\mathbf{\Omega}_{\mathrm{Tx}}, \mathbf{\Omega}_{\mathrm{Rx}}, \tau, \nu) \mathrm{d}\mathbf{\Omega}_{\mathrm{Tx}} \mathrm{d}\mathbf{\Omega}_{\mathrm{Rx}} \mathrm{d}\tau \mathrm{d}\nu. \quad (4)$$

where

$$h(\mathbf{\Omega}_{\mathrm{Tx}}, \mathbf{\Omega}_{\mathrm{Rx}}, \tau, \nu) = \sum_{\ell=1}^{L} \alpha_\ell \delta(\mathbf{\Omega}_{\mathrm{Tx}} - \mathbf{\Omega}_{\mathrm{Tx},\ell}) \delta(\mathbf{\Omega}_{\mathrm{Rx}} - \mathbf{\Omega}_{\mathrm{Rx},\ell}) \delta(\tau - \tau_\ell) \delta(\nu - \nu_\ell). \quad (5)$$

is called spread function.

Property of the spread function

The expectation of the spread function is 0, i.e.

$$\mathrm{E}[h(\mathbf{\Omega}_{\mathrm{Tx}}, \mathbf{\Omega}_{\mathrm{Rx}}, \tau, \nu)] = 0. \tag{6}$$

Under the US assumption:

$$\begin{aligned}\mathrm{E}[h(\mathbf{\Omega}_{\mathrm{Tx}},&\mathbf{\Omega}_{\mathrm{Rx}}, \tau, \nu)h(\mathbf{\Omega}'_{\mathrm{Tx}}, \mathbf{\Omega}'_{\mathrm{Rx}}, \tau', \nu')] = P(\mathbf{\Omega}_{\mathrm{Tx}}, \mathbf{\Omega}_{\mathrm{Rx}}, \tau, \nu) \\ &\delta(\mathbf{\Omega}_{\mathrm{Tx}} - \mathbf{\Omega}'_{\mathrm{Tx}})\delta(\mathbf{\Omega}_{\mathrm{Rx}} - \mathbf{\Omega}'_{\mathrm{Rx}})\delta(\tau - \tau')\delta(\nu - \nu')\end{aligned} \tag{7}$$

where

$$P(\mathbf{\Omega}_{\mathrm{Tx}}, \mathbf{\Omega}_{\mathrm{Rx}}, \tau, \nu) = \mathrm{E}[|h(\mathbf{\Omega}_{\mathrm{Tx}}, \mathbf{\Omega}_{\mathrm{Rx}}, \tau, \nu)|^2] \tag{8}$$

is called the bidirection-delay-Doppler power spectrum

Experimental examples

Power spectrum of direction of departure $\tau = 60$ ns

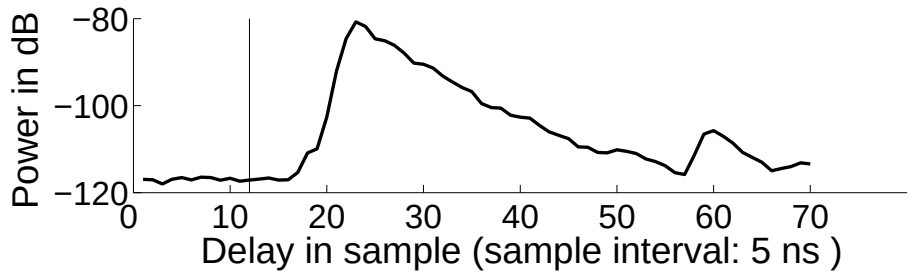

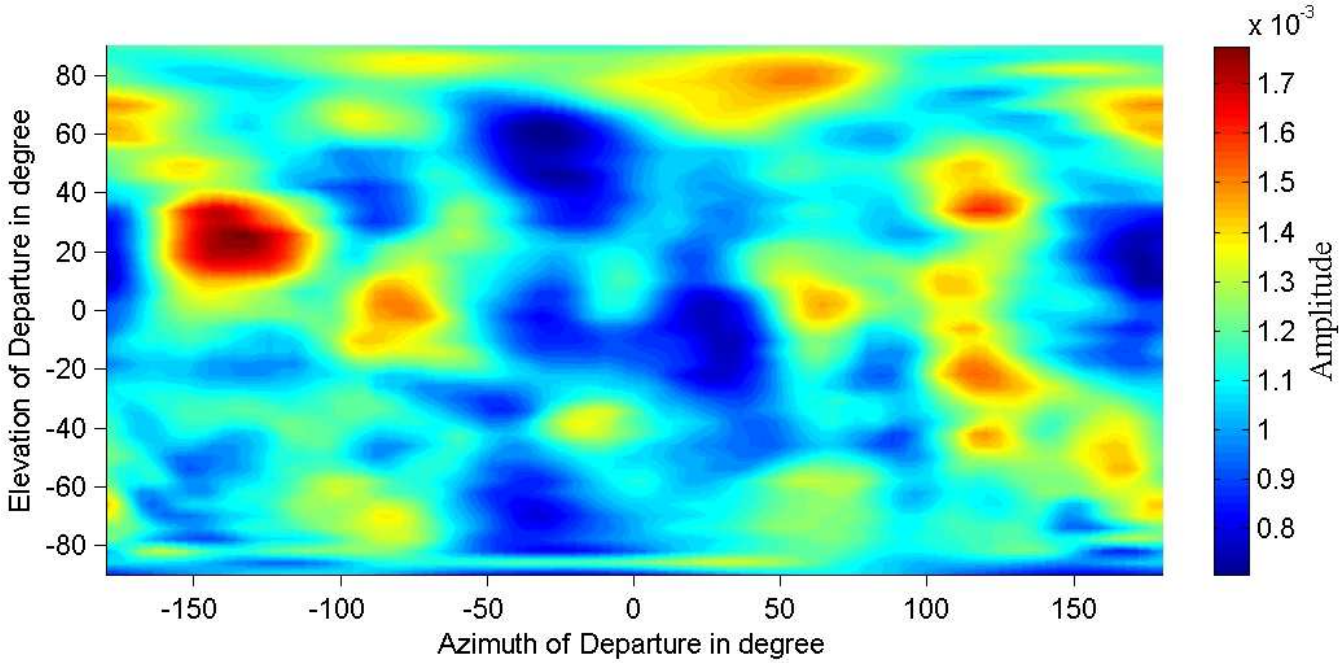

Experimental examples

Power spectrum of direction of departure $\tau = 115$ ns

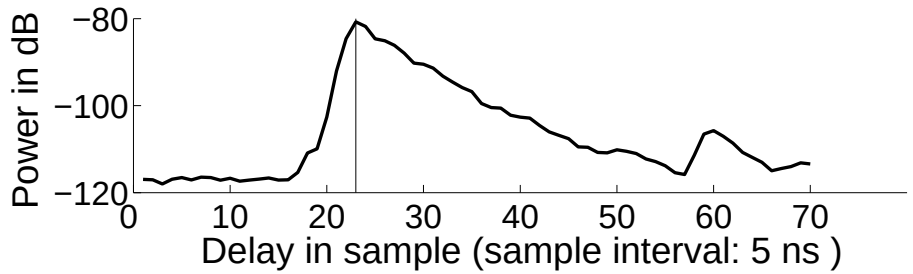

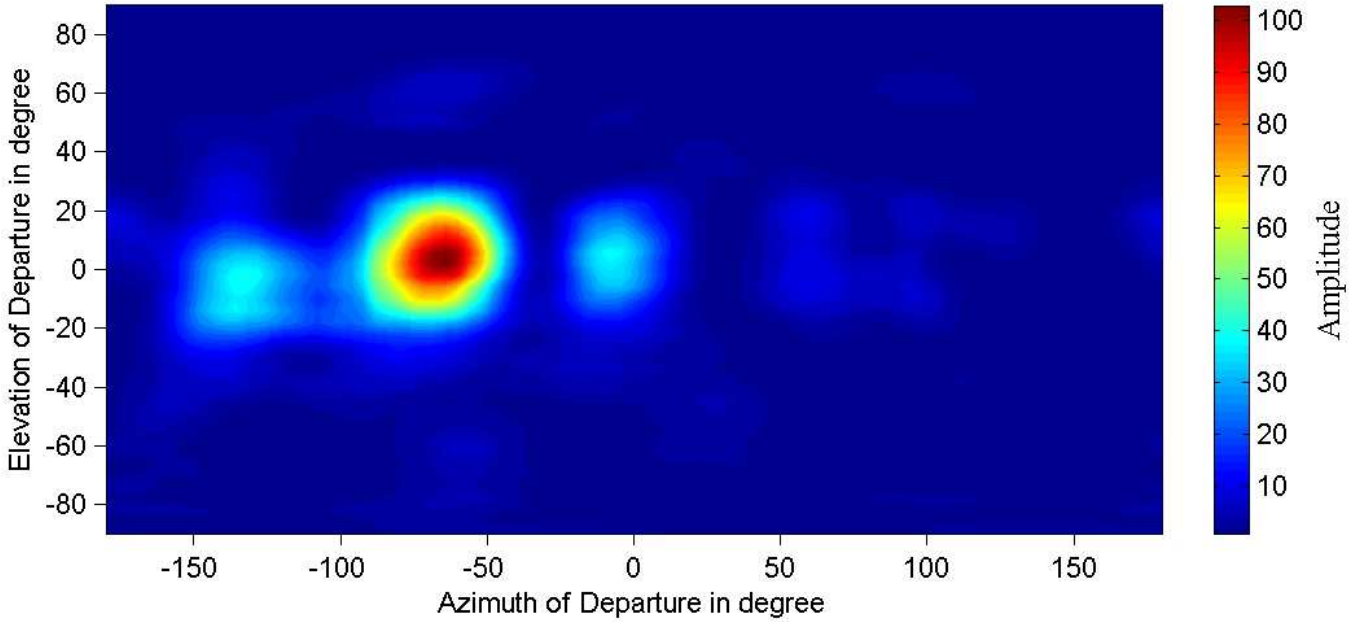

Experimental examples

Power spectrum of direction of departure $\tau = 145$ ns

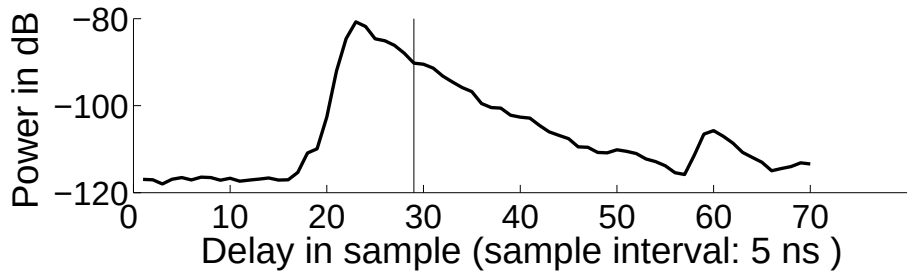

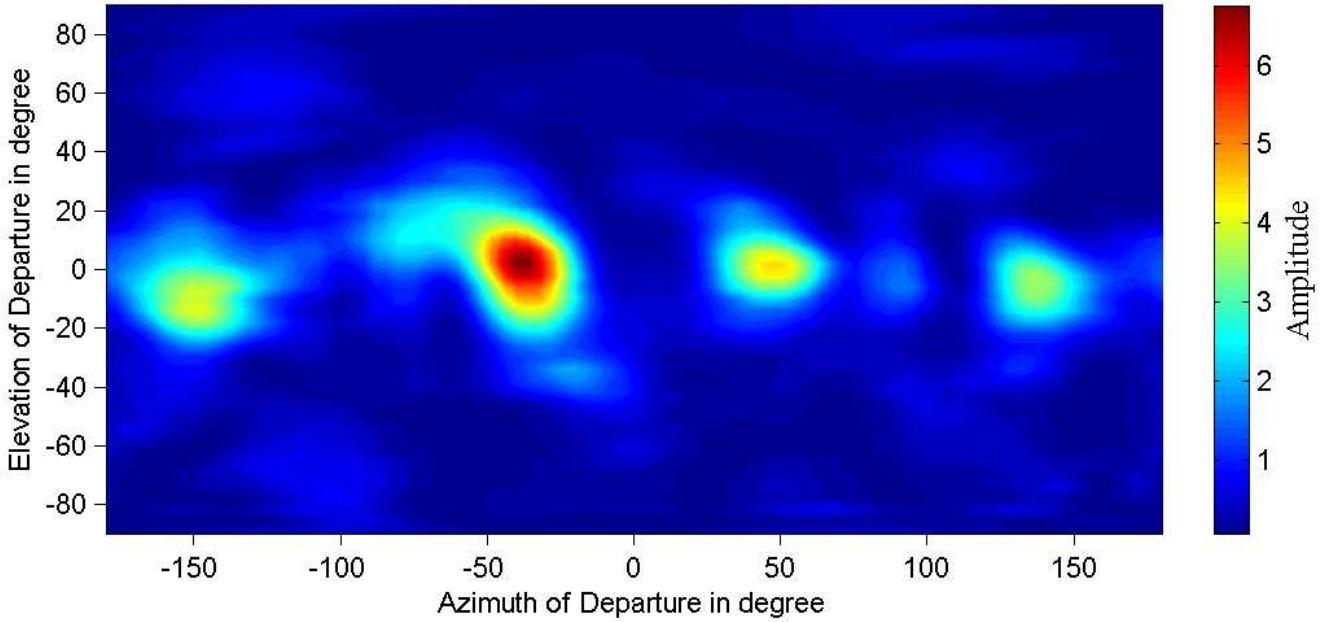

Experimental examples

Power spectrum of direction of departure $\tau = 300$ ns

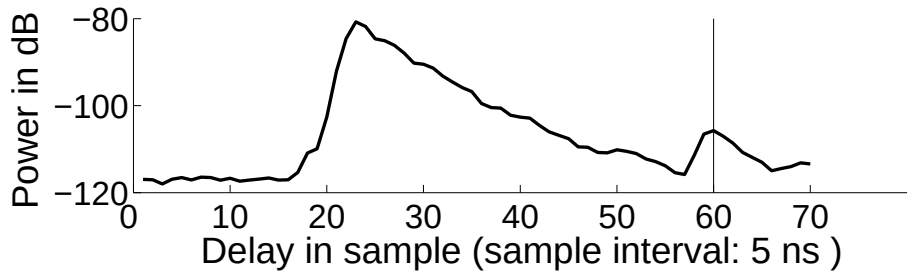

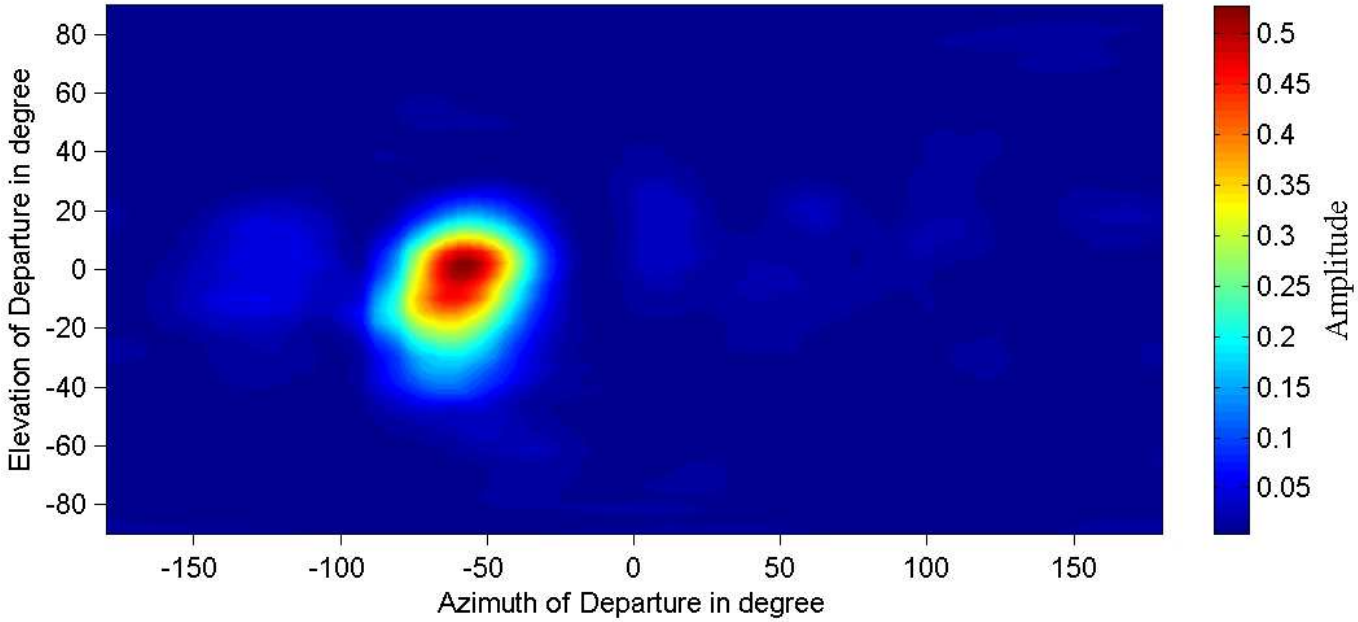

Bidirection spread function

The spread function and the power spectrum of the channel in single dimensions can be calculated by computing the marginal of the multi-dimensional spread function and power spectrum respectively.

$$h(\mathbf{\Omega}_{\mathrm{Tx}}, \mathbf{\Omega}_{\mathrm{Rx}}) = \int \int h(\mathbf{\Omega}_{\mathrm{Tx}}, \mathbf{\Omega}_{\mathrm{Rx}}, \tau, \nu) \mathrm{d}\tau \mathrm{d}\nu. \tag{9}$$

Similarly, the bidirection power spectrum is calculated as

$$P(\mathbf{\Omega}_{\mathrm{Tx}}, \mathbf{\Omega}_{\mathrm{Rx}}) = \int \int P(\mathbf{\Omega}_{\mathrm{Tx}}, \mathbf{\Omega}_{\mathrm{Rx}}, \tau, \nu) \mathrm{d}\tau \mathrm{d}\nu. \tag{10}$$

Chapter 3.3
Specular path model

Scope considered

- Assumption: the electromagnetic waves are considered to propagate along multiple specular paths.
- For parameter estimation, the parameters describing a path may include its delay, direction of arrival (i.e. azimuth and elevation of arrival), direction of departure (i.e. azimuth and elevation of arrival), Doppler frequency and polarization matrix.
- Other parameters may be also included, e.g. the time-variability of these parameters in the time-variant case.
- The bidirection-delay-Doppler-Dual-polarization specular path-model is introduced

Dual polarization

- Dual polarization is specifically considered as the polarization of an electromagnetic wave, especially for the TEM waves, can be projected into two orthogonal directions
- More samples of the channel observation can be obtained to improve the estimation accuracy of the path parameters compared with the signal-polarization
- Since using dual polarized antenna array for boosting the capacity of MIMO system has been considered in advanced wireless communication standards, modeling the channels in the dual-polarization domain becomes popular.
- Therefore, it is necessary to design estimation algorithms for extracting the polarization characteristics of the propagation channel.

Diagram of Dual polarization channel

Contribution of the ℓth wave to the received signal in a MIMO system incorporating dual-antenna arrays

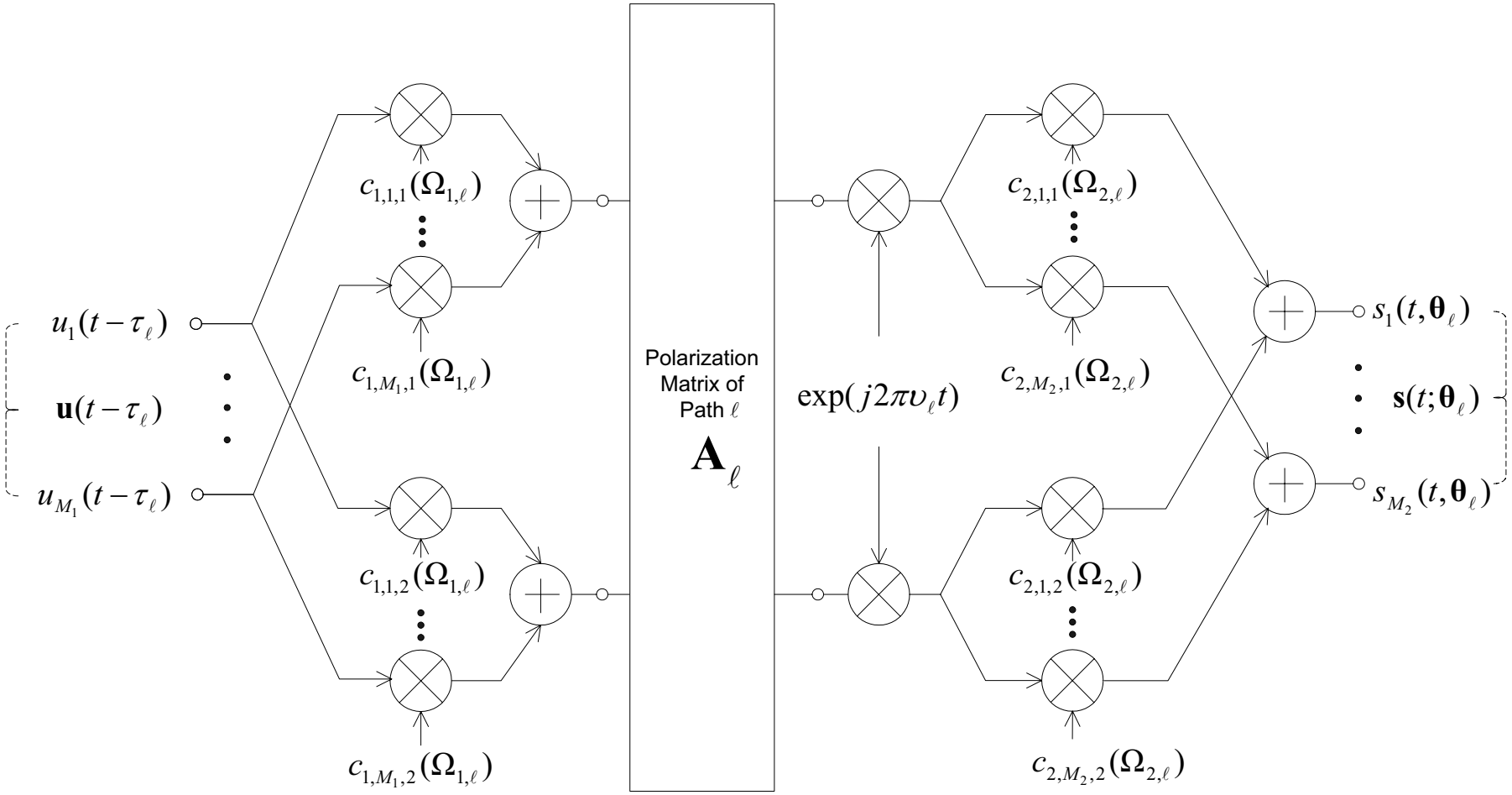

Considerations

- Rx and Tx antenna arrays with dual-polarized antenna configuration considered.
- Each of the dual antenna transmits/receives signal within two polarizations at the same time. This assumption is based on the realistic experience that antennas can not transmit or receive signals in one polarization only.
- To differentiate the two polarizations in the underlying model, one of them is called main polarization, specifying the dominant direction of the signal field pattern. The other is correspondingly referred to the complementary polarization.

Polarization matrix and signal model

- Polarization matrix $\boldsymbol{A}_\ell = \begin{bmatrix} \alpha_{\ell,1,1} & \alpha_{\ell,1,2} \\ \alpha_{\ell,2,1} & \alpha_{\ell,2,2} \end{bmatrix}$ is composed of the complex weights for the attenuations along the propagation paths.
- The signal model describing the contribution of the ℓth wave to the output of the MIMO system reads

$$\boldsymbol{s}(t;\boldsymbol{\theta}_\ell) = \exp(j2\pi\nu_\ell t) \begin{bmatrix} \boldsymbol{c}_{2,1}(\boldsymbol{\Omega}_{2,\ell}) & \boldsymbol{c}_{2,2}(\boldsymbol{\Omega}_{2,\ell}) \end{bmatrix} \boldsymbol{A}_\ell \begin{bmatrix} \boldsymbol{c}_{1,1}(\boldsymbol{\Omega}_{1,\ell}) & \boldsymbol{c}_{1,2}(\boldsymbol{\Omega}_{1,\ell}) \end{bmatrix}^T \boldsymbol{u}(t-\tau_\ell),$$

where

  - $\boldsymbol{c}_{i,p_i}(\boldsymbol{\Omega})$: the steering vector of the transmitter array $(i=1)$ with totally M_1 entries or receiver array $(i=2)$ with totally M_2 entries,
  - M_1 and M_2 are the amount of antennas in the Tx and Rx respectively
  - $p_i, (p_i = 1, 2)$ denotes the polarization inde

Signal model written in matrix form

$$\boldsymbol{s}(t;\boldsymbol{\theta}_\ell) = \exp(j2\pi\nu_\ell t)\boldsymbol{C}_2(\boldsymbol{\Omega}_{2,\ell})\boldsymbol{A}_\ell\boldsymbol{C}_1^{\mathrm{T}}(\boldsymbol{\Omega}_{1,\ell})\boldsymbol{u}(t-\tau_\ell),$$

with

- $\boldsymbol{C}_2(\boldsymbol{\Omega}_{2,\ell}) = \begin{bmatrix}\boldsymbol{c}_{2,1}(\boldsymbol{\Omega}_{2,\ell}) & \boldsymbol{c}_{2,2}(\boldsymbol{\Omega}_{2,\ell})\end{bmatrix}$
- $\boldsymbol{C}_1(\boldsymbol{\Omega}_{1,\ell}) = \begin{bmatrix}\boldsymbol{c}_{1,1}(\boldsymbol{\Omega}_{1,\ell}) & \boldsymbol{c}_{1,2}(\boldsymbol{\Omega}_{1,\ell})\end{bmatrix}$
- $\boldsymbol{u}(t) = [u_1(t), \ldots, u_M(t)]^T$.

$\boldsymbol{s}(t;\boldsymbol{\theta}_\ell)$ can be recast as:

$$\begin{aligned}\boldsymbol{s}(t;\boldsymbol{\theta}_\ell) =& \exp(j2\pi\nu_\ell t)\cdot \\ & \Big\{\Big[\alpha_{\ell,1,1}\boldsymbol{c}_{2,1}(\boldsymbol{\Omega}_{2,\ell})\boldsymbol{c}_{1,1}^{\mathrm{T}}(\boldsymbol{\Omega}_{1,\ell}) + \alpha_{\ell,1,2}\boldsymbol{c}_{2,1}(\boldsymbol{\Omega}_{2,\ell})\boldsymbol{c}_{1,2}^{\mathrm{T}}(\boldsymbol{\Omega}_{1,\ell}) \\ & + \alpha_{\ell,2,1}\boldsymbol{c}_{2,2}(\boldsymbol{\Omega}_{2,\ell})\boldsymbol{c}_{1,1}^{\mathrm{T}}(\boldsymbol{\Omega}_{1,\ell}) + \alpha_{\ell,2,2}\boldsymbol{c}_{2,2}(\boldsymbol{\Omega}_{2,\ell})\boldsymbol{c}_{1,2}^{\mathrm{T}}(\boldsymbol{\Omega}_{1,\ell})\Big]\boldsymbol{u}(t-\tau_\ell)\Big\} \\ =& \exp(j2\pi\nu_\ell t)\cdot\left(\sum_{p_2=1}^{2}\sum_{p_1=1}^{2}\alpha_{\ell,p_2,p_1}\boldsymbol{c}_{2,p_2}(\boldsymbol{\Omega}_{2,\ell})\boldsymbol{c}_{1,p_1}^{T}(\boldsymbol{\Omega}_{1,\ell})\right)\boldsymbol{u}(t-\tau_\ell).\end{aligned}$$

3.3.1 Model for time-division-multiplexing channel sounding

- Channel sounding by using multiple Tx and Rx antennas can be conducted by using RF-switch which connects single Tx antenna with the transmit front-end chain, or Rx antenna with the receiver front-end chain sequentially.
- We call this kind of sounding technique as time-division-multiplexing (TDM) sounding technique.
- Examples of the measurement equipments using the TDM sounding systems are the PROPsound, RUSK, and rBECS.

Timing structure of sounding and sounding window

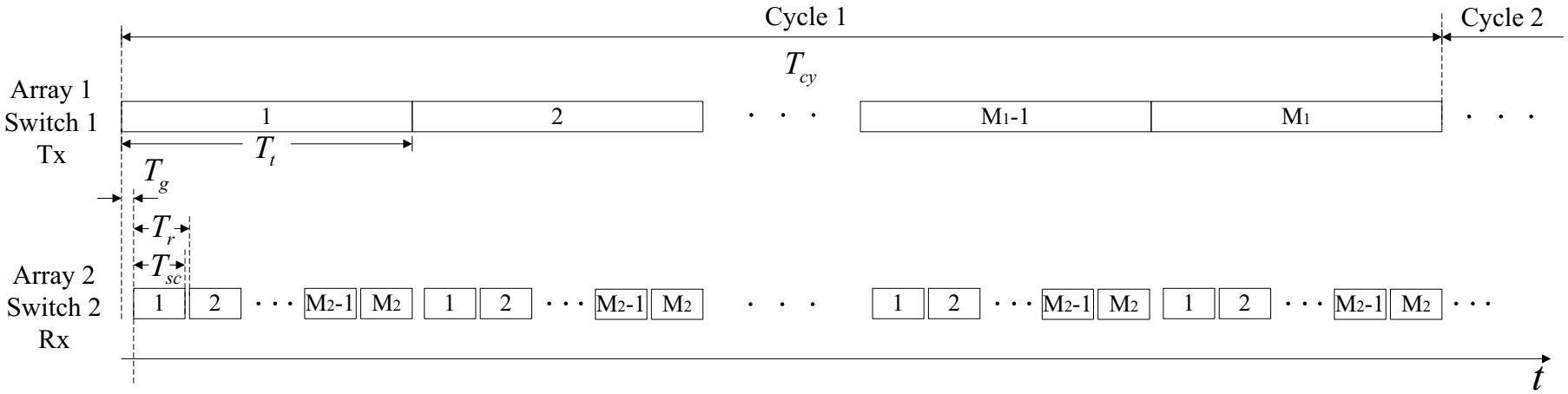

The m_1th antenna element of Array 1 is active during the sounding windows

$$q_{1,m_1}(t) \quad = \quad \sum_{i=1}^{I} q_{T_t}(t - t_{i,m_1} + T_g), \quad m_1 = 1, ..., M_1,$$

where

- i : the cycle index and $t_{i,m_1} = (i-1)T_{cy} + (m_1 - 1)T_t$.
- $q_{1,m_1}(t)$: a real function, with value of 1 or 0 corresponding to the active or inactive moments of the m_1th window.
- Sounding window vector: $\boldsymbol{q}_1(t) \doteq [q_{1,1}(t), ..., q_{1,M_1}(t)]^T$.

Sensing windows

- Sensing window

$$q_{T_{\mathrm{sc}}}(t - t_{i,m_1,m_2}), \quad m_2 = 1, \ldots, M_2, \;\; m_1 = 1, \ldots, M_1$$

corresponds to the case where

- The m_1th Tx antenna is active;
- The m_2th Rx antenna is sensing,

where

$$t_{i,m_2,m_1} = (i-1)T_{cy} + (m_1 - 1)T_t + (m_2 - 1)T_r.$$

The sensing window for the m_2th Rx dual antenna is given by the real function

$$q_{1,m_2}(t) \;\; = \;\; \sum_{i}^{I} \sum_{m_1=1}^{M_1} q_{T_{\mathrm{sc}}}(t - t_{i,m_2,m_1}).$$

Sensing windows

Define the sensing window vector

$$\boldsymbol{q}_2(t) \doteq [q_{2,1}(t), ..., q_{2,M_2}(t)]^T.$$

as well as

$$q_2(t) = \sum_{i=1}^{I} \sum_{m_2=1}^{M_2} \sum_{m_1=1}^{M_1} q_{T_{\mathrm{sc}}}(t - t_{i,m_2,m_1}).$$

3.3.2 Transmitted signal

Making use of the sounding window vector $\boldsymbol{q}_1(t)$, we have the explicit transmitted signal $\boldsymbol{u}(t)$ by concatenating the inputs of the M_1 elements of Array 1

$$\boldsymbol{u}(t) = \boldsymbol{q}_1(t)u(t).$$

3.3.3 Received signal

The signal at the output of Switch 2 can be written as

$$Y(t) = \sum_{\ell=1}^{L} \boldsymbol{s}(t;\boldsymbol{\theta}_\ell) + \sqrt{\frac{N_o}{2}} q_2(t) W(t),$$

with

$$\begin{aligned}
\boldsymbol{s}(t;\boldsymbol{\theta}_\ell) &= \exp(j2\pi\nu_\ell t)\boldsymbol{q}_2^{\mathrm{T}}(t)\boldsymbol{C}_2(\boldsymbol{\Omega}_{2,\ell})\boldsymbol{A}_\ell\boldsymbol{C}_1(\boldsymbol{\Omega}_{1,\ell})^{\mathrm{T}}\boldsymbol{q}_1(t-\tau_\ell)u(t-\tau_\ell) \\
&= \exp(j2\pi\nu_\ell t)\cdot\sum_{p_2=1}^{2}\sum_{p_1=1}^{2}\alpha_{\ell,p_2,p_1}\boldsymbol{q}_2^{\mathrm{T}}(t)\boldsymbol{c}_{2,p_2}(\boldsymbol{\Omega}_{2,\ell})\boldsymbol{c}_{1,p_1}^{\mathrm{T}}(\boldsymbol{\Omega}_{1,\ell})\boldsymbol{q}_1(t) \\
&\quad \cdot u(t-\tau_\ell).
\end{aligned}$$

3.3.3 Received signal

Define the $M_2 \times M_1$ sounding matrices

$$\boldsymbol{U}(t;\tau_\ell) = \boldsymbol{q}_2(t)\boldsymbol{q}_1(t)^{\mathrm{T}} u(t-\tau_\ell).$$

With this definition, $s(t;\boldsymbol{\theta}_\ell)$ can be further written as

$$s(t;\boldsymbol{\theta}_\ell) \quad = \quad \exp(j2\pi\nu_\ell t) \sum_{p_2=1}^{2} \sum_{p_1=1}^{2} \alpha_{\ell,p_2,p_1} \boldsymbol{c}_{2,p_2}^{\mathrm{T}}(\boldsymbol{\Omega}_{2,\ell}) \boldsymbol{U}(t;\tau_\ell) \boldsymbol{c}_{1,p_1}(\boldsymbol{\Omega}_{1,\ell}).$$

We can also express $s(t;\boldsymbol{\theta}_\ell)$ as

$$s(t;\boldsymbol{\theta}_\ell) = \sum_{p_2=1}^{2} \sum_{p_1=1}^{2} s_{p_2,p_1}(t;\boldsymbol{\theta}_\ell),$$

where

$$s_{p_2,p_1}(t;\boldsymbol{\theta}_\ell) \doteq \alpha_{\ell,p_2,p_1} \exp(j2\pi\nu_\ell t) \boldsymbol{c}_{2,p_2}^{\mathrm{T}}(\boldsymbol{\Omega}_{2,\ell}) \boldsymbol{U}(t;\tau_\ell) \boldsymbol{c}_{1,p_1}(\boldsymbol{\Omega}_{1,\ell})$$

Chapter 3.4
Dispersive-path model

Motivation

- Unrealistic US assumption adopted: the parameters of paths have differences larger than the intrinsic resolutions of the measurement equipment, therefore they can be well separated.
- Based on the US assumption, these paths are supposed to be uncorrelated/resolvable.
- In real situation, the propagation paths could be correlated/nonresolvable.
- The mismatch between the non-correlated single-wave model and the reality of correlation leads to the poor performance of the SAGE algorithm.
- Another issue is that the number of paths is large, which corresponds to the diffuse scattering scenario, the computational complexity becomes prohibitive for practical implementation.
- It is therefore necessary to find an appropriate solution for this special case.

Diffuse scattering cluster estimation

- Or slightly spatially distributed source estimation
- Two classes of estimation methods proposed historically:
  1) Find approximate models for the slightly distributed sources, such as the first order Taylor expansion approximation model [Tan,Beach,Nix,2003] and a two-ray model proposed by [Bengtsson, 2000];
  2) Find high-resolution estimators for estimating the slightly distributed sources, such as DSPE [Valaee, 1995], DISPARE [Meng,Stoica,Wong,1996] and [Trump, Ottersten, 1996], and spread root-MUSIC, ESPRIT, MODE [Bengtsson, 2000]
- These high-resolution estimators are derived more or less by employing subspace fitting techniques or covariance matrix fitting techniques.
- It is necessary to extend the SAGE algorithm for estimating diffuse scattering cluster.

3.4.2 Original model of slightly distributed sources

The contribution of multiple slightly distributed sources to the received signal at the output of the mth Rx antenna array can be modelled as

$$s_m(\boldsymbol{\theta}) = \sum_{c=1}^{C} \sum_{\ell=1}^{L_c} \gamma_{c,\ell} \cdot c_m(\theta_{c,\ell}), \quad \text{where}$$

- C is the number of clusters,
- L_c is the number of multipaths in cth cluster,
- m is the data index in the frequency and spatial domain,
- $\boldsymbol{\theta}$ is a parameter vector containing all the unknown parameters in the model,
- $\gamma_{c,\ell}$ is the path weight of the ℓth path in cth cluster,
- $c_m(\theta_{c,\ell})$ denotes the response which has the expression as $c_m(\theta_{c,\ell}) \doteq e^{-j2\pi(m-1)(\Delta s/\lambda)\sin(\theta_{c,\ell})}$. Here
  - Δs is the array element spacing, λ is the carrier wavelength.
  - $\theta_{c,\ell}$ is the direction-of-arrival (DoA) of the ℓth path in cth cluster

Assumptions

- Phases of $\gamma_{c,\ell}$ are independent random variables uniformly distributed on $[-\pi, \pi]$, and $\gamma_{c,\ell}$ are random variables
- Deviation of the direction of arrival, calculated as $\tilde{\theta}_{c,\ell} = \theta_{c,\ell} - \theta_c$ with θ_c denoting the nominal direction of arrival of all rays, are assumed to be random variables, following approximately Gaussian distribution $\mathcal{N} \sim (0, \sigma_\theta^2)$.

One cluster scenario with the contribution of the cth cluster written as

$$s_m(\boldsymbol{\theta}_c) = \sum_{\ell=1}^{L_c} \gamma_{c,\ell} \cdot c_m(\theta_{c,\ell})$$

For unitary $u(t)$, the received signal is described as

$$x_m = s_m(\boldsymbol{\theta}_c) + w_m = \sum_{\ell=1}^{L_c} \gamma_{c,\ell} \cdot c_m(\theta_{c,\ell}) + w_m$$

where w is complex circularly symmetric additive white Gaussian noise with variance of σ_w^2.

First-order Taylor expansion model I

- The first order Taylor expansion with respect to the spread of the parameter is

$$a(\phi_o + \tilde{\phi}) \approx a(\phi_o) + \tilde{\phi}\frac{\partial a(\phi_o)}{\partial \phi_o},$$

  where ϕ_o represents the nominal value and $\tilde{\phi}$ denotes the spread.
- Applying this principle, we obtain an approximation model for slightly distributed sources as

$$\begin{aligned} s_m(\boldsymbol{\theta}_c) &= \sum_{\ell=1}^{L_c} \gamma_{c,\ell} \cdot c_m(\theta_{c,\ell}) = \sum_{\ell=1}^{L_c} \gamma_{c,\ell} \cdot c_m(\theta_c + \tilde{\theta}_{c,\ell}) \\ &\approx \sum_{\ell=1}^{L_c} \gamma_{c,\ell} \cdot c_m(\theta_c) + \sum_{\ell=1}^{L_c} \gamma_{c,\ell} \cdot \tilde{\theta}_{c,\ell} \cdot \frac{\partial c_m(\theta_c)}{\partial \theta_c}, \end{aligned}$$

  where θ_c is the nominal direction of arrival and $\tilde{\theta}_{c,\ell}$ is the angle spread of the ℓth wave in the cth distributed source.

First-order Taylor expansion model I (Conti.)

- Introducing parameters

$$\gamma_c = \sum_{\ell=1}^{L_c} \gamma_{c,\ell}, \quad \psi_c = \sum_{\ell=1}^{L_c} \gamma_{c,\ell} \cdot \tilde{\theta}_{c,\ell}, \quad \text{and}$$

- noticing that when the field pattern of the antenna elements is assumed to be isotropic, the steering vector and its derivative can be written as

$$\begin{aligned} c_m(\theta_c) &= e^{-j2\pi(m-1)(\Delta s/\lambda)\sin(\theta_c)}, \\ \frac{\partial c_m(\theta_c)}{\partial \theta_c} &= (-j2\pi(m-1)(\Delta s/\lambda)\cos(\theta_c)) \\ &\quad \cdot e^{-j2\pi(m-1)(\Delta s/\lambda)\sin(\theta_c)}. \end{aligned} \tag{11}$$

First-order Taylor expansion model I (Conti.)

- So Equation (11) can be written to be

$$s_m(\boldsymbol{\theta}_c) \approx \gamma_c \cdot e^{-j2\pi(m-1)(\Delta s/\lambda)\sin(\theta_c)} - \psi_c \cdot j2\pi(m-1) \cdot(\Delta s/\lambda)\cos(\theta_c))e^{-j2\pi(m-1)(\Delta s/\lambda)\sin(\theta_c)}.$$

- Written in matrix notation $\boldsymbol{s}(\boldsymbol{\theta}_c)$ is

$$\boldsymbol{s}(\boldsymbol{\theta}_c) = \boldsymbol{D}(\bar{\boldsymbol{\theta}}_c)\boldsymbol{\beta}_c, \quad \text{where} \tag{12}$$

  - $\bar{\boldsymbol{\theta}}_c \doteq [\theta_c]$,
  - $\boldsymbol{\beta}_c$ is a column vector $\boldsymbol{\beta}_c \doteq [\gamma_c, \psi_c]^T$, and
  - $\boldsymbol{D}(\bar{\boldsymbol{\theta}}_c)$ is $2 \times M$ matrix defined as follows

$$\boldsymbol{D}(\bar{\boldsymbol{\theta}}_c) \doteq [\boldsymbol{a}(\bar{\boldsymbol{\theta}}_c)\ \boldsymbol{b}(\bar{\boldsymbol{\theta}}_c)], \quad \text{with}$$
$$\boldsymbol{a}(\bar{\boldsymbol{\theta}}_c) \doteq [c_m(\theta_c); m = 1, \ldots, M]^T,$$
$$\boldsymbol{b}(\bar{\boldsymbol{\theta}}_c) \doteq [\frac{\partial c_m(\theta_c)}{\partial \theta_c}; m = 1, \ldots, M]^T$$

First-order Taylor expansion model I (Conti.)

- The received signal is

$$\begin{aligned} \boldsymbol{x} &= \boldsymbol{s}(\boldsymbol{\theta}_c) + \boldsymbol{w} \\ &= \boldsymbol{D}(\bar{\boldsymbol{\theta}}_c)\boldsymbol{\beta}_c + \boldsymbol{w}. \end{aligned}$$

- Properties of the parameters:
  - The nominal incident angle θ_c is constant across all the snapshots
  - The angle spreads $\tilde{\theta}_{c,\ell}, \ell = 1, \ldots, L_c$ could have different constellations from snapshot to snapshot
  - We assume that $\tilde{\theta}_{c,\ell}, \ell = 1, \ldots, L_c$ follows the Gaussian distribution with zero mean and variance σ_θ^2, and they are independent with the complex attenuations
  - The complex attenuation $\alpha_{c,\ell}, \ell = 1, \ldots, L_c$ is assumed to be random variable with $\mathcal{N}(0, \frac{1}{L_c}\sigma_{\gamma_c}^2)$

First-order Taylor expansion model I (Conti.)

- Properties of the parameters (Conti.): it can be shown that

$$E[\gamma_c] = E[\sum_{\ell=1}^{L_c} \gamma_\ell] = \sum_{\ell=1}^{L_c} E[\gamma_\ell] = 0,$$

$$E[\psi_c] = E[\sum_{\ell=1}^{L_c} \gamma_\ell \tilde{\theta}_\ell] = \sum_{\ell=1}^{L_c} E[\gamma_\ell] E[\tilde{\theta}_\ell] = 0,$$

$$E[\gamma_c \gamma_c^*] = E[\sum_{\ell=1}^{L_c} \gamma_\ell \sum_{\ell'=1}^{L_c} \gamma_{\ell'}^*] = \sum_{\ell=1}^{L_c} E[\gamma_\ell \gamma_\ell^*] = \sigma_{\gamma_c}^2,$$

$$E[\psi_c \psi_c^*] = E[\sum_{\ell=1}^{L_c} \gamma_\ell \tilde{\theta}_\ell \sum_{\ell'=1}^{L_c} \gamma_{\ell'}^* \tilde{\theta}_\ell^*] = \sum_{\ell=1}^{L_c} E[\gamma_\ell \gamma_\ell^*] E[\tilde{\theta}_\ell \tilde{\theta}_\ell^*]$$

$$= L_c \frac{1}{L_c} \sigma_{\gamma_c}^2 \sigma_\theta^2 = \sigma_{\gamma_c}^2 \sigma_\theta^2$$

$$E[\gamma_c \psi_c^*] = 0.$$

We use $\sigma_{\psi_c}^2$ to denote $\sigma_{\gamma_c}^2 \sigma_\theta^2$.

First-order Taylor expansion model I (Conti.)

- Properties of the parameters (Conti.): The covariance matrix of the received signal $\boldsymbol{x}$ which consists of the signal of a single source, can be calculated to be

$$\begin{aligned}\boldsymbol{R} &= E[\boldsymbol{x}\boldsymbol{x}^H] \\ &= \boldsymbol{D}(\bar{\boldsymbol{\theta}}_c)E[\boldsymbol{\beta}_c\boldsymbol{\beta}_c^*]\boldsymbol{D}(\bar{\boldsymbol{\theta}}_c)^H + \sigma_w^2\boldsymbol{I} \\ &= \boldsymbol{c}(\boldsymbol{\theta}_c)\boldsymbol{P}_c\boldsymbol{c}(\boldsymbol{\theta}_c)^H + \sigma_w^2\boldsymbol{I}\end{aligned}$$

where

$$\boldsymbol{P}_c = \begin{bmatrix}\sigma_{\gamma_c}^2 & 0 \\ 0 & \sigma_{\psi_c}^2\end{bmatrix}.$$

First-order Taylor expansion model II

- Another approximate model using the first order Taylor expansion can be written as

$$\begin{aligned} s_m(\boldsymbol{\theta}_c) &\approx \gamma_c \cdot c_m(\theta_c) + \psi_c \cdot \frac{\partial c_m(\theta_c)}{\partial \theta_c} \\ &\approx \gamma_c \cdot c_m(\theta_c + \frac{\psi_c}{\gamma_c}) \\ &= \gamma_c \cdot e^{-j2\pi(m-1)(\Delta s/\lambda)\sin(\theta_c + j\Delta\theta_c)}, \end{aligned} \tag{13}$$

where θ_c is redefined to be $\theta_c + \mathcal{R}\{\frac{\psi_c}{\gamma_c}\}$, and $\Delta\theta_c \doteq \mathcal{I}\{\frac{\psi_c}{\gamma_c}\}$ is the angle spread. Written in vector notation we obtained

$$\boldsymbol{s}(\boldsymbol{\theta}_c) = \gamma_c \cdot \boldsymbol{c}(\bar{\boldsymbol{\theta}}_c), \tag{14}$$

where $\bar{\boldsymbol{\theta}}_c = [\theta_c, \Delta\theta_c]$. The received signal can be written in vector notation as

$$\boldsymbol{x} = \boldsymbol{c}(\bar{\boldsymbol{\theta}}_c)\gamma_c + \boldsymbol{w}.$$

First-order Taylor expansion model II (Conti.)

- The parameter θ_c and $\Delta\theta_c$ are assumed to be deterministic over realizations. The covariance matrix of the received signal $\boldsymbol{x}$ is written as

$$\begin{aligned}\boldsymbol{R} &= E[\boldsymbol{x}\boldsymbol{x}^H] \\ &= \boldsymbol{c}(\bar{\boldsymbol{\theta}}_c)E[\gamma_c\gamma_c^*]\boldsymbol{c}(\bar{\boldsymbol{\theta}}_c)^H + \sigma_w^2\boldsymbol{I} \\ &= \sigma_{\gamma_c}^2\boldsymbol{c}(\bar{\boldsymbol{\theta}}_c)\boldsymbol{c}(\bar{\boldsymbol{\theta}}_c)^H + \sigma_w^2\boldsymbol{I}.\end{aligned}$$

Chapter 3.5
Time-evolution model

Motivation

- Temporal behavior of paths are considered as an additional degree of freedom for path clustering.
- The evolution of clusters of paths is included into models.
- The used estimation methods are derived under the assumption that the path parameters in different observation snapshots are independent. This (unrealistic) assumption results in a "loss of information" in the estimation of the path evolution in time..
- Due to model-order mismatch and heuristic settings in these algorithms, such as the (usually fixed) dynamic range, a time-variant path may remain undetected in some snapshots
- As a result, a time-variant path can be erroneously considered as several paths.
- It is therefore of great importance to use appropriate algorithms to estimate the temporal characteristics of paths directly.

Tracking Time-Variant Cluster Parameters in MIMO Channel Measurements: Algorithm and Results [Czink 2007]

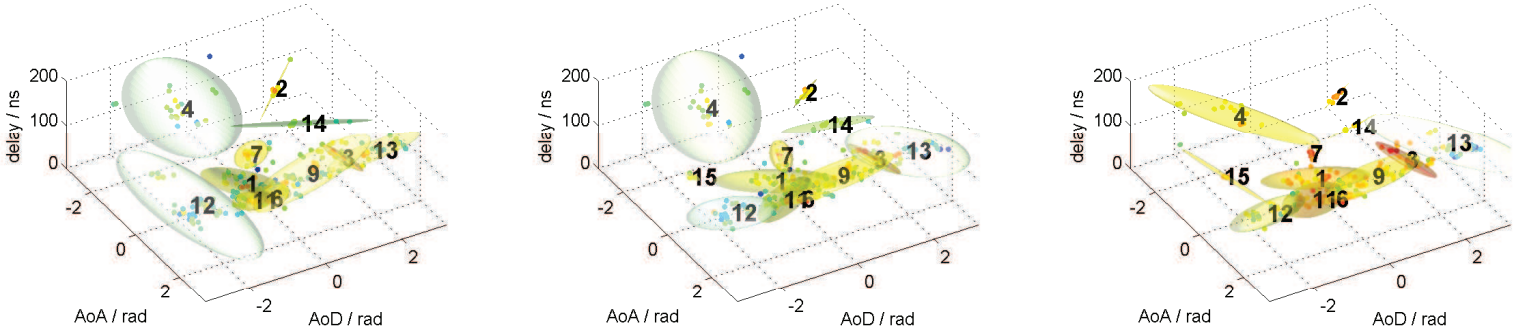

(a) (b) (c)

Figure 2: Tracked clusters from indoor scenario; (a)-(c) show the clusters' evolution over time

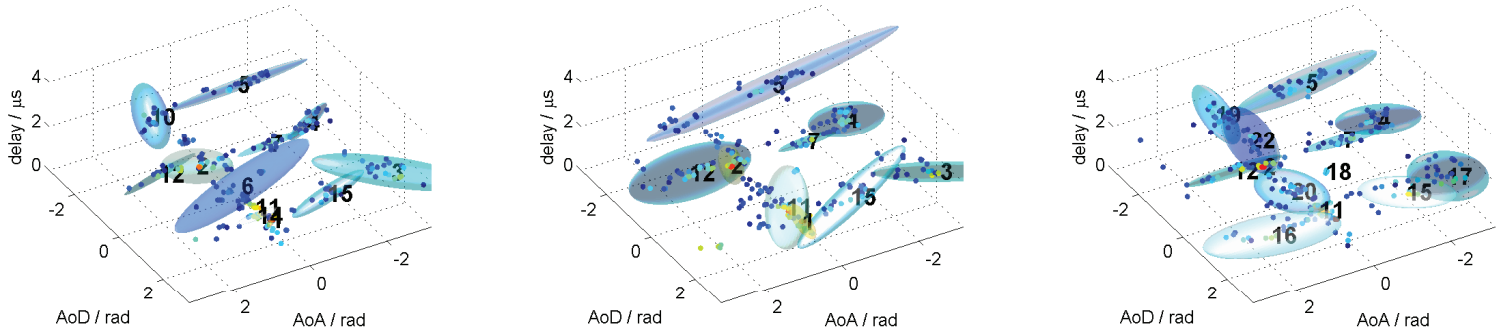

(a) (b) (c)

Figure 3: Tracked clusters from rural outdoor scenario; (a)-(c) show the clusters' evolution over time

Recent development

- Methods proposed to track time-variant paths when the linear approximation of the non-linear observation model is accurate
  - *Recursive expectation-maximization (EM)* and *recursive space-alternating generalized EM (SAGE)*-inspired algorithms for tracking of AoAs [Chung2005a]
  - *Extended Kalman filter (EKF)* for tracking of the delays, DoAs, DoDs and complex amplitudes [Richter2006,Salmi2006]
- Drawbacks
  - When parameters fluctuate dramatically, the linear approximation based on Taylor-series expansions is inaccurate, leading to *"loss of track"* errors.
  - Parameter updating requires the *second-order derivatives* of the received signal w.r.t. the path parameters. Calibration errors leads to erroneous derivatives
- Monte-Carlo method: a so-called "particle filter (PF)" [Yin2008e,Yin2008d] used for the nonlinear observation model

Experimental results for PF usage [Yin2008e]

Photographs and the map of the investigated environment

Tx surroundings

Rx surroundings

Map of the premises

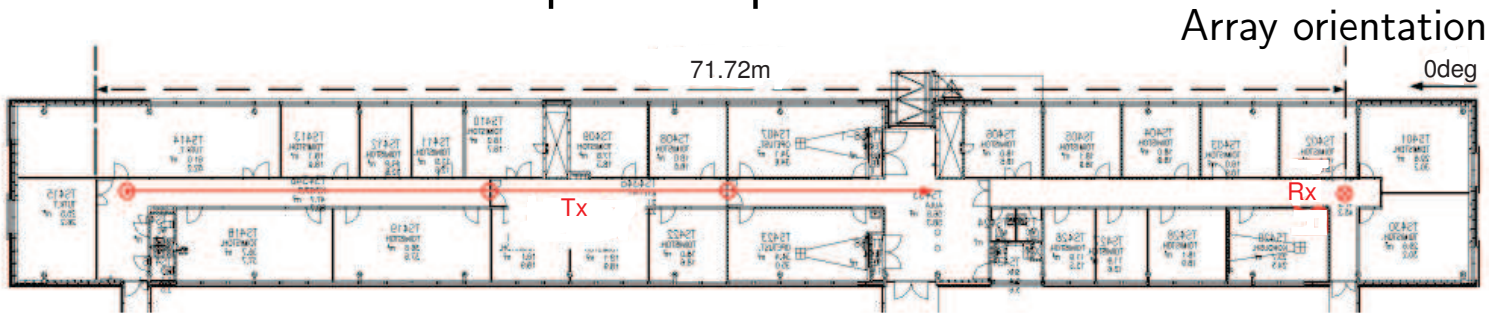

Experimental results for PF usage [Yin2008e]

Average power delay profiles of the received signals from 50 bursts

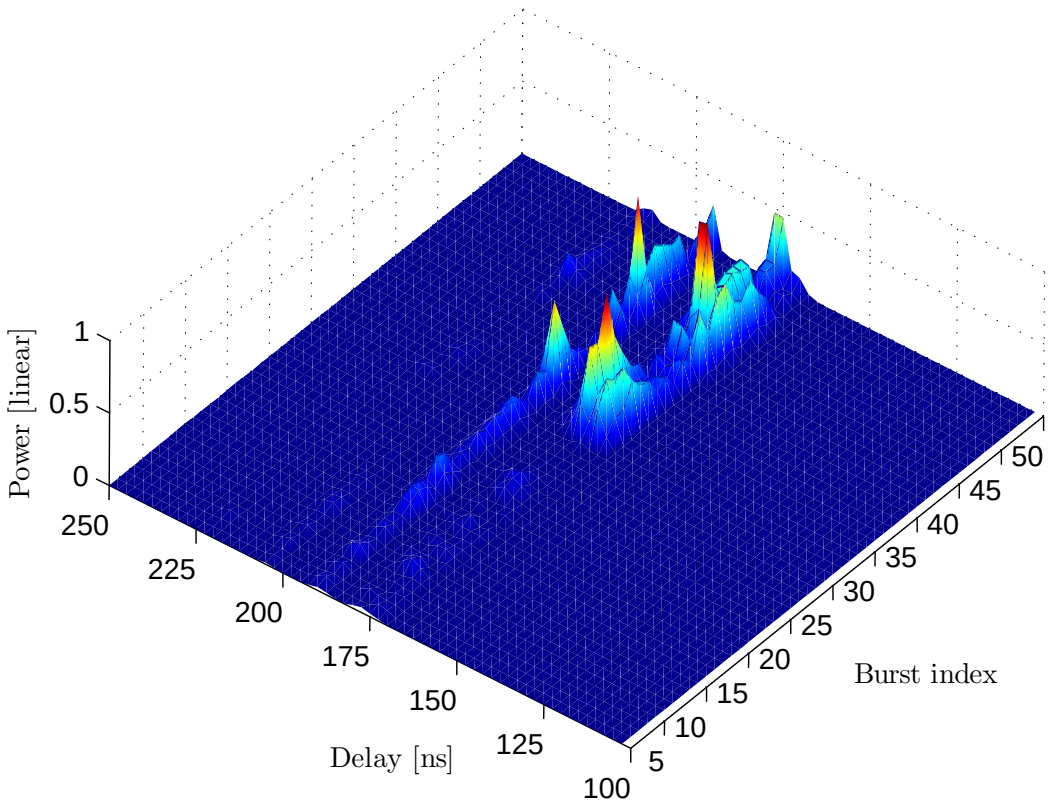

Estimates obtained using ISIS

601 to 650 Cycles

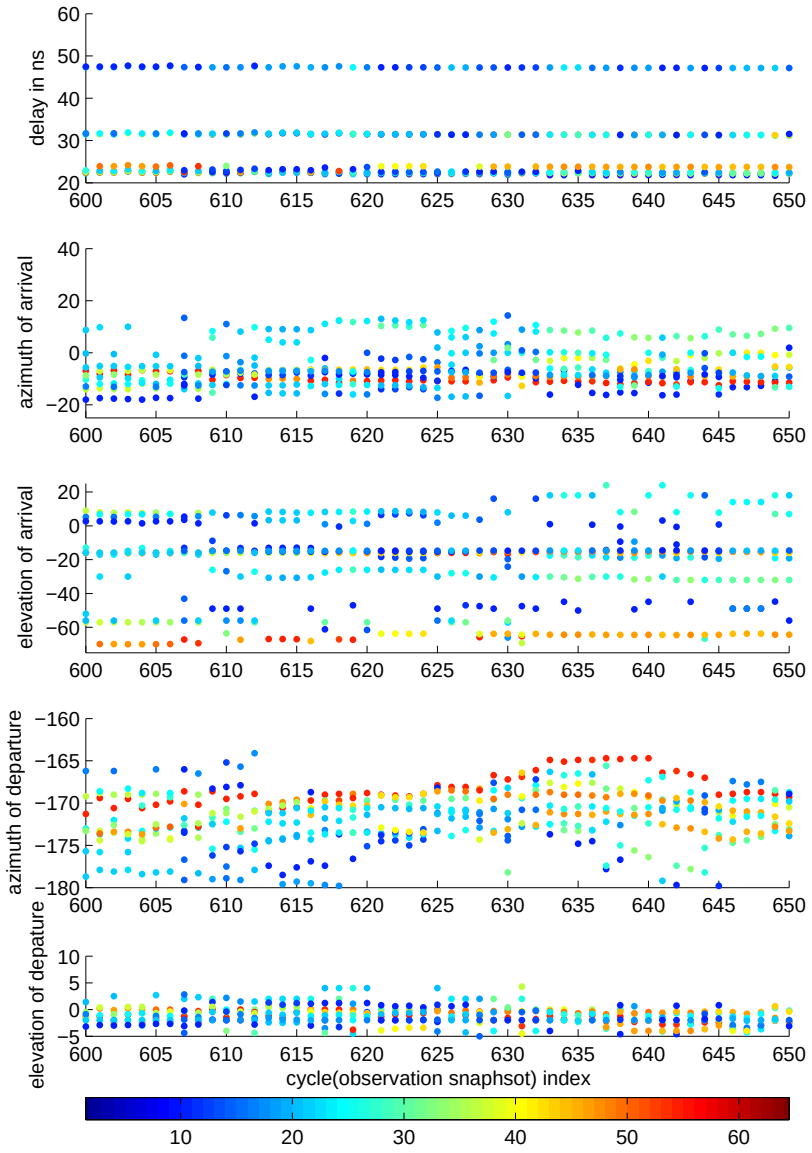

101 to 200 Cycles

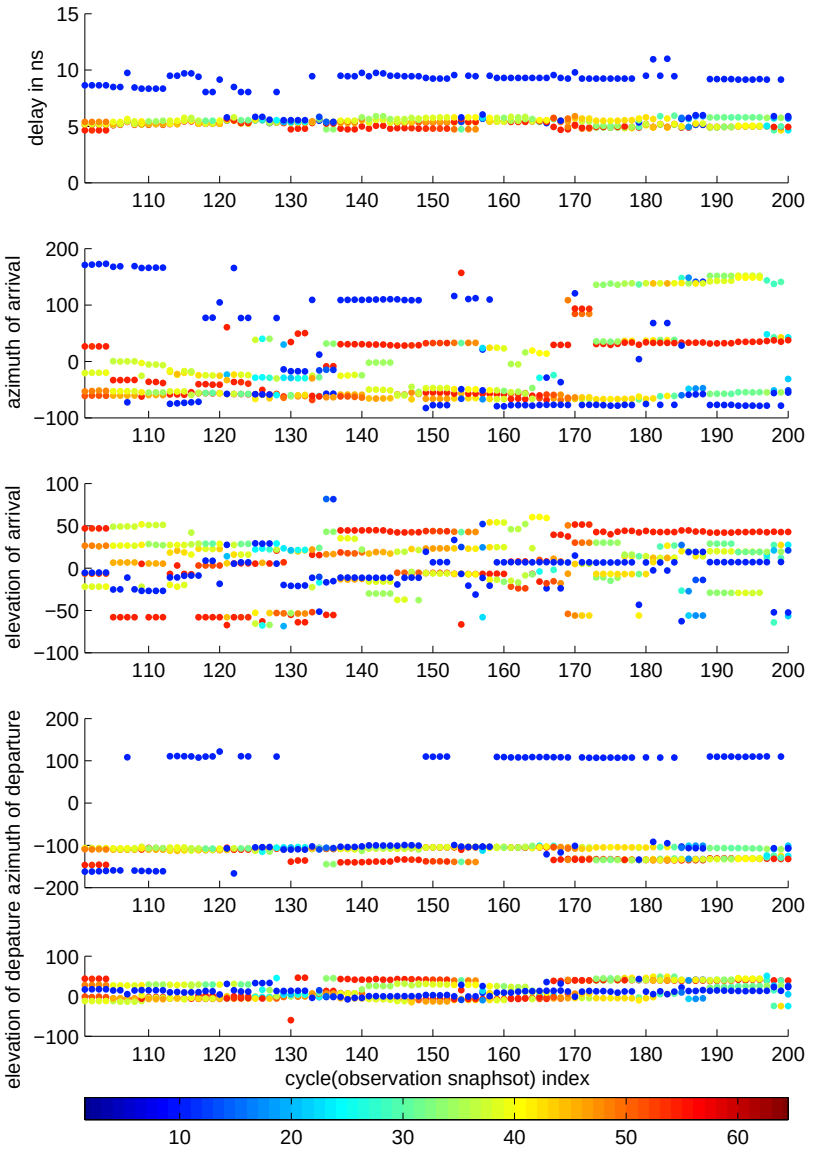

Experimental results for PF usage [Yin2008e]

Doppler frequency Estimates obtained using ISIS. TxR1, Cycle 600 to 650

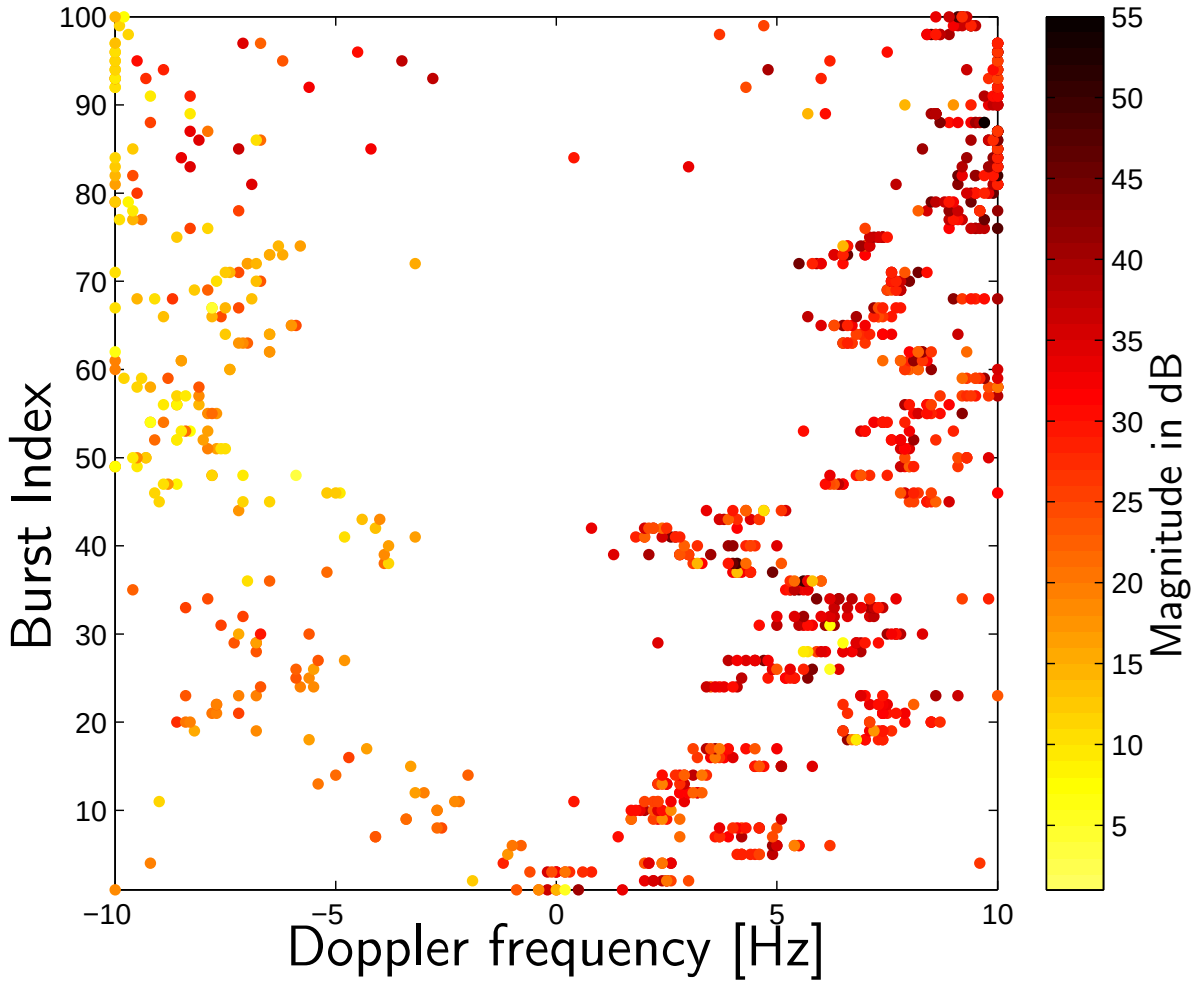

Experimental results for PF usage [Yin2008e]

Performance of the PF in tracking of three time-variant paths.

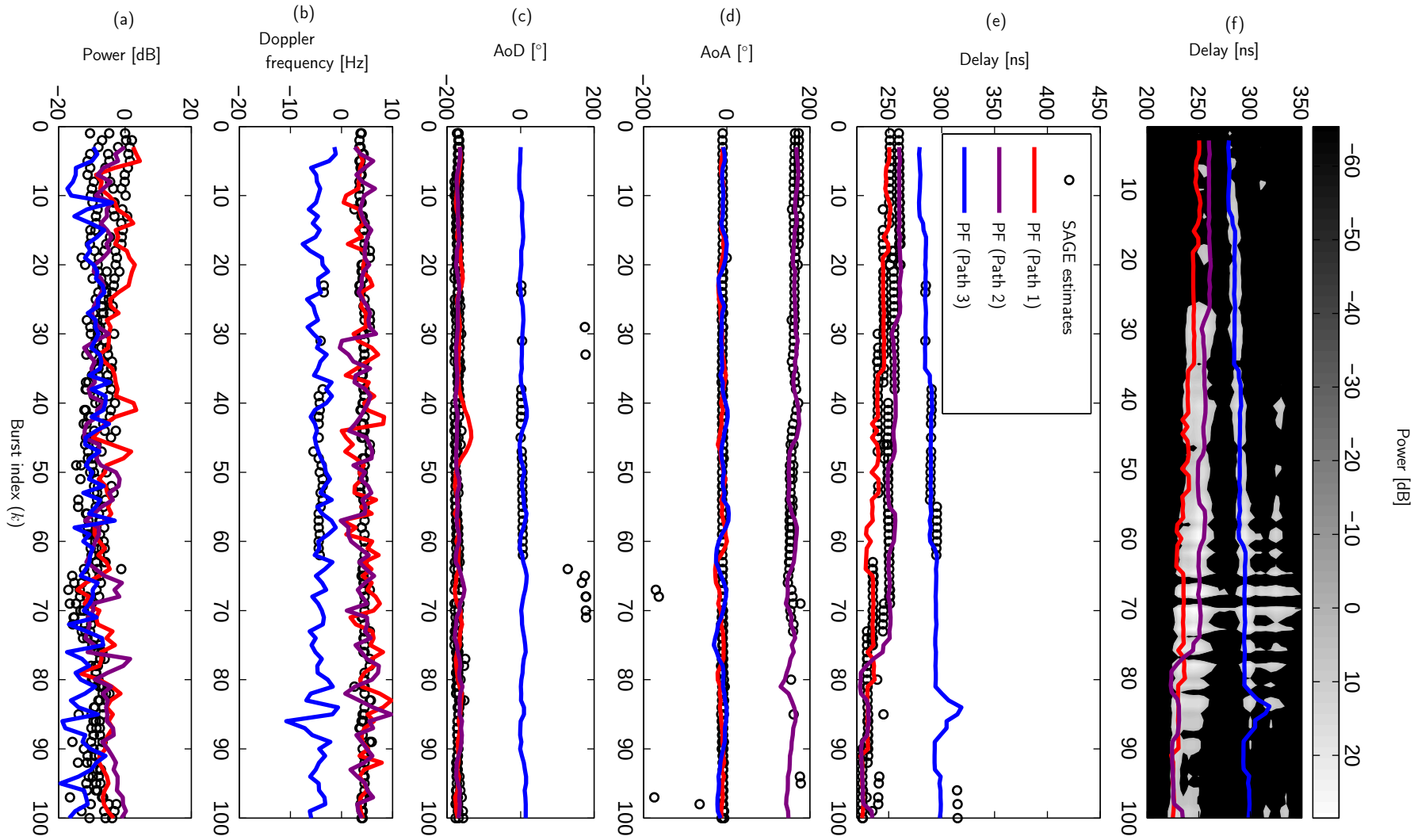

State-Space Model

- We consider a scenario where the environment consists of time-variant specular paths.
- The parameters of a path are

$$\boldsymbol{\Omega}_k = [\boldsymbol{P}_k^{\mathrm{T}}, \boldsymbol{\alpha}_k^{\mathrm{T}}, \boldsymbol{\Delta}_k^{\mathrm{T}}]^{\mathrm{T}},$$

where

  - $\boldsymbol{P}_k \doteq [\tau_k, \phi_{1,k}, \phi_{2,k}, \nu_k]^{\mathrm{T}}$: the "position" parameter vector, delay τ, azimuth of departure (AoD) ϕ_1, AoA ϕ_2, Doppler frequency ν
  - $\boldsymbol{\Delta}_k \doteq [\Delta\tau_k, \Delta\phi_{1,k}, \Delta\phi_{2,k}, \Delta\nu_k]^{\mathrm{T}}$: the "rate-of-change" parameter vector
  - $\boldsymbol{\alpha}_k \doteq [|\alpha_k|, \arg(\alpha_k)]^{\mathrm{T}}$ is the amplitude vector with $|\alpha_k|$ and $\arg(\alpha_k)$ representing the magnitude and the argument of α_k respectively

State-Space Model (Conti.)

- The state vector $\boldsymbol{\Omega}_k$ is modelled as a Markov process, i.e.

$$p(\boldsymbol{\Omega}_k|\boldsymbol{\Omega}_{1:k-1}) = p(\boldsymbol{\Omega}_k|\boldsymbol{\Omega}_{k-1}), \quad k \in [1, \ldots, K],$$

  where
  - $\boldsymbol{\Omega}_{1:k-1} \doteq \{\boldsymbol{\Omega}_1, \ldots, \boldsymbol{\Omega}_{k-1}\}$ is a sequence of state values from the 1st to the $(k-1)$th observation, and
  - K denotes the total number of observations.
- The transition of $\boldsymbol{\Omega}_k$ w.r.t. k is modelled as

$$\underbrace{\begin{bmatrix} \boldsymbol{P}_k \\ \boldsymbol{\alpha}_k \\ \boldsymbol{\Delta}_k \end{bmatrix}}_{\boldsymbol{\Omega}_k} = \underbrace{\begin{bmatrix} \boldsymbol{I}_4 & \boldsymbol{0}_{4\times 2} & T_k\boldsymbol{I}_4 \\ \boldsymbol{J}_k & \boldsymbol{I}_2 & \boldsymbol{0}_{2\times 4} \\ \boldsymbol{0}_{4\times 4} & \boldsymbol{0}_{4\times 2} & \boldsymbol{I}_4 \end{bmatrix}}_{\boldsymbol{F}_k \doteq} \underbrace{\begin{bmatrix} \boldsymbol{P}_{k-1} \\ \boldsymbol{\alpha}_{k-1} \\ \boldsymbol{\Delta}_{k-1} \end{bmatrix}}_{\boldsymbol{\Omega}_{k-1}} + \underbrace{\begin{bmatrix} \boldsymbol{0}_{4\times 1} \\ \boldsymbol{v}_{\boldsymbol{\alpha},k} \\ \boldsymbol{v}_{\Delta,k} \end{bmatrix}}_{\boldsymbol{v}_k \doteq},$$

State-Space Model (Conti.)

- The transition of $\boldsymbol{\Omega}_k$ w.r.t. k is modelled as

$$\underbrace{\begin{bmatrix}\boldsymbol{P}_k\\ \boldsymbol{\alpha}_k\\ \boldsymbol{\Delta}_k\end{bmatrix}}_{\boldsymbol{\Omega}_k} = \underbrace{\begin{bmatrix}\boldsymbol{I}_4 & \mathbf{0}_{4\times 2} & T_k\boldsymbol{I}_4\\ \boldsymbol{J}_k & \boldsymbol{I}_2 & \mathbf{0}_{2\times 4}\\ \mathbf{0}_{4\times 4} & \mathbf{0}_{4\times 2} & \boldsymbol{I}_4\end{bmatrix}}_{\boldsymbol{F}_k \doteq} \underbrace{\begin{bmatrix}\boldsymbol{P}_{k-1}\\ \boldsymbol{\alpha}_{k-1}\\ \boldsymbol{\Delta}_{k-1}\end{bmatrix}}_{\boldsymbol{\Omega}_{k-1}} + \underbrace{\begin{bmatrix}\mathbf{0}_{4\times 1}\\ \boldsymbol{v}_{\boldsymbol{\alpha},k}\\ \boldsymbol{v}_{\Delta,k}\end{bmatrix}}_{\boldsymbol{v}_k \doteq},$$

  - $\boldsymbol{I}_n$ represents the $n \times n$ identity matrix,
  - $\mathbf{0}_{b\times c}$ is the all-zero matrix of dimension $b \times c$,
  - $\boldsymbol{J}_k = \begin{bmatrix}0 & 0 & 0 & 0\\ 0 & 0 & 0 & 2\pi T_k\end{bmatrix}$, and T_k denotes the interval between the starts of the $(k-1)$th and the kth observation periods.
  - $\boldsymbol{v}_{\boldsymbol{\alpha},k} \doteq \left[v_{|\alpha|,k},\ v_{\arg(\alpha),k}\right]^{\mathrm{T}}$
  - $\boldsymbol{v}_{\boldsymbol{\Delta},k} \doteq \left[v_{\Delta\tau,k},\ v_{\Delta\phi_1,k},\ v_{\Delta\phi_2,k},\ v_{\Delta\nu,k}\right]^{\mathrm{T}}$
  - $v_{(\cdot),k}$ are independent Gaussian random variables $v_{(\cdot),k} \sim \mathcal{N}(0, \sigma^2_{(\cdot)})$.
- Consider the case with $T_k = T$, $k \in [1, \ldots, K]$ and the subscript k in $\boldsymbol{F}_k$ is dropped.

Observation Model

- In the kth observation period, the discrete-time signals at the output of the m_2th Rx antenna when the m_1th Tx antenna transmits can be written as

$$\begin{aligned} y_{k,m_1,m_2}(t) = x_{k,m_1,m_2}(t;\boldsymbol{\Omega}_k) + n_{k,m_1,m_2}(t), \\ t \in [t_{k,m_1,m_2}, t_{k,m_1,m_2} + T), \\ m_1 = 1,\ldots,M_1,\ m_2 = 1,\ldots,M_2, \end{aligned} \tag{15}$$

  where
  - t_{k,m_1,m_2}: the time instant when the m_2th Rx antenna starts to receive signals while the m_1th Tx antenna transmits
  - T: the sensing duration of each Rx antenna,
  - M_1 and M_2 : the total number of Tx antennas and Rx antennas respectively.
- The vector $\boldsymbol{y}_k$ is used to represent all the samples received in the kth observation period
- $\boldsymbol{y}_{1:k} \doteq \{\boldsymbol{y}_1, \boldsymbol{y}_2, \ldots, \boldsymbol{y}_k\}$ denotes a sequence of observations.

Observation Model (Conti.)

- The signal contribution $x_{k,m_1,m_2}(t;\mathbf{\Omega}_k)$ reads

$$x_{k,m_1,m_2}(t;\mathbf{\Omega}_k) = \alpha_k \exp(j2\pi\nu_k t) c_{1,m_1}(\phi_{k,1}) c_{2,m_2}(\phi_{k,2}) \cdot u(t-\tau_k).$$

  where
  - $c_{1,m_1}(\phi)$ and $c_{2,m_2}(\phi)$ represent respectively the response in azimuth of the m_1th Tx antenna, and the response in azimuth of the m_2th Rx antenna,
  - $u(t-\tau_k)$ denotes the transmitted signal delayed by τ_k.
  - The noise $n_{k,m_1,m_2}(t)$ is a zero-mean Gaussian process with spectrum height σ_n^2.

Chapter 3.6
Power spectral density model

Objective

- Derive a 6-*dimensional power spectral density (PSD)* and use it to characterize the shape of the bidirection (direction of departure and direction of arrival), delay and Doppler frequency PSD of individual components in the response of a propagation channel.
- This PSD maximizes the entropy under the constraint that the multi-dimensional PSD of each component exhibits a fixed center of gravity, specific spreads and dependence of the spreads in bidirection, delay and Doppler frequency.
- The *power spectrum (PS) of the channel* is modeled as the superposition of the component PSDs multiplied with the component average power.

Definition of dispersive components (Revisited)

- Due to the heterogeneity of the propagation environment, the received signal at the receiver (Rx) of a radio communication system is the superposition of a number of components.
- Each component is contributed by an electromagnetic wave propagating along a path from the transmitter (Tx) to the Rx.
- Along its path, the wave interacts with a certain number of objects referred to as scatterers.
- Due to the geometrical and electromagnetic properties of the scatterers, the individual components may be dispersive in delay, direction of departure (DoD), direction of arrival (DoA), polarizations, as well as in Doppler frequency.
- Dispersion of individual components in these dimensions significantly influences the performance of communication systems using multiple-input multiple-output (MIMO) techniques.

Conventional models of dispersive components

- Dispersed component is modeled using a cluster of multiple specular components [Correia2001], [Medbo2006] and [Czink2007]
  - Wideband channel sounder RUSK ATM.
  - RiMAX is used to estimate multiple specular paths.

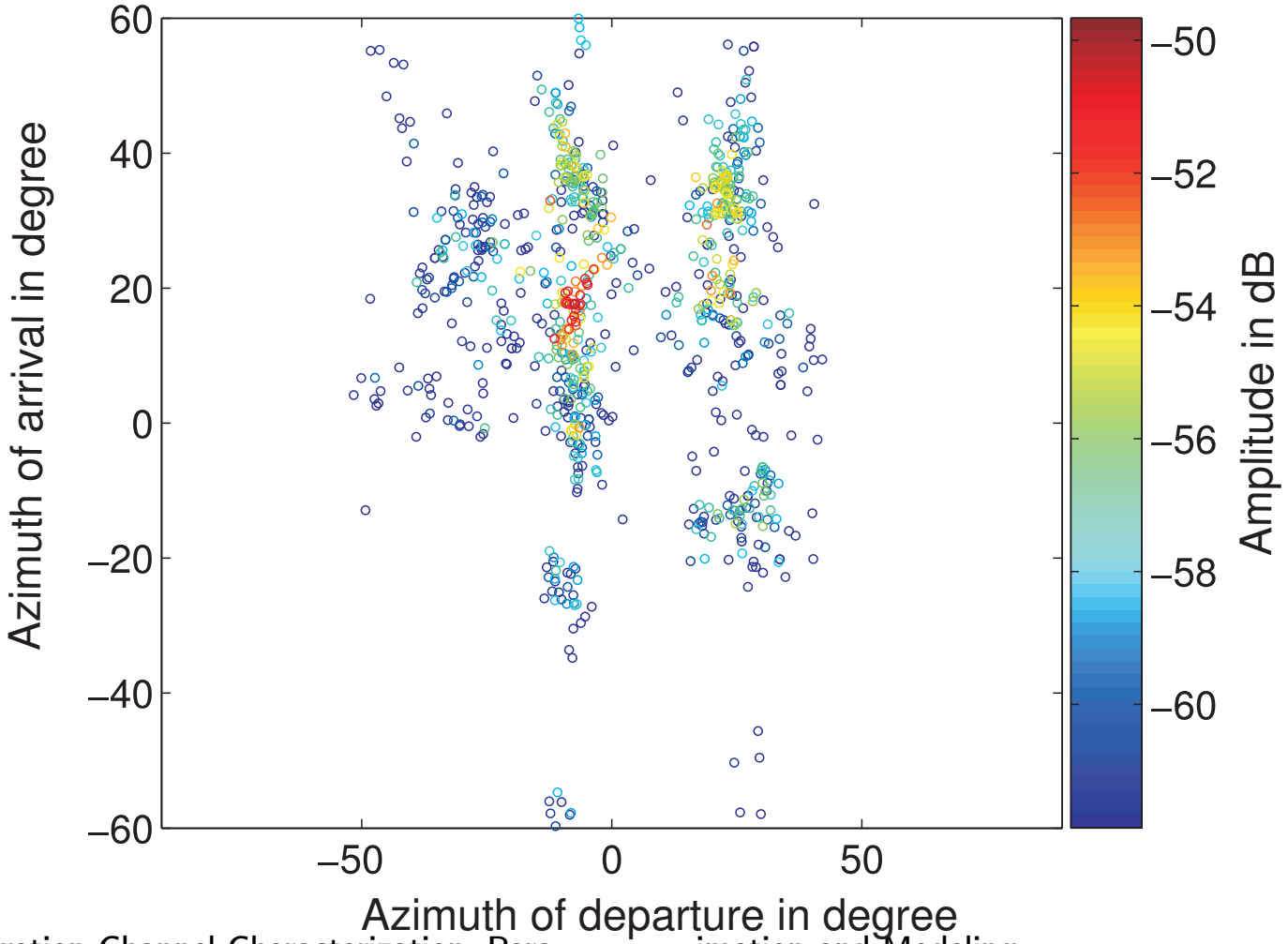

Problems in estimation of dispersive components

- Extracted dispersion parameters of specular components do not accurately characterize the true behavior of a dispersed component [Bengtsson-01].

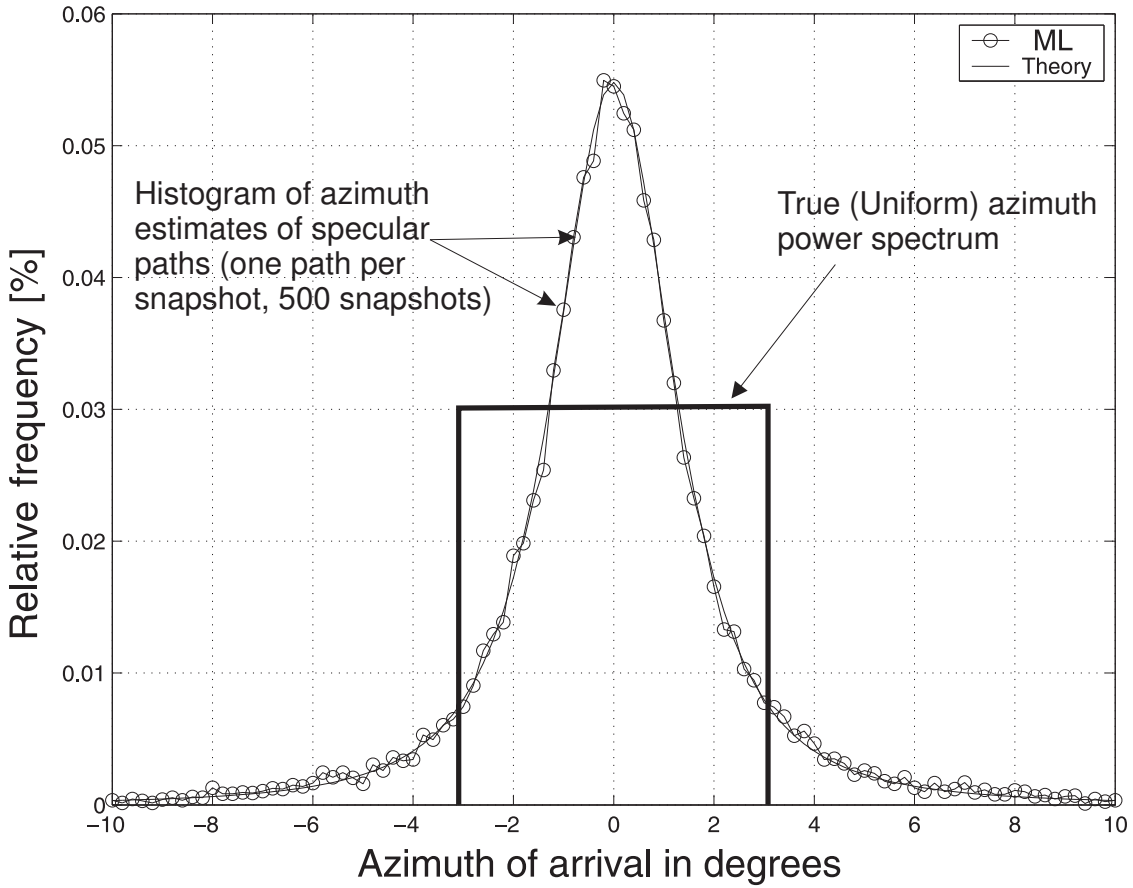

- We need suitable generic parametric models characterizing the dispersive components and use efficient parameter estimators to get accurate estimates from real measurements.

Conventional approaches for PSD estimation for dispersive components

- Various algorithms have been proposed for the estimation of the dispersive characteristics of individual components in the channel response by using *the power spectral density (PSD)* of each component. [Betlehem2006],[Trump-Ottersten-96],[BessonStoica-1999],[Ribeiro2004].

- A component PSD can be irregular in real environments and thus, a gross description relying on certain characteristic parameters, e.g. *the center of gravity and spreads* of the PSD, is usually adopted.

- These algorithms estimate these parameters by approximating the shape of the normalized component PSD with *a certain probability density function (pdf)*, e.g. in azimuth-of-arrival (AoA) as described in [Trump-Ottersten-96,BessonStoica-1999,Ribeiro2004], and in AoA and azimuth of departure (AoD) [Betlehem2006].

Problems for PSD estimation for dispersive components

- The parameter estimates obtained by using these algorithms depend on the selected pdfs.
- However, no rationale behind the selection is given in these contributions.
- Furthermore, the applicability of these pdfs in characterizing the PSD, as well as the performance of the estimation algorithms have not been investigated experimentally with real measurement data.

Using the maximum-entropy principle to derive generic PSD models

- The maximum-entropy (ME) principle [Jaynes2003] is proposed in [Yin-06,Yin2007,Yin2007a,Yin2006] for the selection/derivation of the PSD characterizing the component power distribution.
- This rationale assumes that each component has a fixed center of gravity and spread, and that no additional information about the PSD exists.
- The center of gravity and the spreads of a component PSD are described by the first and second moments of the corresponding power distribution.
- Using the ME principle, we derive a PSD that has fixed first and second moments, while maximizing the entropy of any other constraint.

Using the maximum-entropy principle to derive generic PSD models

- The estimates of the dispersion parameters obtained by modeling the component PSD with this entropy-maximizing PSD provide the "safest" results in the sense that, they are more accurate than the estimates computed using another form of PSD subject to any constraint that is invalid in real situations.
- Based on this rationale, we derived the ME PSDs to characterize the component power distribution in
  - BiAzimuth: Von-Mises pdf [Yin-06] [Mardia2003]
  - Azimuth-elevation: Fisher-Bingham-5 pdf [Kent1982,Yin2007,Yin2007a]
  - Azimuth-elevation-delay: Von-Mises-Fisher pdf
  - Azimuth of arrival - azimuth of departure - delay: Von-Mises-Fisher pdf [Mardia2003]
- Preliminary investigations using measurement data demonstrate that these characterizations are applicable in real environments.

Dispersion in Azimuth

We seek for a density function with

- specified first moment $\boldsymbol{\mu}_{\boldsymbol{\Omega}} \doteq \int \boldsymbol{\Omega} f(\boldsymbol{\Omega}) \mathrm{d}\boldsymbol{\Omega}$
- the entropy maximized.

This function is the density function of the von-Mises distribution [Mardia, 1975]:

$$f(\boldsymbol{\Omega}) = c(\kappa) \exp\{\kappa \bar{\boldsymbol{\Omega}}^{\mathrm{T}} \boldsymbol{\Omega}\}$$

with

- $\bar{\boldsymbol{\Omega}} = \|\boldsymbol{\mu}_{\boldsymbol{\Omega}}\|^{-1} \boldsymbol{\mu}_{\boldsymbol{\Omega}}$: the mode of the distribution
- κ: concentration parameter
- $c(\kappa)$: normalization factor.

Horizontal-only propagation: $\boldsymbol{\Omega} = \boldsymbol{e}(\phi) \doteq [\cos(\phi) \sin(\phi)]^{\mathrm{T}}$.
Via the mapping $\phi \mapsto \boldsymbol{e}(\phi)$, we obtain the azimuth density function:

$$f(\phi) = \frac{1}{2\pi I_0(\kappa)} \exp\{\kappa \cos(\phi - \bar{\phi})\}.$$

Dispersion in Biazimuth (AoA-AoD)

The entropy-maximizing density function $f(\boldsymbol{\Omega}_1, \boldsymbol{\Omega}_2)$ with specified

- first moments $\boldsymbol{\mu}_{\boldsymbol{\Omega}_1}$, $\boldsymbol{\mu}_{\boldsymbol{\Omega}_2}$
- second moments in $\int \boldsymbol{\Omega}_1 \boldsymbol{\Omega}_2^{\mathrm{T}} f(\boldsymbol{\Omega}_1, \boldsymbol{\Omega}_2) \mathrm{d}\boldsymbol{\Omega}_1 \mathrm{d}\boldsymbol{\Omega}_2$

is the von-Mises-Fisher density function [Mardia, 1975]

$$f(\boldsymbol{\Omega}_1, \boldsymbol{\Omega}_2) \propto \exp\{\boldsymbol{a}_1^{\mathrm{T}} \boldsymbol{\Omega}_1 + \boldsymbol{a}_2^{\mathrm{T}} \boldsymbol{\Omega}_2 + \boldsymbol{\Omega}_1^{\mathrm{T}} \boldsymbol{A} \boldsymbol{\Omega}_2\},$$

with $\boldsymbol{a}_1$, $\boldsymbol{a}_2$ and $\boldsymbol{A}$ being free parameters.

A biazimuth density function $f(\phi_1, \phi_2)$ derived via the mapping $[\phi_1, \phi_2] \mapsto [\boldsymbol{e}(\phi_1)^{\mathrm{T}}, \boldsymbol{e}(\phi_2)^{\mathrm{T}}]$ reads,

$$\begin{aligned} f(\phi_1, \phi_2) \;=\; & c(\kappa_1, \kappa_2, \rho) \cdot \exp\Bigg\{ \left(\frac{\kappa_1 - \rho\sqrt{\kappa_1 \kappa_2}}{1 - \rho^2} \right) \cos(\phi_1 - \bar{\phi}_1) \\ & + \left(\frac{\kappa_2 - \rho\sqrt{\kappa_1 \kappa_2}}{1 - \rho^2} \right) \cos(\phi_2 - \bar{\phi}_2) + \frac{\rho\sqrt{\kappa_1 \kappa_2}}{1 - \rho^2} \cos[(\phi_1 - \bar{\phi}_1) - (\phi_2 - \bar{\phi}_2)] \Bigg\} \end{aligned}$$

Dispersion in Biazimuth (Cont.)

Contour plots of the biazimuth density function:

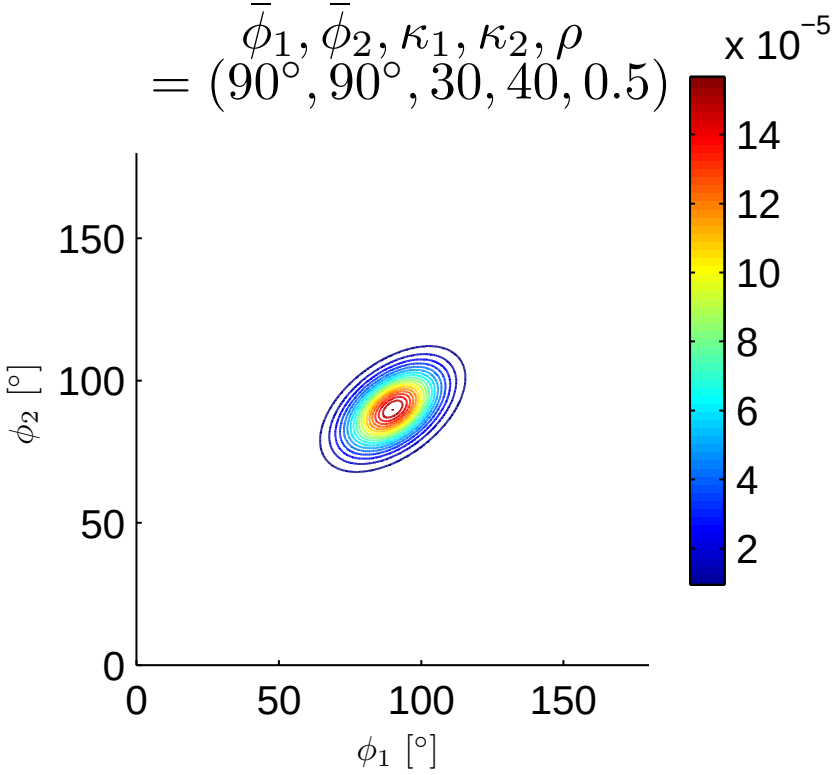

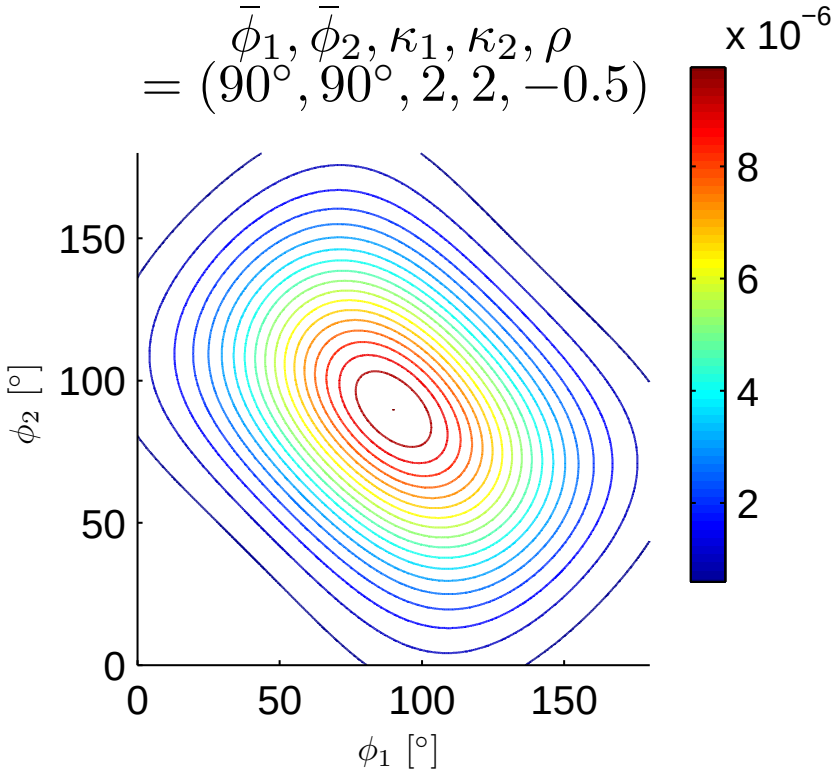

Dispersion in Direction (Azimuth-Elevation)

Definition of a direction:

$$\boldsymbol{\Omega} = \boldsymbol{e}(\phi, \theta) \doteq \begin{bmatrix} \cos(\phi)\sin(\theta) \\ \sin(\phi)\sin(\theta) \\ \cos(\theta) \end{bmatrix} \in \mathbb{S}_2$$

where

- $\mathbb{S}_2$: unit sphere
- ϕ: azimuth
- θ: elevation

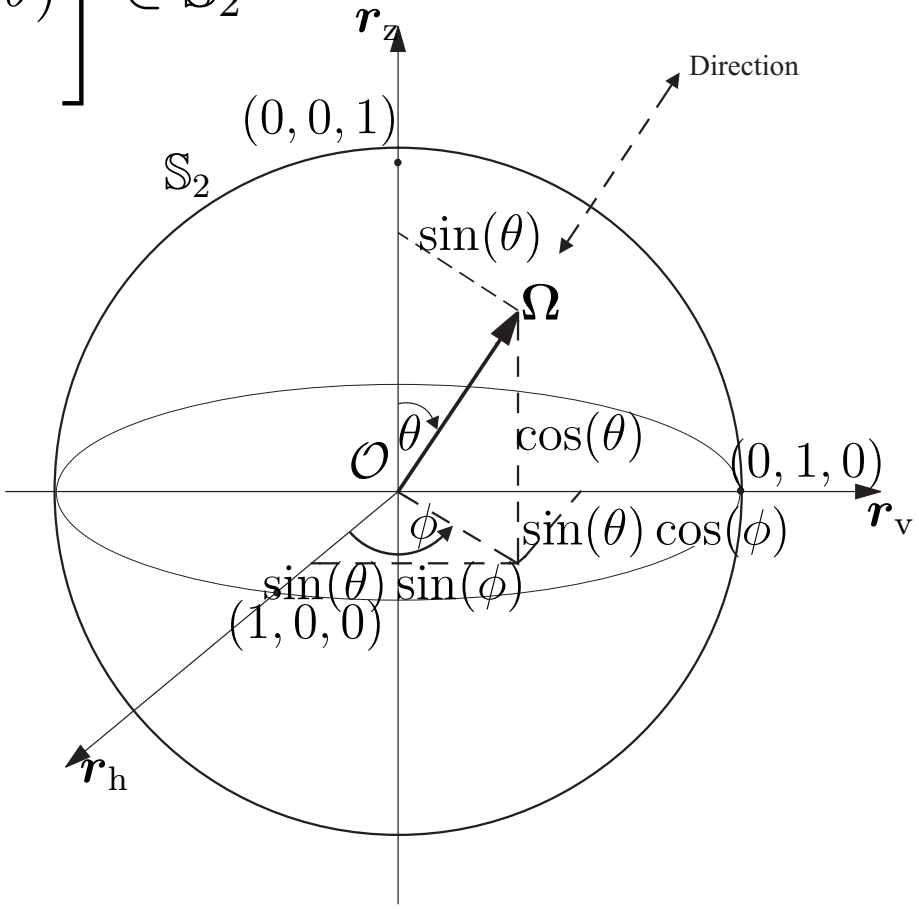

Dispersion in Direction (Azimuth-Elevation)

The entropy-maximizing density function on $\mathbb{S}_2$ with specified

- first moment (mean direction) $\mu_{\mathbf{\Omega}} \doteq \int \mathbf{\Omega} f(\mathbf{\Omega}) \mathrm{d}\mathbf{\Omega}$
- second moment matrix $\int \mathbf{\Omega}\mathbf{\Omega}^{\mathrm{T}} f(\mathbf{\Omega}) \mathrm{d}\mathbf{\Omega}$

is the density function of the Fisher-Bingham 5 distribution [Kent 1982]:

$$f(\mathbf{\Omega}) = c(\kappa, \beta) \cdot \exp\left\{\kappa \boldsymbol{\gamma}_1^{\mathrm{T}} \mathbf{\Omega} + \beta[(\boldsymbol{\gamma}_2^{\mathrm{T}} \mathbf{\Omega})^2 - (\boldsymbol{\gamma}_3^{\mathrm{T}} \mathbf{\Omega})^2]\right\},$$

where

- κ: concentration parameter
- β: ovalness parameter
- $\boldsymbol{\gamma}_1, \boldsymbol{\gamma}_2, \boldsymbol{\gamma}_3$: orthonormal vectors determined by angles $\bar{\phi}, \bar{\theta}, \alpha$
- $\bar{\phi}$: azimuth of the mean direction $\mu_{\mathbf{\Omega}}$
- $\bar{\theta}$: elevation of $\mu_{\mathbf{\Omega}}$
- α : angle describing how the distribution is tilted on $\mathbb{S}_2$.

Dispersion in Direction (Azimuth-Elevation) (Cont.)

Two examples of the direction density function $f(\mathbf{\Omega})$:

$$(\bar{\phi}, \bar{\theta}, \alpha, \kappa, \beta) = (0°, 45°, 160°, 5, 1.5)$$

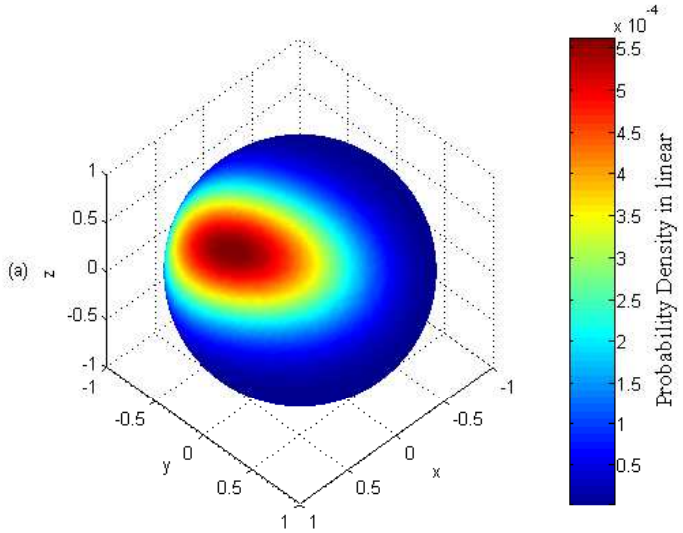

$$(\bar{\phi}, \bar{\theta}, \alpha, \kappa, \beta) = (45°, 70°, 35°, 200, 100)$$

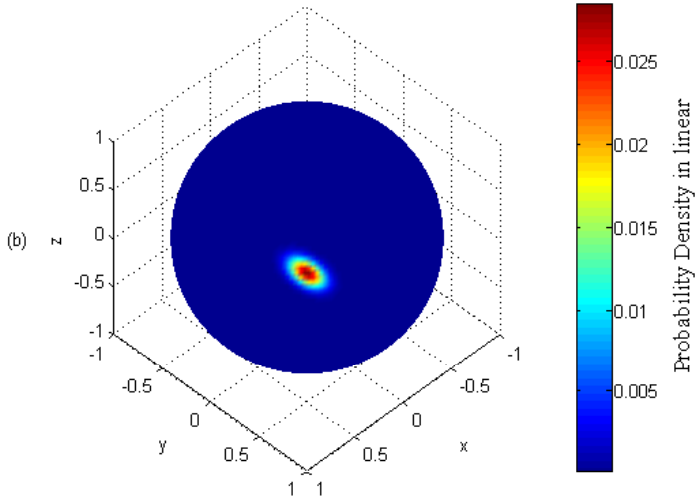

The azimuth-elevation density function $f(\phi, \theta)$ induced by $f(\mathbf{\Omega})$ reads

$$f(\phi, \theta) = c(\kappa, \beta) \cdot \exp\left\{\kappa \boldsymbol{\gamma}_1^{\mathrm{T}} \mathbf{\Omega} + \beta[(\boldsymbol{\gamma}_2^{\mathrm{T}} \mathbf{\Omega})^2 - (\boldsymbol{\gamma}_3^{\mathrm{T}} \mathbf{\Omega})^2]\right\} \cdot \sin(\theta).$$

Dispersion in Biazimuth and Delay

Define $\boldsymbol{\psi} \doteq [\boldsymbol{\Omega}_1^{\mathrm{T}}, \boldsymbol{\Omega}_2^{\mathrm{T}}, \tau]^{\mathrm{T}}$.
The entropy-maximizing density function $f(\boldsymbol{\psi})$ with specified

- first moments $\boldsymbol{\mu}_{\boldsymbol{\psi}}$
- second moments $\int \boldsymbol{\psi}\boldsymbol{\psi}^{\mathrm{T}} f(\boldsymbol{\psi}) \mathrm{d}\boldsymbol{\psi}$

is [Mardia, 1975]

$$f(\boldsymbol{\psi}) \propto \exp\{\boldsymbol{b}^{\mathrm{T}}\boldsymbol{\psi} + \boldsymbol{\psi}^{\mathrm{T}}\boldsymbol{B}\boldsymbol{\psi}\},$$

where $\boldsymbol{b} \in \mathbb{R}^{5\times 1}$ and $\boldsymbol{B} \in \mathbb{R}^{5\times 5}$ are free parameters.

Via the mapping $[\phi_1, \phi_2, \tau] \mapsto [\boldsymbol{e}(\phi_1)^{\mathrm{T}}, \boldsymbol{e}(\phi_2)^{\mathrm{T}}, \tau]$, the biazimuth-delay density function $f(\phi_1, \phi_2, \tau)$ can be induced by $f(\boldsymbol{\Omega}_1, \boldsymbol{\Omega}_2, \tau)$,

$$\begin{aligned} f(\phi_1, \phi_2, \tau) = C \exp\big\{ & c_1 \cos(\phi_1 - \bar{\phi}_1) + c_2 \cos(\phi_2 - \bar{\phi}_2) \\ & + (\tau - \bar{\tau})[c_3 \sin(\phi_1 - \bar{\phi}_1) + \ c_4 \sin(\phi_2 - \bar{\phi}_2)] \\ & + c_5(\tau - \bar{\tau})^2 + \ c_6 \cos[(\phi_1 - \bar{\phi}_1) - (\phi_2 - \bar{\phi}_2)]\big\}. \end{aligned}$$

Dispersion in Biazimuth and Delay (Cont.)

3dB-spread surfaces $\left\{(\phi_1, \phi_2, \tau) : f(\phi_1, \phi_2, \tau) = \frac{1}{2} f(\bar{\phi}_1, \bar{\phi}_2, \bar{\tau})\right\}$:

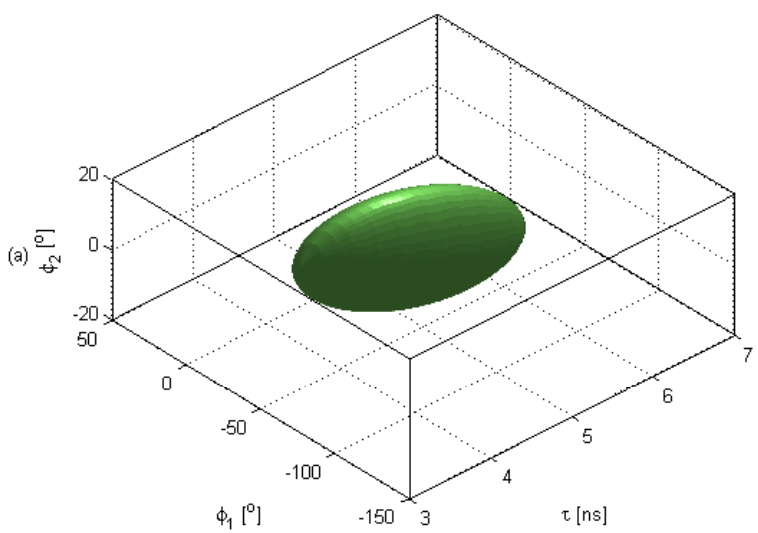

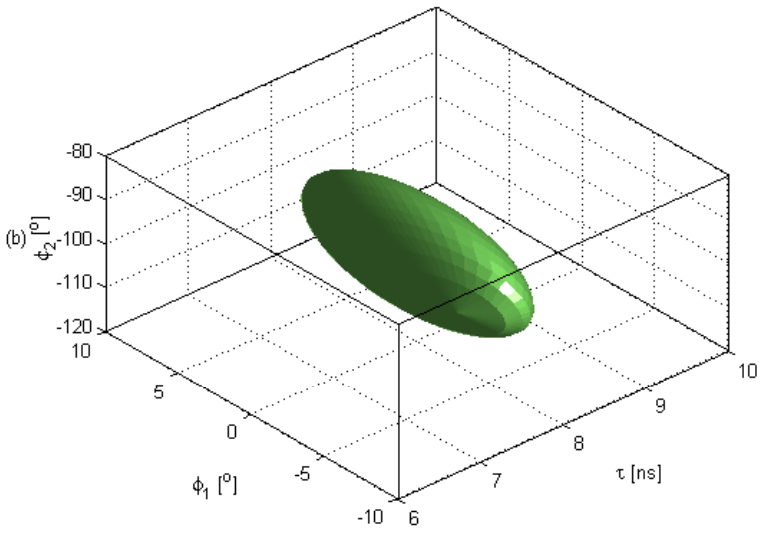

	$\bar{\tau}$ [ns]	$\bar{\phi}_1$ [°]	$\bar{\phi}_2$ [°]	σ_τ [ns]	κ_1	σ_{ϕ_1} [°]	κ_2	σ_{ϕ_2} [°]	ρ_{12}	ρ_1	ρ_2
(a)	5	−40	0	1	5	25.6	10	18.1	−0.4	−0.3	−0.3
(b)	8	0	−100	0.5	50	8.1	30	10.5	−0.5	0.6	−0.2

Direction-Delay Dispersion

The entropy-maximizing pdf of direction $\boldsymbol{\Omega}$ and delay τ with specified first moment and second moment is of the form

$$f_{\mathrm{ME}}(\boldsymbol{\Omega}, \tau) \propto \exp\left\{ \begin{bmatrix} \boldsymbol{\Omega} - \bar{\boldsymbol{\Omega}} \\ \tau - \bar{\tau} \end{bmatrix}^{\mathrm{T}} \begin{bmatrix} \boldsymbol{A} & \boldsymbol{c} \\ \boldsymbol{c}^{\mathrm{T}} & -b \end{bmatrix} \begin{bmatrix} \boldsymbol{\Omega} - \bar{\boldsymbol{\Omega}} \\ \tau - \bar{\tau} \end{bmatrix} \right\}.$$

Two conditions are used to derive the expressions of the parameters:

- The conditional pdf of direction is Fisher-Bingham-5 (FB5)
  Two examples of FB5 pdf:

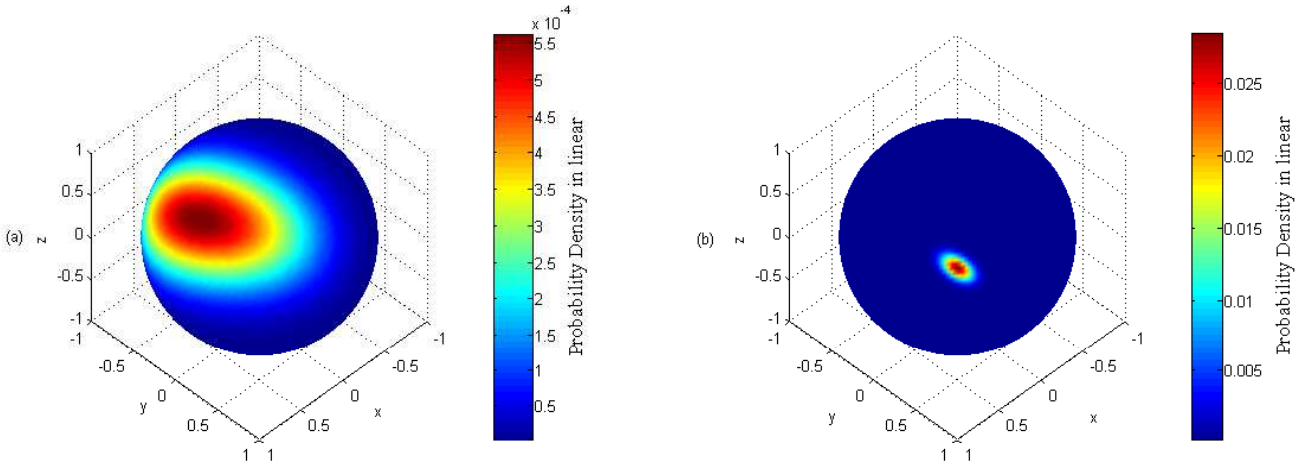

- The conditional pdf of delay is Gaussian.

Direction-Delay Dispersion (Cont.)

The direction-delay pdf is calculated to be

$$f_{\mathrm{ME}}(\boldsymbol{\Omega},\tau) = C \cdot \exp\Big(\kappa \bar{\boldsymbol{\Omega}}^{\mathrm{T}} \boldsymbol{\Omega} + \boldsymbol{\Omega}^{\mathrm{T}} \boldsymbol{A}(\tau,\zeta,\alpha,\beta)\boldsymbol{\Omega} - b(\tau-\bar{\tau})^2 - 2\eta \boldsymbol{g}^{\mathrm{T}}(\boldsymbol{\Omega}-\bar{\boldsymbol{\Omega}})(\tau-\bar{\tau})\Big),$$

where

- C: Constant for normalization
- $\bar{\Omega}$: Mean direction (equivalently $\bar{\phi}, \bar{\theta}$)
- $\bar{\tau}$: Mean delay
- κ: Concentration parameter in direction
- b: Concentration parameter in delay
- ζ: Ovalness parameter in direction
- η: Dependence between the spread in direction and in delay
- α, β: Two angles describing how the pdf is tilted on $\mathbb{S}_2$
- $\boldsymbol{g}$: Vector jointly determined by $\bar{\Omega}$ and β

3-dB spread surface of $f_{\mathrm{ME}}(\boldsymbol{\Omega},\tau)$ with parameter setting

$\bar{\theta}$ [°]	$\bar{\phi}$ [°]	$\bar{\tau}$ [ms]	κ	ζ
0	0	58	100	0.01

α [°]	β [°]	η	b
60	270	1×10^3	4×10^4

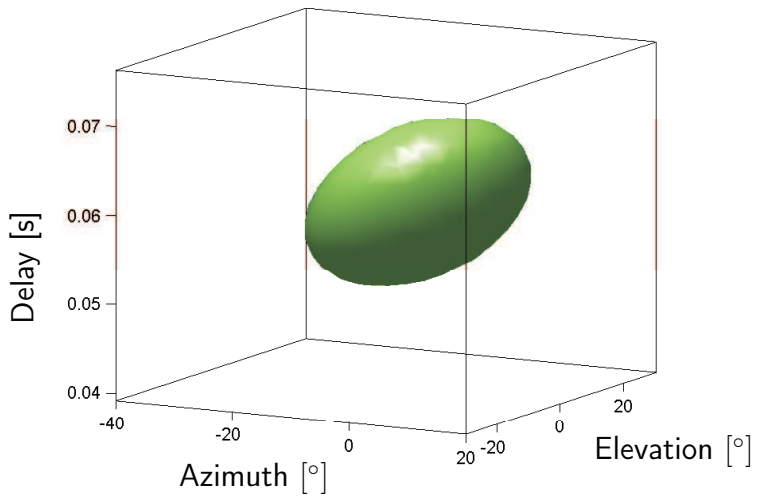

Bidirection, delay and Doppler frequency Dispersion

- Dispersion vector considered:

$$\boldsymbol{\psi} \triangleq [\boldsymbol{\Omega}_1, \boldsymbol{\Omega}_2, \tau, \nu]^{\mathrm{T}}$$

with range $\mathcal{A}^* = \mathcal{S}_2 \times \mathcal{S}_2 \times \mathcal{R}_+ \times \mathcal{R}$, where

$$\mathcal{S}_2 = \{\boldsymbol{x} \in \mathcal{R}^3 : \|\boldsymbol{x}\| = 1\} \subset \mathcal{R}^3$$

denotes a unit sphere.

- We are interested at knowing the centers of gravity, the spreads and the coupling coefficients of the power spectral density $f(\boldsymbol{\psi})$ in the six dispersion dimensions, i.e. $\boldsymbol{\Omega}_1$, $\boldsymbol{\Omega}_2$, τ and ν.
- Recent studies reported in [Betlehem2006] show that the capacity and the diversity gains of MIMO systems depend on the coupling of the DoA and DoD dimensions. Thus, it is necessary to include the coupling coefficients of the PSD into our consideration.

Constraints for deriving the PSD

- Center of gravity fixed:
  The centers of gravity of the bidirection-delay-Doppler frequency power distribution are determined by the mean DoD $\boldsymbol{\mu}_{\boldsymbol{\Omega}_1}$, mean DoA $\boldsymbol{\mu}_{\boldsymbol{\Omega}_2}$, mean delay μ_τ and mean Doppler frequency μ_ν. They are defined as respectively,

$$\boldsymbol{\mu}_{\boldsymbol{\Omega}_k} = \int_{\mathcal{A}^*} \boldsymbol{\Omega}_k f(\boldsymbol{\psi}) \mathrm{d}\boldsymbol{\psi},\ k = 1, 2,$$

$$\mu_\tau = \int_{\mathcal{A}^*} \tau f(\boldsymbol{\psi}) \mathrm{d}\boldsymbol{\psi},$$

$$\mu_\nu = \int_{\mathcal{A}^*} \nu f(\boldsymbol{\psi}) \mathrm{d}\boldsymbol{\psi}$$

Constraints for deriving the PSD (Conti.)

- Spreads fixed:
  the spreads of $f(\boldsymbol{\psi})$ in DoD, DoA, delay and Doppler frequency, denoted with $\sigma_{\boldsymbol{\Omega}_1}$, $\sigma_{\boldsymbol{\Omega}_2}$, σ_τ and σ_ν respectively, can be computed as

$$\sigma_{\boldsymbol{\Omega}_k} = \sqrt{1 - |\boldsymbol{\mu}_{\boldsymbol{\Omega}_k}|^2},\ k = 1, 2,$$

$$\sigma_\tau = \sqrt{\int_{\mathcal{A}^*} (\tau - \mu_\tau)^2 f(\boldsymbol{\psi}) \mathrm{d}\boldsymbol{\psi}},$$

$$\sigma_\nu = \sqrt{\int_{\mathcal{A}^*} (\nu - \mu_\nu)^2 f(\boldsymbol{\psi}) \mathrm{d}\boldsymbol{\psi}},$$

  where $|\cdot|$ denotes the Euclidean norm.

Constraints for deriving the PSD (Conti.)

- Coupling coefficients fixed:
  - $\boldsymbol{\Omega}_k \triangleq \boldsymbol{e}(\phi_k, \theta_k)$, $k = 1, 2$.
  - In the case where only azimuths are considered, the coupling coefficient of two directions can be defined as one scalar.
  - However, when both azimuth and elevation are considered, we need to introduce a covariance matrix, which is used to describe the correlation of the components of directions on three axes of the Cartesian coordinate system.
  - define the coupling coefficient matrix $\boldsymbol{\rho}_{\boldsymbol{\Omega}_1\boldsymbol{\Omega}_2}$ of two directions $\boldsymbol{\Omega}_1$ and $\boldsymbol{\Omega}_2$ as

$$\boldsymbol{\rho}_{\boldsymbol{\Omega}_1\boldsymbol{\Omega}_2} \triangleq \frac{1}{\sigma_{\boldsymbol{\Omega}_1}\sigma_{\boldsymbol{\Omega}_2}} \int_{\mathcal{A}^*} (\boldsymbol{\Omega}_1 - \boldsymbol{\mu}_{\boldsymbol{\Omega}_1})^{\mathrm{T}} \boldsymbol{R}_1 \boldsymbol{R}_2^{\mathrm{T}} (\boldsymbol{\Omega}_2 - \boldsymbol{\mu}_{\boldsymbol{\Omega}_2}) f(\boldsymbol{\psi}) \mathrm{d}\boldsymbol{\psi} \in \mathcal{R}^{3\times 3},$$

  $\boldsymbol{R}_k$, $k = 1, 2$ are two orthonormal matrices.

Constraints for deriving the PSD (Conti.)

$$\boldsymbol{\rho}_{\boldsymbol{\Omega}_1\boldsymbol{\Omega}_2} \triangleq \frac{1}{\sigma_{\boldsymbol{\Omega}_1}\sigma_{\boldsymbol{\Omega}_2}} \int_{\mathcal{A}^*} (\boldsymbol{\Omega}_1 - \boldsymbol{\mu}_{\boldsymbol{\Omega}_1})^{\mathrm{T}} \boldsymbol{R}_1 \boldsymbol{R}_2^{\mathrm{T}} (\boldsymbol{\Omega}_2 - \boldsymbol{\mu}_{\boldsymbol{\Omega}_2}) f(\boldsymbol{\psi}) \mathrm{d}\boldsymbol{\psi} \in \mathcal{R}^{3\times 3},$$

- The function of $\boldsymbol{R}_k$ is to align the difference vectors $\boldsymbol{\Omega}_k - \boldsymbol{\mu}_{\boldsymbol{\Omega}_k}$ to the same Cartesian coordinate system.
- The expression of $\boldsymbol{R}_k$ can be easily defined in the case where directions are determined by azimuth only, i.e. with directions' ends located on a unit circle.
- However, it is non-trivial to write an analytical expression of $\boldsymbol{R}_k$ when the directions' ends are located on a unit sphere.
- In the following, we provide a method for computing $(\boldsymbol{\Omega}_k - \boldsymbol{\mu}_{\boldsymbol{\Omega}_k})^{\mathrm{T}} \boldsymbol{R}_k$ rather than giving explicitly the exact expression of $\boldsymbol{R}_k$. This computation method allows aligning $(\boldsymbol{\Omega}_k - \boldsymbol{\mu}_{\boldsymbol{\Omega}_k})$, $k = 1, 2$ in the same spherical coordinate system as required for computing $\boldsymbol{\rho}_{\boldsymbol{\Omega}_1\boldsymbol{\Omega}_2}$.

Constraints for deriving the PSD (Conti.)

- The direction $\boldsymbol{\Omega}$ in the spherical coordinate system can be written as

$$\boldsymbol{\Omega} = \boldsymbol{e}_r \cdot 1 + \boldsymbol{e}_\theta \cdot \theta + \boldsymbol{e}_\phi \cdot \phi,$$

  where $\boldsymbol{e}_r$, $\boldsymbol{e}_\theta$ and $\boldsymbol{e}_\phi$ denote respectively the radius, the co-elevation and the azimuth axes of the spherical coordinate system.
- Rotating $\boldsymbol{\Omega}$ to the direction $\boldsymbol{\Omega}' = \boldsymbol{e}(\phi', \theta')$ can be expressed as follows:

$$\boldsymbol{\Omega} \oplus \Delta\boldsymbol{\Omega} = \boldsymbol{\Omega}',$$

  where $\Delta\boldsymbol{\Omega} = \boldsymbol{e}_r \cdot 0 + \boldsymbol{e}_\theta \cdot (\theta' - \theta) + \boldsymbol{e}_\phi \cdot (\phi' - \phi)$, and $\oplus$ denotes the axis-wise summation.

Constraints for deriving the PSD (Conti.)

- Thus, the operation $(\boldsymbol{\Omega}_1 - \boldsymbol{\mu}_{\boldsymbol{\Omega}_1})^{\mathrm{T}} \boldsymbol{R}_1$ can be performed using the following steps:
  1. Calculate $(\boldsymbol{\Omega}_1 - \boldsymbol{\mu}_{\boldsymbol{\Omega}_1})$ in the spherical coordinate system
  2. Specify a rotational vector
     $\Delta\boldsymbol{\Omega} = \boldsymbol{e}_r \cdot 0 + \boldsymbol{e}_\theta \cdot (\bar{\theta}_2 - \bar{\theta}_1) + \boldsymbol{e}_\phi \cdot (\bar{\phi}_2 - \bar{\phi}_1)$
  3. Perform the operation $(\boldsymbol{\Omega}_1 - \boldsymbol{\mu}_{\boldsymbol{\Omega}_1}) \oplus \Delta\boldsymbol{\Omega}$.
  4. Rewrite the obtained vector in the Cartesian coordinate system.
- The same method is used for computing $(\boldsymbol{\Omega}_2 - \boldsymbol{\mu}_{\boldsymbol{\Omega}_2})^{\mathrm{T}} \boldsymbol{R}_2$, with the rational vector $\Delta\boldsymbol{\Omega} = \boldsymbol{e}_r \cdot 0 + \boldsymbol{e}_\theta \cdot (\bar{\theta}_1 - \bar{\theta}_2) + \boldsymbol{e}_\phi \cdot (\bar{\phi}_1 - \bar{\phi}_2)$.
- The calculation of $(\boldsymbol{\Omega}_1 - \boldsymbol{\mu}_{\boldsymbol{\Omega}_1})^{\mathrm{T}} \boldsymbol{R}_1 \boldsymbol{R}_2^{\mathrm{T}} (\boldsymbol{\Omega}_2 - \boldsymbol{\mu}_{\boldsymbol{\Omega}_2})$ can be calculated as the outer product of two obtained vectors represented in the Cartesian coordinate system.

Constraints for deriving the PSD (Conti.)

- The correlation coefficient between the dispersion in a direction $\boldsymbol{\Omega}_k$, $k \in [1, 2]$ and in the delay τ, as well as the Doppler frequency ν are defined as

$$\boldsymbol{\rho}_{\boldsymbol{\Omega}_k \tau} \triangleq \frac{1}{\sigma_{\boldsymbol{\Omega}_k} \sigma_\tau} \int_{\mathcal{A}^*} (\boldsymbol{\Omega}_k - \boldsymbol{\mu}_{\boldsymbol{\Omega}_k})^{\mathrm{T}} \boldsymbol{R}_k (\tau - \mu_\tau) f(\boldsymbol{\psi}) \mathrm{d}\boldsymbol{\psi} \in \mathcal{R}^{1\times 3},$$

$$\boldsymbol{\rho}_{\boldsymbol{\Omega}_k \nu} \triangleq \frac{1}{\sigma_{\boldsymbol{\Omega}_k} \sigma_\nu} \int_{\mathcal{A}^*} (\boldsymbol{\Omega}_k - \boldsymbol{\mu}_{\boldsymbol{\Omega}_k})^{\mathrm{T}} \boldsymbol{R}_k (\nu - \mu_\nu) f(\boldsymbol{\psi}) \mathrm{d}\boldsymbol{\psi} \in \mathcal{R}^{1\times 3},$$

$$k = 1, 2.$$

- The coupling coefficient between the dispersion in τ and ν is defined as

$$\rho_{\tau\nu} \triangleq \frac{1}{\sigma_\tau \sigma_\nu} \int_{\mathcal{A}^*} (\tau - \mu_\tau)(\nu - \mu_\nu) f(\boldsymbol{\psi}) \mathrm{d}\boldsymbol{\psi} \in \mathcal{R}, \quad k = 1, 2.$$

Constraints for deriving the PSD (Conti.)

- We also introduce $(\boldsymbol{\Omega}_k - \boldsymbol{\mu}_{\boldsymbol{\Omega}_k})^{\mathrm{T}} \boldsymbol{R}_k$ in order to maintain the rotational invariance of $\boldsymbol{\rho}_{\boldsymbol{\Omega}_k \tau}, \boldsymbol{\rho}_{\boldsymbol{\Omega}_k \nu}$, i.e. $\boldsymbol{\rho}_{\boldsymbol{\Omega}_k \tau}$ and $\boldsymbol{\rho}_{\boldsymbol{\Omega}_k \nu}$ do not change when the center of gravity of $f(\boldsymbol{\Omega}_k, \tau, \nu) \triangleq \int_{\mathcal{A}^*} f(\boldsymbol{\psi}) \mathrm{d}\boldsymbol{\Omega}_{k'}$ with $k' \in [1, 2]$ and $k' \neq k$ is changed.

Properties of the coupling coefficients

- Coefficients in the matrix $\boldsymbol{\rho}_{\boldsymbol{\Omega}_1\boldsymbol{\Omega}_2}$, the vectors $\boldsymbol{\rho}_{\boldsymbol{\Omega}_1\tau}$, $\boldsymbol{\rho}_{\boldsymbol{\Omega}_1\nu}$, $\boldsymbol{\rho}_{\boldsymbol{\Omega}_2\tau}$, $\boldsymbol{\rho}_{\boldsymbol{\Omega}_2\nu}$ and $\rho_{\tau\nu}$ range within $[-1, 1]$
- They are equal to zero when the spreads in the corresponding dimensions are decoupled, i.e. in the case where the bidirection-delay-Doppler-frequency PSD can be factorized as the product of the marginal PSDs in the considered dimensions
- When the spreads in any pair (a, b) of $\boldsymbol{\Omega}_1$, $\boldsymbol{\Omega}_2$,τ and ν are linearly dependent, i.e. the marginal PSD $f(a, b)$ is a straight line, the coefficient ρ_{ab} is close to 1 or -1, with sign determined by the increasing or decreasing slope of the line
- They are rotational invariant, and have analytical expressions.
- They can enter the component MaxEnt normalized PSD as explicit parameters
- Allowing deriving the maximum likelihood estimators of these parameters

Deriving the 6-D PSD

- For notational convenience, we use

$$\begin{aligned}\boldsymbol{\theta} = (&\mu_\tau, \mu_\nu, \boldsymbol{\mu}_{\boldsymbol{\Omega}_1}, \boldsymbol{\mu}_{\boldsymbol{\Omega}_2},\\ &\sigma_\tau, \sigma_\nu, \sigma_{\boldsymbol{\Omega}_1}, \sigma_{\boldsymbol{\Omega}_2},\\ &\boldsymbol{\rho}_{\boldsymbol{\Omega}_1\boldsymbol{\Omega}_2}, \boldsymbol{\rho}_{\boldsymbol{\Omega}_1\tau}, \boldsymbol{\rho}_{\boldsymbol{\Omega}_1\nu}, \boldsymbol{\rho}_{\boldsymbol{\Omega}_2\tau}, \boldsymbol{\rho}_{\boldsymbol{\Omega}_2\nu}, \rho_{\boldsymbol{\tau}\nu})\end{aligned}$$

  to denote the parameters characterizing the bidirection-delay-Doppler frequency PSD $f(\boldsymbol{\psi})$.

- We seek for a bidirection-delay-Doppler frequency PSD that maximizes the entropy under the constraint that the parameters are all fixed.
- Such a PSD leaves the highest uncertainty about the shape of the PSD of a path component provided the parameters are known. .
- This means that estimation of the these parameters with any other form of PSD can be better than using the MaxEnt PSD.

Derivation : Step 1

Specify the constraints:

Constraint 1: $\int_{\mathcal{A}^*} \boldsymbol{\Omega}_1 f(\boldsymbol{\psi}) \mathrm{d}\boldsymbol{\psi}$ is fixed,

Constraint 2: $\int_{\mathcal{A}^*} \boldsymbol{\Omega}_2 f(\boldsymbol{\psi}) \mathrm{d}\boldsymbol{\psi}$ is fixed,

Constraint 3: $\int_{\mathcal{A}^*} \tau f(\boldsymbol{\psi}) \mathrm{d}\boldsymbol{\psi}$ is fixed,

Constraint 4: $\int_{\mathcal{A}^*} \tau^2 f(\boldsymbol{\psi}) \mathrm{d}\boldsymbol{\psi}$ is fixed,

Constraint 5: $\int_{\mathcal{A}^*} \boldsymbol{\Omega}_2^{\mathrm{T}} \boldsymbol{R}_1 \boldsymbol{R}_2^{\mathrm{T}} \boldsymbol{\Omega}_1 f(\boldsymbol{\psi}) \mathrm{d}\boldsymbol{\psi}$ is fixed,

Constraint 6: $\int_{\mathcal{A}^*} \boldsymbol{\Omega}_1^{\mathrm{T}} \boldsymbol{R}_1 \tau f(\boldsymbol{\psi}) \mathrm{d}\boldsymbol{\psi}$ is fixed,

Constraint 7: $\int_{\mathcal{A}^*} \boldsymbol{\Omega}_2^{\mathrm{T}} \boldsymbol{R}_2 \tau f(\boldsymbol{\psi}) \mathrm{d}\boldsymbol{\psi}$ is fixed.

Derivation : Step 1

Specify the constraints:

Constraint 8: $\int_{\mathcal{A}^*} \nu f(\boldsymbol{\psi}) \mathrm{d}\boldsymbol{\psi}$ is fixed,

Constraint 9: $\int_{\mathcal{A}^*} \nu^2 f(\boldsymbol{\psi}) \mathrm{d}\boldsymbol{\psi}$ is fixed,

Constraint 10: $\int_{\mathcal{A}^*} \boldsymbol{\Omega}_1^{\mathrm{T}} \boldsymbol{R}_1 \nu f(\boldsymbol{\psi}) \mathrm{d}\boldsymbol{\psi}$ is fixed,

Constraint 11: $\int_{\mathcal{A}^*} \boldsymbol{\Omega}_2^{\mathrm{T}} \boldsymbol{R}_2 \nu f(\boldsymbol{\psi}) \mathrm{d}\boldsymbol{\psi}$ is fixed.

Constraint 12: $\int_{\mathcal{A}^*} \tau \nu f(\boldsymbol{\psi}) \mathrm{d}\boldsymbol{\psi}$ is fixed,

Derivation : Step 2

Lagrange principle: Invoking the MaxEnt theorem, the sought PSD can be calculated to be

$$f_{\mathrm{MaxEnt}}(\boldsymbol{\psi}) = \exp\{b_0 + \boldsymbol{b}_1^{\mathrm{T}}\boldsymbol{\Omega}_1 + \boldsymbol{b}_2^{\mathrm{T}}\boldsymbol{\Omega}_2 + b_3\tau + b_4\tau^2 + \boldsymbol{b}_5\boldsymbol{\Omega}_2^{\mathrm{T}}\boldsymbol{R}_1\boldsymbol{R}_2^{\mathrm{T}}\boldsymbol{\Omega}_1 + \boldsymbol{b}_6\boldsymbol{\Omega}_1^{\mathrm{T}}\boldsymbol{R}_1\tau + \boldsymbol{b}_7\boldsymbol{\Omega}_2^{\mathrm{T}}\boldsymbol{R}_2\tau + b_8\nu + b_9\nu^2 + \boldsymbol{b}_{10}\boldsymbol{\Omega}_1^{\mathrm{T}}\boldsymbol{R}_1\nu + \boldsymbol{b}_{11}\boldsymbol{\Omega}_2^{\mathrm{T}}\boldsymbol{R}_2\nu + b_{12}\tau\nu\},$$

where

- b_0 is the normalization factor such that $\int_{\mathcal{A}^*} f_{\mathrm{MaxEnt}}(\boldsymbol{\psi})\mathrm{d}\boldsymbol{\psi} = 1$, and
- $\boldsymbol{b}_1, \boldsymbol{b}_2, b_3, \cdots, b_{12}$ are obtained by applying Constraints $1, 2, \cdots, 12$ respectively.
- $\boldsymbol{b} = (\boldsymbol{b}_1, \boldsymbol{b}_2, b_3, b_4, \boldsymbol{b}_5, \boldsymbol{b}_6, \boldsymbol{b}_7, b_8, b_9, \boldsymbol{b}_{10}, \boldsymbol{b}_{11}, b_{12})$ with $\boldsymbol{b}_1, \boldsymbol{b}_2, \boldsymbol{b}_6, \boldsymbol{b}_7, \boldsymbol{b}_{10}, \boldsymbol{b}_{11} \in \mathbb{R}^3$, $\boldsymbol{b}_5 \in \mathbb{R}^{3\times 3}$.
- The total number of the parameters of the PSD is 30
- The constraint that the directions are all unit vectors may reduce the 30 parameters to 21, similar with the case of 6-variate Gaussian distribution.

Derivation : Step 3 Approximation

Consider the case where $f_{\mathrm{MaxEnt}}(\boldsymbol{\psi})$ is highly concentrated:

- In such a case, the entropy-maximizing PSD can be approximated by the Gaussian PSD with $\boldsymbol{\theta}$ as the parameters.
- By change of parameters, we may identify the expression of $\boldsymbol{b}$ in terms of $\boldsymbol{\theta}$, and then obtain a novel expression of $f_{\mathrm{MaxEnt}}(\boldsymbol{\psi})$ parameterized by $\boldsymbol{\theta}$.
- Since this newly expressed $f_{\mathrm{MaxEnt}}(\boldsymbol{\psi})$ still satisfies the maximum-entropy requirement subject to the constraints defined, the PSD is applicable regardless of the condition that the power distribution is highly concentrated.
- The benefit of using this new expression of $f_{\mathrm{MaxEnt}}(\boldsymbol{\psi})$ in terms of $\boldsymbol{\theta}$ is that it allows estimation of $\boldsymbol{\theta}$ directly by using e.g. maximum-likelihood-based algorithms derived based on the generic form of the PSD from the received signals.

Special case of highly-concentrated PSD

- $f(\boldsymbol{\omega})$ is used to denote the PSD of the biazimuth-bielevation-delay-Doppler-frequency power distribution, where the vector

$$\boldsymbol{\omega} \triangleq [\phi_1, \theta_1, \phi_2, \theta_2, \tau, \nu]^{\mathrm{T}}$$

has the support
$\mathcal{C} \triangleq (0, 2\pi] \times [-\pi/2, \pi/2\pi] \times (0, 2\pi] \times [-\pi/2, \pi/2\pi] \times \mathcal{R}_+ \times \mathcal{R}$.

- The center of gravity

$$\mu_{\boldsymbol{\omega}} = [\mu_{\phi_1}, \mu_{\theta_1}, \mu_{\phi_2}, \mu_{\theta_2}, \mu_{\tau}, \mu_{\nu}]^{\mathrm{T}}$$

of the biazimuth-bielevation-delay-Doppler frequency component PSD $f(\boldsymbol{\omega})$ is calculated as

$$\mu_{\boldsymbol{\omega}} = \int_{\mathcal{C}} \boldsymbol{\omega} f(\boldsymbol{\omega}) \mathrm{d}\boldsymbol{\omega}.$$

- The spreads of $f(\boldsymbol{\omega})$ in biazimuth, bielevation, delay and Doppler

Special case of highly-concentrated PSD

- The spreads of $f(\boldsymbol{\omega})$ in biazimuth, bielevation, delay and Doppler frequency are computed as

$$\boldsymbol{\sigma}_{\boldsymbol{\omega}} = \begin{bmatrix} \sigma_{\phi_1} \\ \sigma_{\theta_1} \\ \sigma_{\phi_2} \\ \sigma_{\theta_2} \\ \sigma_{\tau} \\ \sigma_{\nu} \end{bmatrix} = \sqrt{\int_{\mathcal{C}} (\boldsymbol{\omega} - \mu_{\boldsymbol{\omega}})^2 f(\boldsymbol{\omega}) \mathrm{d}\boldsymbol{\omega}}.$$

- The coupling coefficients of the spreads in different dimensions are defined by analogy with the correlation coefficients of two linear random variables as

$$\rho_{ab}^2 = \int_{\mathcal{C}} (a - \mu_a)(b - \mu_b) f(\boldsymbol{\omega}) \mathrm{d}\boldsymbol{\omega}$$

with a and b representing any pair of ϕ_1,θ_1,ϕ_2,θ_2,τ and ν .

Special case of highly-concentrated PSD

- For notational convenience, we use

$$\begin{aligned}\boldsymbol{\eta} = (&\mu_{\phi_1},\mu_{\theta_1},\mu_{\phi_2},\mu_{\theta_2},\mu_\tau,\mu_\nu,\sigma_{\phi_1},\sigma_{\theta_1},\sigma_{\phi_2},\sigma_{\theta_2},\sigma_\tau,\sigma_\nu,\\ &\rho_{\phi_1\phi_2},\rho_{\phi_1\theta_1},\rho_{\phi_1\theta_2},\rho_{\phi_1\tau},\rho_{\phi_1\nu},\rho_{\phi_2\theta_1},\rho_{\phi_2\theta_2},\rho_{\phi_2\tau},\\ &\rho_{\phi_2\nu},\rho_{\theta_1\theta_2},\rho_{\theta_1\tau},\rho_{\theta_1\nu},\rho_{\theta_2\tau},\rho_{\theta_2\nu},\rho_{\tau\nu})\end{aligned}$$

  to denote the parameters of the bidirection-delay-Doppler frequency PSD $f(\boldsymbol{\omega})$.

- Thus, the estimates of $\boldsymbol{\theta}$ can be approximated by the estimates of $\boldsymbol{\eta}$.

Special case of highly-concentrated PSD

The PSD that maximizes the entropy subject to the constraint of fixed $\boldsymbol{\eta}$:

$$f_{\mathrm{MaxEnt}}(\boldsymbol{\omega}) \propto \exp\left[-\frac{1}{2|\boldsymbol{B}|}\sum_{j=1}^{6}\sum_{i=1}^{6}|\boldsymbol{B}|_{jk}\left(\frac{\boldsymbol{\omega}_j-\boldsymbol{\mu}_{\boldsymbol{\omega},j}}{\sigma_{\boldsymbol{\omega},j}}\right)\left(\frac{\boldsymbol{\omega}_k-\boldsymbol{\mu}_{\boldsymbol{\omega},k}}{\sigma_{\boldsymbol{\omega},k}}\right)\right],$$

where

$$\boldsymbol{\mu}_{\boldsymbol{\omega}} = \begin{bmatrix}\mu_{\phi_1}\\ \mu_{\theta_1}\\ \mu_{\phi_2}\\ \mu_{\theta_2}\\ \mu_{\tau}\\ \mu_{\nu}\end{bmatrix},\ \boldsymbol{B} = \begin{bmatrix} 1 & \rho_{\phi_1\theta_1} & \rho_{\phi_1\phi_2} & \rho_{\phi_1\theta_2} & \rho_{\phi_1\tau} & \rho_{\phi_1\nu}\\ \rho_{\theta_1\phi_1} & 1 & \rho_{\theta_1\phi_2} & \rho_{\theta_1\theta_2} & \rho_{\theta_1\tau} & \rho_{\theta_1\nu}\\ \rho_{\phi_2\phi_1} & \rho_{\phi_2\theta_1} & 1 & \rho_{\phi_2\theta_2} & \rho_{\phi_2\tau} & \rho_{\phi_2\nu}\\ \rho_{\theta_2\phi_1} & \rho_{\theta_2\theta_1} & \rho_{\theta_2\phi_2} & 1 & \rho_{\theta_2\tau} & \rho_{\theta_2\nu}\\ \rho_{\tau\phi_1} & \rho_{\tau\theta_1} & \rho_{\tau\phi_2} & \rho_{\tau\theta_2} & 1 & \rho_{\tau\nu}\\ \rho_{\nu\phi_1} & \rho_{\nu\theta_1} & \rho_{\nu\phi_2} & \rho_{\nu\theta_2} & \rho_{\nu\tau} & 1\end{bmatrix},$$

$|\boldsymbol{B}|$ denotes the determinant of $\boldsymbol{B}$, $|\boldsymbol{B}|_{jk}$ is the cofactor of $\boldsymbol{B}_{jk}$, where $\boldsymbol{B}_{jk}$ represents the (j,k)th entry, $\boldsymbol{\mu}_{\boldsymbol{\omega},j}$ denotes the jth entry of the column vector $\boldsymbol{\mu}_{\boldsymbol{\omega},j}$, and $\boldsymbol{\sigma}_{\boldsymbol{\omega},j}$ represents the jth entry of $\boldsymbol{\sigma}_{\boldsymbol{\omega}}$.

Remarks

- The subtraction of angular variables, e.g. $\phi_k - \mu_{\phi_k}$, $\theta_k - \mu_{\theta_k}$, $k = 1, 2$ arising when calculating $\boldsymbol{\omega} - \boldsymbol{\mu}_{\boldsymbol{\omega}}$ is defined in such a way that the resulting azimuth lies in the range $[-\pi, \pi)$ and elevation lies in the range $[-\pi/2, \pi/2)$. This rationale is applicable for the subtraction of angular variables throughout this report.
- Notice that the MaxEnt biazimuth-bielevation-delay-Doppler frequency PSD $f_{\mathrm{MaxEnt}}(\boldsymbol{\omega})$ in (??) has the same form as a truncated Gaussian pdf with the support of $\mathcal{C}$.
- Strictly speaking the traditional meaning of σ_{ϕ_1},σ_{θ_1},σ_{ϕ_2}, σ_{θ_2}, $\rho_{\phi_1\theta_1}$,$\rho_{\phi_1\phi_2}$,$\rho_{\phi_1\theta_2}$,$\rho_{\phi_1\tau}$,$\rho_{\phi_1\nu}$, $\rho_{\theta_1\phi_2}$,$\rho_{\theta_1\theta_2}$,$\rho_{\theta_1\tau}$,$\rho_{\theta_1\nu}$, $\rho_{\phi_2\theta_2}$,$\rho_{\phi_2\tau}$,$\rho_{\phi_2\nu}$,$\rho_{\theta_2\tau}$,$\rho_{\theta_2\nu}$, and $\rho_{\tau\nu}$ as second-order central moments of a 6-variate Gaussian distribution does not apply anymore here, due to the fact that the angular ranges are bounded.
- However, these parameters provide good approximations of these moments when σ_{ϕ_1},σ_{θ_1},σ_{ϕ_2} and σ_{θ_2} are small.

Remarks

- According to the MaxEnt theorem [Mardia1976], a pdf which maximizes the entropy subject to certain constraints is unique.
- As $f_{\mathrm{MaxEnt}}(\boldsymbol{\omega})$ and $f_{\mathrm{MaxEnt}}(\boldsymbol{\omega})$ both maximize the entropy subject to the similar constraints, it is reasonable to postulate that the approximation

$$f_{\mathrm{MaxEnt}}(\boldsymbol{\psi})\big|_{\boldsymbol{\psi}=(\boldsymbol{e}(\phi_1,\theta_1),\boldsymbol{e}(\phi_2,\theta_2),\tau,\nu)} \approx f_{\mathrm{MaxEnt}}(\boldsymbol{\omega})$$

holds in the case of highly-concentrated PSD. This postulation is used to find the expression of $\boldsymbol{b}$ in terms of $\boldsymbol{\theta}$ in the sequel.

Expression of b in terms of θ

- Rewrite $\boldsymbol{b}_1$ and $\boldsymbol{b}_2$ in $f_{\mathrm{MaxEnt}}(\boldsymbol{\psi})$ as

$$\boldsymbol{b}_i = \kappa_i \boldsymbol{e}(\bar{\phi}_k, \bar{\theta}_k),\ k = 1, 2,\ \text{with } \kappa_i = |\boldsymbol{b}_i|$$
$$\boldsymbol{R}_1 \triangleq \boldsymbol{e}_r \cdot 0 + \boldsymbol{e}_\theta \cdot (\bar{\theta}_2 - \bar{\theta}_1) + \boldsymbol{e}_\phi \cdot (\bar{\phi}_2 - \bar{\phi}_1),$$
$$\boldsymbol{R}_2 \triangleq \boldsymbol{e}_r \cdot 0 + \boldsymbol{e}_\theta \cdot (\bar{\theta}_1 - \bar{\theta}_2) + \boldsymbol{e}_\phi \cdot (\bar{\phi}_1 - \bar{\phi}_2)$$

.

- Inserting $f_{\mathrm{MaxEnt}}(\boldsymbol{\psi})$, with slight abuse of notation we obtain

$$\begin{aligned}
f_{\mathrm{MaxEnt}}(\boldsymbol{\omega}; \boldsymbol{b}) = \exp\{ & b_0 \\
& + b_1 \cos(\phi_1 - \bar{\phi}_1) + b_2 \cos(\theta_1 - \bar{\theta}_1) + b_3 \cos(\phi_2 - \bar{\phi}_2) + b_4 \cos(\theta_2 - \bar{\theta}_2) + b_5 (\tau - \bar{\tau})^2 + b_6 (\nu - \bar{\nu})^2 \\
& + b_7 \cos((\phi_1 - \bar{\phi}_1) - (\phi_2 - \bar{\phi}_2)) + b_8 \cos((\theta_1 - \bar{\theta}_1) - (\theta_2 - \bar{\theta}_2)) + b_9 \cos((\phi_1 - \bar{\phi}_1) - (\theta_2 - \bar{\theta}_2)) \\
& + b_{10} \cos((\theta_1 - \bar{\theta}_1) - (\phi_2 - \bar{\phi}_2)) + b_{11} \cos((\phi_1 - \bar{\phi}_1) - (\theta_1 - \bar{\theta}_1)) + b_{12} \cos((\phi_2 - \bar{\phi}_2) - (\theta_2 - \bar{\theta}_2)) \\
& + b_{13} (\tau - \bar{\tau}) \sin(\phi_1 - \bar{\phi}_1) + b_{14} (\tau - \bar{\tau}) \sin(\theta_1 - \bar{\theta}_1) + b_{15} (\tau - \bar{\tau}) \sin(\phi_2 - \bar{\phi}_2) \\
& + b_{16} (\tau - \bar{\tau}) \sin(\theta_2 - \bar{\theta}_2) + b_{17} (\nu - \bar{\nu}) \sin(\phi_1 - \bar{\phi}_1) + b_{18} (\nu - \bar{\nu}) \sin(\theta_1 - \bar{\theta}_1) \\
& + b_{19} (\nu - \bar{\nu}) \sin(\phi_2 - \bar{\phi}_2) + b_{20} (\nu - \bar{\nu}) \sin(\theta_2 - \bar{\theta}_2) + b_{21} (\tau - \bar{\tau})(\nu - \bar{\nu}) \}.
\end{aligned}$$

Expression of b in η

- In the case where the component PSD is highly concentrated, the following approximations hold:

$$\cos(\phi_k - \bar{\phi}_k) \approx 1 - (\phi_k - \bar{\phi}_k)^2/2, \sin(\phi_k - \bar{\phi}_k) \approx \phi_k - \bar{\phi}_k,$$
$$\cos(\theta_k - \bar{\theta}_k) \approx 1 - (\theta_k - \bar{\theta}_k)^2/2, \sin(\theta_k - \bar{\theta}_k) \approx \theta_k - \bar{\theta}_k,\ k = 1, 2.$$

- Analytical expressions of $\boldsymbol{b} = b_1, b_2, ..., b_{12}$ in terms of $\boldsymbol{\eta}$:

$$b_1 = \frac{|\boldsymbol{B}|_{11}}{|\boldsymbol{B}|\sigma_{\phi_1^2}} - (b_7 + b_9 + b_{11}),\ \ b_2 = \frac{|\boldsymbol{B}|_{22}}{|\boldsymbol{B}|\sigma_{\theta_1^2}} - (b_8 + b_{10} + b_{11}),\ \ b_3 = \frac{|\boldsymbol{B}|_{33}}{|\boldsymbol{B}|\sigma_{\phi_2^2}} - (b_7 + b_{10} + b_{12})$$

$$b_4 = \frac{|\boldsymbol{B}|_{44}}{|\boldsymbol{B}|\sigma_{\theta_2^2}} - (b_8 + b_9 + b_{12}),\ \ b_5 = -\frac{|\boldsymbol{B}|_{55}}{2|\boldsymbol{B}|\sigma_\tau^2},\ \ b_6 = -\frac{|\boldsymbol{B}|_{66}}{2|\boldsymbol{B}|\sigma_\nu^2},\ \ b_7 = \frac{-|\boldsymbol{B}|_{13} - |\boldsymbol{B}|_{31}}{2|\boldsymbol{B}|\sigma_{\phi_1}\sigma_{\phi_2}}$$

$$b_8 = \frac{-|\boldsymbol{B}|_{24} - |\boldsymbol{B}|_{42}}{2|\boldsymbol{B}|\sigma_{\theta_1}\sigma_{\theta_2}},\ \ b_9 = \frac{-|\boldsymbol{B}|_{14} - |\boldsymbol{B}|_{41}}{2|\boldsymbol{B}|\sigma_{\phi_1}\sigma_{\theta_2}},\ \ b_{10} = \frac{-|\boldsymbol{B}|_{23} - |\boldsymbol{B}|_{32}}{2|\boldsymbol{B}|\sigma_{\theta_1}\sigma_{\phi_2}},\ \ b_{11} = \frac{-|\boldsymbol{B}|_{12} - |\boldsymbol{B}|_{21}}{2|\boldsymbol{B}|\sigma_{\phi_1}\sigma_{\theta_1}}$$

$$b_{12} = \frac{-|\boldsymbol{B}|_{34} - |\boldsymbol{B}|_{43}}{2|\boldsymbol{B}|\sigma_{\phi_2}\sigma_{\theta_2}},\ \ b_{13} = \frac{-|\boldsymbol{B}|_{15} - |\boldsymbol{B}|_{51}}{2|\boldsymbol{B}|\sigma_{\phi_1}\sigma_\tau},\ \ b_{14} = \frac{-|\boldsymbol{B}|_{25} - |\boldsymbol{B}|_{52}}{2|\boldsymbol{B}|\sigma_{\theta_1}\sigma_\tau},\ \ b_{15} = \frac{-|\boldsymbol{B}|_{35} - |\boldsymbol{B}|_{53}}{2|\boldsymbol{B}|\sigma_{\phi_2}\sigma_\tau}$$

$$b_{16} = \frac{-|\boldsymbol{B}|_{45} - |\boldsymbol{B}|_{54}}{2|\boldsymbol{B}|\sigma_{\theta_2}\sigma_\tau},\ \ b_{17} = \frac{-|\boldsymbol{B}|_{16} - |\boldsymbol{B}|_{61}}{2|\boldsymbol{B}|\sigma_{\phi_1}\sigma_\nu},\ \ b_{18} = \frac{-|\boldsymbol{B}|_{26} - |\boldsymbol{B}|_{62}}{2|\boldsymbol{B}|\sigma_{\theta_1}\sigma_\nu}$$

$$b_{19} = \frac{-|\boldsymbol{B}|_{36} - |\boldsymbol{B}|_{63}}{2|\boldsymbol{B}|\sigma_{\phi_2}\sigma_\nu},\ \ b_{20} = \frac{-|\boldsymbol{B}|_{46} - |\boldsymbol{B}|_{64}}{2|\boldsymbol{B}|\sigma_{\theta_2}\sigma_\nu},\ \ b_{21} = \frac{-|\boldsymbol{B}|_{56} - |\boldsymbol{B}|_{65}}{2|\boldsymbol{B}|\sigma_\tau\sigma_\nu}$$

Remarks

- Replacing the elements of $\boldsymbol{\eta}$ by their approximates in $\boldsymbol{\theta}$, we can obtain the mapping between $\boldsymbol{b}$ and $\boldsymbol{\theta}$.
- Using this mapping, $f_{\mathrm{MaxEnt}}(\boldsymbol{\psi};\boldsymbol{b})$ can be written as $f_{\mathrm{MaxEnt}}(\boldsymbol{\psi};\boldsymbol{\theta})$.
- Notice that in the case where the component PSD is highly concentrated, the parameters $\boldsymbol{\theta}$ of $f_{\mathrm{MaxEnt}}(\boldsymbol{\psi};\boldsymbol{\theta})$ represent the parameters of interests, i.e. the values of $\boldsymbol{\theta}$ can be considered as the estimates of the parameters of interests.
- When the component PSD is not highly concentrated, the expression $f_{\mathrm{MaxEnt}}(\boldsymbol{\psi};\boldsymbol{\theta})$ is still applicable. However, the values of $\boldsymbol{\theta}$ when the spreads of the PSD are large do not have the meaning of the parameters of interests.
- In such a case, the parameters of interest $\boldsymbol{\theta}$ have to be calculated based on their definitions by using $f_{\mathrm{MaxEnt}}(\boldsymbol{\psi};\boldsymbol{\theta})$.

Model of the received signal in MIMO systems

- For the case where totally D propagation paths existing between the Tx and the Rx, the bidirection-delay-Doppler-dual-polarized spread function $\boldsymbol{H}(\boldsymbol{\Omega}_1, \boldsymbol{\Omega}_2, \tau, \nu)$ of the channel can be written as

$$\boldsymbol{H}(\boldsymbol{\Omega}_1, \boldsymbol{\Omega}_2, \tau, \nu) = \sum_{d=1}^{D} \boldsymbol{H}_d(\boldsymbol{\Omega}_1, \boldsymbol{\Omega}_2, \tau, \nu),$$

where

$$\begin{aligned} \boldsymbol{H}_d(\boldsymbol{\Omega}_1, \boldsymbol{\Omega}_2, \tau, \nu) &= [H_{d,p_1,p_2}(\boldsymbol{\Omega}_1, \boldsymbol{\Omega}_2, \tau, \nu); \{p_1, p_2\} \in [1, 2]] \\ &= \begin{bmatrix} H_{d,1,1}(\boldsymbol{\Omega}_1, \boldsymbol{\Omega}_2, \tau, \nu) & H_{d,2,1}(\boldsymbol{\Omega}_1, \boldsymbol{\Omega}_2, \tau, \nu) \\ H_{d,1,2}(\boldsymbol{\Omega}_1, \boldsymbol{\Omega}_2, \tau, \nu) & H_{d,2,2}(\boldsymbol{\Omega}_1, \boldsymbol{\Omega}_2, \tau, \nu) \end{bmatrix} \end{aligned}$$

represents the dual-polarization-bidirection-delay-Doppler frequency spread function of the dth component, p_i, $i = 1, 2$ denote polarization status, with $p_i = 1$ being the vertical polarization and $p_i = 2$ being the horizontal polarization.

Baseband representation of the output signal

- The baseband representation of the output signal of the considered $M_1 \times M_2$ MIMO sounding system can be written as

$$\boldsymbol{Y}(t) = \int_{\mathbb{S}_2}\int_{\mathbb{S}_2}\int_{-\infty}^{+\infty}\int_{-\infty}^{+\infty} \boldsymbol{C}_2(\boldsymbol{\Omega}_2)\boldsymbol{H}(\boldsymbol{\Omega}_1,\boldsymbol{\Omega}_2,\tau,\nu)\boldsymbol{C}_1(\boldsymbol{\Omega}_1)^{\mathrm{T}} u(t-\tau) \exp\{j2\pi\nu t\}\mathrm{d}\boldsymbol{\Omega}_1\mathrm{d}\boldsymbol{\Omega}_2\mathrm{d}\tau\mathrm{d}\nu + \boldsymbol{W}(t),$$

  where
  - $\boldsymbol{Y}(t) \in \mathcal{C}^{M_2\times M_1}$ is a $M_2 \times M_1$ matrix with the (m_2, m_1)th entry $Y_{m_2,m_1}(t)$ being the output of the m_2th Rx antenna when the m_1th Tx antenna transmits.
  - $\boldsymbol{C}_1(\boldsymbol{\Omega}_1)$ and $\boldsymbol{C}_2(\boldsymbol{\Omega}_2)$ represent the dual-polarized array response of the Tx and Rx respectively. They are written as

$$\boldsymbol{C}_i(\boldsymbol{\Omega}_i) = [\boldsymbol{c}_{i,1}(\boldsymbol{\Omega}_1), \boldsymbol{c}_{i,2}(\boldsymbol{\Omega}_1)] \in \mathcal{C}^{M_i\times 2},\ i = 1, 2$$

$$\text{with } \boldsymbol{c}_{i,p_i}(\boldsymbol{\Omega}_i) = [c_{i,1,p_i}(\boldsymbol{\Omega}_i), \ldots, c_{i,M_i,p_i}(\boldsymbol{\Omega}_i)]^{\mathrm{T}}$$

Baseband representation of the output signal

- Rewrite $\boldsymbol{Y}(t)$ as

$$\boldsymbol{Y}(t) = \sum_{d=1}^{D} \boldsymbol{S}_d(t) + \boldsymbol{W}(t),$$

with $\boldsymbol{S}_d(t)$ being the contribution of the dth component, i.e.

$$\boldsymbol{S}_d(t) = \int_{\mathbb{S}_2} \int_{\mathbb{S}_2} \int_{-\infty}^{+\infty} \int_{-\infty}^{+\infty} \boldsymbol{C}_2(\boldsymbol{\Omega}_2) \boldsymbol{H}_d(\boldsymbol{\Omega}_1, \boldsymbol{\Omega}_2, \tau, \nu) \boldsymbol{C}_1(\boldsymbol{\Omega}_1)^{\mathrm{T}} u(t-\tau) \exp\{j2\pi\nu t\} \mathrm{d}\boldsymbol{\Omega}_1 \mathrm{d}\boldsymbol{\Omega}_2 \mathrm{d}\tau \mathrm{d}\nu + \boldsymbol{W}(t).$$

The stochastic properties of the channel

- Assume that the dual-polarized component spread function $H_{d,p_1,p_2}(\mathbf{\Omega}_1, \mathbf{\Omega}_2, \tau, \nu)$, $d \in \{1, \ldots, D\}$ are uncorrelated complex (zero-mean) orthogonal stochastic measures, i.e.

$$\begin{aligned}\mathrm{E}[H_{d,p_1,p_2}(\mathbf{\Omega}_1,\mathbf{\Omega}_2, \tau, \nu) H_{d',p_1',p_2'}(\mathbf{\Omega}_1', \mathbf{\Omega}_2', \tau', \nu')^*] = \\ P_{d,p_1,p_2}(\mathbf{\Omega}_1, \mathbf{\Omega}_2, \tau, \nu)\delta_{dd'}\delta_{p_1p_1'}\delta_{p_2p_2'} \\ \delta(\mathbf{\Omega}_1 - \mathbf{\Omega}_1')\delta(\mathbf{\Omega}_2 - \mathbf{\Omega}_2')\delta(\tau - \tau')\delta(\nu - \nu'),\end{aligned}$$

  where $(\cdot)^*$ denotes complex conjugation, $\delta_{..}$ and $\delta(\cdot)$ represent the Kronecker delta and the Dirac delta function respectively
- $P_{d,p_1,p_2}(\mathbf{\Omega}_1, \mathbf{\Omega}_2, \tau, \nu)$ represents the power spectrum (PS) of the dth component with Tx polarization p_1 and Rx polarization p_2, which can be calculated as

$$P_{d,p_1,p_2}(\mathbf{\Omega}_1, \mathbf{\Omega}_2, \tau, \nu) = \mathrm{E}[|H_{d,p_1,p_2}(\mathbf{\Omega}_1,\mathbf{\Omega}_2, \tau, \nu)|^2].$$

The stochastic properties of the channel

- The polarized component PS $P_{d,p_1,p_2}(\mathbf{\Omega}_1, \mathbf{\Omega}_2, \tau, \nu)$ can be further written as

$$P_{d,p_1,p_2}(\mathbf{\Omega}_1, \mathbf{\Omega}_2, \tau, \nu) = P_{d,p_1,p_2} \cdot f_{d,p_1,p_2}(\mathbf{\Omega}_1, \mathbf{\Omega}_2, \tau, \nu),$$

  where P_{d,p_1,p_2} represents the average power of the dth (p_1, p_2)-polarized component, and
- $f_{d,p_1,p_2}(\mathbf{\Omega}_1, \mathbf{\Omega}_2, \tau, \nu)$ denotes the power spectral density (PSD) of the dth component at polarizations (p_1, p_2).

The stochastic properties of the channel

- It can be easily shown from the property defined in (??) that

$$\begin{aligned}\mathrm{E}[\boldsymbol{H}_d(\boldsymbol{\Omega}_1,\boldsymbol{\Omega}_2,\tau,\nu)\odot\boldsymbol{H}_{d'}(\boldsymbol{\Omega}_1',\boldsymbol{\Omega}_2',\tau',\nu')^*] = \\ \boldsymbol{P}_d(\boldsymbol{\Omega}_1,\boldsymbol{\Omega}_2,\tau,\nu)\delta_{dd'}\delta(\boldsymbol{\Omega}_1-\boldsymbol{\Omega}_1')\delta(\boldsymbol{\Omega}_2-\boldsymbol{\Omega}_2') \\ \delta(\tau-\tau')\delta(\nu-\nu'),\end{aligned}$$

  where $\odot$ is element-wise product,
- $\boldsymbol{P}_d(\boldsymbol{\Omega}_1,\boldsymbol{\Omega}_2,\tau,\nu)$ is called "dual-polarized component PS matrix":

$$\begin{aligned}\boldsymbol{P}_d(\boldsymbol{\Omega}_1,\boldsymbol{\Omega}_2,\tau,\nu) &= \mathrm{E}[\boldsymbol{H}_d(\boldsymbol{\Omega}_1,\boldsymbol{\Omega}_2,\tau,\nu)\odot\boldsymbol{H}_d(\boldsymbol{\Omega}_1,\boldsymbol{\Omega}_2,\tau,\nu)^*] \\ &= \begin{bmatrix} P_{d,1,1}(\boldsymbol{\Omega}_1,\boldsymbol{\Omega}_2,\tau,\nu) & P_{d,1,2}(\boldsymbol{\Omega}_1,\boldsymbol{\Omega}_2,\tau,\nu) \\ P_{d,2,1}(\boldsymbol{\Omega}_1,\boldsymbol{\Omega}_2,\tau,\nu) & P_{d,2,2}(\boldsymbol{\Omega}_1,\boldsymbol{\Omega}_2,\tau,\nu)\end{bmatrix}.\end{aligned}$$

The stochastic properties of the channel

- We can further rewrite $\boldsymbol{P}_d(\boldsymbol{\Omega}_1, \boldsymbol{\Omega}_2, \tau, \nu)$ as

$$\boldsymbol{P}_d(\boldsymbol{\Omega}_1, \boldsymbol{\Omega}_2, \tau, \nu) = \boldsymbol{P}_d \odot \boldsymbol{f}_d(\boldsymbol{\Omega}_1, \boldsymbol{\Omega}_2, \tau, \nu),$$

  where
  - $\boldsymbol{P}_d = \begin{bmatrix} P_{d,1,1} & P_{d,1,2} \\ P_{d,2,1} & P_{d,2,2} \end{bmatrix}$: the average power matrix
  - $\boldsymbol{f}_d(\boldsymbol{\Omega}_1, \boldsymbol{\Omega}_2, \tau, \nu) = \begin{bmatrix} f_{d,1,1}(\boldsymbol{\Omega}_1, \boldsymbol{\Omega}_2, \tau, \nu) & f_{d,1,2}(\boldsymbol{\Omega}_1, \boldsymbol{\Omega}_2, \tau, \nu) \\ f_{d,2,1}(\boldsymbol{\Omega}_1, \boldsymbol{\Omega}_2, \tau, \nu) & f_{d,2,2}(\boldsymbol{\Omega}_1, \boldsymbol{\Omega}_2, \tau, \nu) \end{bmatrix}$: the dual-polarized PSD matrix of the dth component.
- the dual-polarized spread function matrix $\boldsymbol{H}(\boldsymbol{\Omega}_1, \boldsymbol{\Omega}_2, \tau, \nu)$ of the channel is also an orthogonal stochastic measure, i.e.

$$\mathrm{E}[\boldsymbol{H}(\boldsymbol{\Omega}_1, \boldsymbol{\Omega}_2, \tau, \nu) \odot \boldsymbol{H}(\boldsymbol{\Omega}_1', \boldsymbol{\Omega}_2', \tau', \nu')] = \boldsymbol{P}(\boldsymbol{\Omega}_1, \boldsymbol{\Omega}_2, \tau, \nu)$$
$$\delta(\boldsymbol{\Omega}_1 - \boldsymbol{\Omega}_1')\delta(\boldsymbol{\Omega}_2 - \boldsymbol{\Omega}_2')\delta(\tau - \tau')\delta(\nu - \nu'),$$

The stochastic properties of the channel

- $\boldsymbol{P}(\boldsymbol{\Omega}_1, \boldsymbol{\Omega}_2, \tau, \nu)$ is the dual-polarized bidirection-delay-Doppler PS matrix of the channel considered:

$$\begin{aligned}\boldsymbol{P}(\boldsymbol{\Omega}_1, \boldsymbol{\Omega}_2, \tau, \nu) &= \mathrm{E}[\boldsymbol{H}(\boldsymbol{\Omega}_1, \boldsymbol{\Omega}_2, \tau, \nu) \odot \boldsymbol{H}(\boldsymbol{\Omega}_1, \boldsymbol{\Omega}_2, \tau, \nu)^*] \\ &= \sum_{d=1}^{D} \boldsymbol{P}_d(\boldsymbol{\Omega}_1, \boldsymbol{\Omega}_2, \tau, \nu).\end{aligned}$$

- Assume that the PSDs of the dth component with different combinations of polarizations are identical, i.e.

$$f_{d,p_1,p_2}(\boldsymbol{\Omega}_1, \boldsymbol{\Omega}_2, \tau, \nu) = f_d(\boldsymbol{\Omega}_1, \boldsymbol{\Omega}_2, \tau, \nu), \text{for } p_1 = 1, 2,\ p_2 = 1, 2.$$

- Under this assumption, $\boldsymbol{P}_d(\boldsymbol{\Omega}_1, \boldsymbol{\Omega}_2, \tau, \nu) = \boldsymbol{P}_d \cdot f_d(\boldsymbol{\Omega}_1, \boldsymbol{\Omega}_2, \tau, \nu)$.
- We are interested at extracting the PS matrix $\boldsymbol{P}(\boldsymbol{\Omega}_1, \boldsymbol{\Omega}_2, \tau, \nu)$ of a propagation channel from measurement data.